INVESTIGATING THE ROLES OF MICRORNAS IN BIOTIC STRESS RESPONSES AND FUNCTIONAL CHARACTERIZATION OF A NOVEL ZTL-TYPE F-BOX PROTEIN *VIA* VIRUS INDUCED GENE SILENCING

A THESIS SUBMITTED TO
THE GRADUATE SCHOOL OF NATURAL AND APPLIED SCIENCES
OF
MIDDLE EAST TECHNICAL UNIVERSITY

BY

YASİN FATİH DAĞDAŞ

IN PARTIAL FULFILLMENT OF THE REQUIREMENTS
FOR
THE DEGREE OF MASTER OF SCIENCES
IN
BIOTECHNOLOGY

JUNE 2009

Approval of the thesis

INVESTIGATING THE ROLES OF MICRORNAS IN BIOTIC STRESS RESPONSES AND FUNCTIONAL CHARACTERIZATION OF A NOVEL ZTL-TYPE F-BOX PROTEIN *VIA* VIRUS INDUCED GENE SILENCING

submitted by **YASİN FATİH DAĞDAŞ** in partial fulfillment of the requirements for the degree of **Master of Science in Biotechnology Programme, METU** by

Prof. Dr. Canan Özgen
Dean, Graduate School of Natural and Applied Sciences _____

Prof. Dr. Gulay Ozcengiz
Head of Department, Biotechnology _____

Prof. Dr. Mahinur S. Akkaya
Supervisor, Chemistry Dept., METU _____

Examining Committee Members:
Prof. Dr. Mahinur S. Akkaya
Chemistry Dept., METU _____

Prof. Dr. Mesude İşcan
Biology Dept., METU _____

Assist. Prof. Dr. Tolga Can
Comp. Eng. Dept., METU _____

Assist. Prof. Dr. Tülin Yanık
Biology Dept., METU _____

Assist Prof. Dr. Çağdaş Son
Biology Dept., METU _____

Date: 23.06.2009

I here by declare that all information in this document has been obtained and presented in accordance with academic rules and ethical conduct. I also declare that, as required by these rules and conduct, I have fully cited and referenced all materials and results that are not original to this work.

Name, Last name: Yasin Fatih Dağdaş

Signature :

ABSTRACT

INVESTIGATING THE ROLES OF MicroRNAS IN BIOTIC STRESS RESPONSES AND FUNCTIONAL CHARACTERIZATION OF A NOVEL ZTL-TYPE F-BOX PROTEIN *VIA* VIRUS INDUCED GENE SILENCING

Dağdaş, Yasin Fatih

M. Sc., Department of Biotechnology

Supervisor: Prof. Dr. Mahinur S. Akkaya

June 2009, 170 pages

Barley and wheat are the two most important crop species in Turkey. Molecular studies for increasing crop yield of these species are very important for the economic benefits of Turkey. Powdery mildew and yellow rust are the two main pathogens, infecting barley and wheat, respectively in our country and causing a great amount of yield loss each year. Till now, classical genetics studies were performed in order to develop resistant barley and wheat cultivars, but these studies have not been succesful. Therefore, molecular plant-pathogen interactions studies are starting to become the new tool to fight against pathogens. In this thesis, two important aspects of plant microbe interactions were investigated.

In the first part, the role of microRNAs (miRNAs) in powdery mildew-barley pathosysytem, and yellow rust-wheat pathosystem were studied. The expression levels

of miRNAs and their putative targets were investigated *via* miRNA microarray analysis and qRT-PCR, respectively, in response to virulent and avirulent pathogen infections. These data were used to establish a new model for powdery mildew-barley and yellow rust-wheat pathosystems.

In the second part, functional analysis of a novel F-box gene, which was a ZTL-type F-box, was performed by using Barley Stripe Mosaic Virus mediated Virus Induced Gene Silencing. This F-box gene (HvDRF) (*Hordeum vulgare* Disease Related F-box) was induced upon yellow rust infection and we studied its role in powdery mildew infection. The results confirmed HvDRF as a positive regulator of race specific immunity and enlarged the roles of ZTL-type F-box proteins to biotic stress responses.

Key Words: miRNA, F-box protein, yellow rust, powdery mildew, E3 ligase, miR159, miR169, qRT-PCR, miRNA microarray analysis, VIGS.

ÖZ

MiKRORNA`LARIN BiYOTiK STRES KOŞULLARINDAKİ GÖREVLERİNİN ARAŞTIRILMASI VE YENİ BİR ZTL-TİPİ F-BOX PROTEİNİNİN VIRÜS İNDÜKLENMESİ İLE GEN SUSTURULMASI YÖNTEMİ İLE FONKSİYONEL KARAKTERİZASYONU

Dağdaş, Yasin Fatih

Yüksek Lisans, Biyoteknoloji Bölümü

Tez yöneticisi: Prof.Dr.Mahinur S. Akkaya

Haziran 2009, 170 sayfa

Arpa ve buğday Türkiye'de üretilen en önemli tahılların başında gelmektedir ve bu bitkilerin ürün verimini arttıracak moleküler çalışmalar ülke ekonomisinin gelişmesi için çok önemlidir. Külleme ve sarı pas bu bitkileri hasta eden patojenlerin başında gelmektedir ve her yıl önemli miktarda ürün kaybına neden olmaktadır. Şimdiye kadar bu patojenlere karşı klasik genetik çalışmaları ile karşı konulmaya çalışılmıştır, ancak bu çalışmalar başarılı olamamıştır. Dolayısıyla, moleküler bitki-patojen ilişkisi çalışmaları patojenlerle savaşabilmek ve ürün kaybının önüne geçmek için yaygın olarak kullanılmaya başlamıştır. Bu tezde bitki-patojen ilişkilerinin iki farklı boyutu

incelenmiştir.

İlk kısımda arpa-külleme ve sarı pas-buğday patojen sistemlerinde mikroRNA`ların rolu araştırılmıştır. Virulent ve avirulent patojen enfekte edilmiş bitkilerde mikroRNA`ların ve onların hedef genlerinin ekspresyon seviyeleri mikroRNA mikrodizin analizi ve qRT-PCR deneyleri ile saptanmış ve bu veriler ışığında bu iki sistem icin mikroRNA`ları içeren yeni bir model ortaya konulmuştur.

İkinci kısımda, sarı pas enfekte edilmiş buğdaylarda arttığı bulunmuş ZTL-tipi yeni bir F-box proteinin (HvDRF) BSMV aracılığı ile VIGS yöntemi ile külleme bulaştırılmış arpalarda fonksiyonel karakterizasyonu yapılmıştır. Gen susturması sonuçları bu F-box proteininin ırk-spesifik direnç mekanizmalarında pozitif regülatör olarak görev aldığını kanıtlamış ve ZTL tipi F-box proteinlerinin biyotik stres koşullarında da görev aldıklarını ispatlamıştır.

Anahtar kelimeler: MikroRNA, F-box proteini, külleme, sarı pas, E3 ligaz, miR159, miR169, qRT-PCR, mikroRNA mikrodizin analizi, VIGS.

I dedicate my thesis to the “arms race” between plants and pathogens.

ACKNOWLEDGEMENTS

I would like to express my gratitude to my advisor Dr. Mahinur Akkaya for giving me the opportunity to work with her, for believing in me and my abilities and for her great encouragement, friendship and support.

I would like to thank to Dr. Turgay Unver for his guidance and support throughout my Msc studies.

I would also like to thank to my wife, Gulay, for her kind support and motivation.

I am grateful to the members of Akkaya Laboratory for their great friendship and motivation.

I gratefully acknowledge the kind financial supports of TÜBİTAK (TBAG-107T877) and BAP.

TABLE OF CONTENTS

LIST OF TABLES

TABLES

LIST OF FIGURES

FIGURES

LIST OF ABBREVIATIONS

ug : Microgram

uL : Microliter

uM : Micromolar

ACRE : Avr/Cf Rapid Elicidated

ADP : Adenosine Di phosphate

As : Anti sense

At : *Arabidopsis thaliana*

Avo : Avocet

Avr : Avirulence

Bgh : *Blumeria graminis hordei*

BSMV: Barley Stripe Mosaic Virus

Cf : *Clodisporium fulvum*

DNA : Deoxyribonucleic acid

dNTP : Deoxy-nucleotidetriphosphate

Dpi : Day post inoculation

ds : Double stranded

DTT : Dithiothretiol solution

DUB : Deubiquitinase

EDTA : Ethylenediaminetetraacetic acid

ETI : Effector Triggered Immunity

ETS : Effector Triggered Susceptibility

GFP : Green Flourescent Protein

h. : Hour

Hai : Hour after inoculation

HR : Hypersensitive response

HSP90 : Heat Shock Protein 90

kb : Kilobase

LiCl : Lithium Chloride

LRR : Leucine rich repeat

M : Molar

mg : Miligram

min. : Minute

miRNA: microRNA

mL : Mililiter

Mla : Mildew Locus A

mM : Milimolar

NB : Nucleotide binding

NEB : New England Biolabs

ng : Nanogram

nm : Nanometer

NTC : No Template Control

Os : *Oryza sativa*

p : plasmid

PAMP : Pathogen Associated Molecular Pattern

PCD : Programmed Cell Death

PCR : Polymerase Chain Reaction

PDS : Phytoene Desaturase

pmol : Picomole

PR : Pathogenesis Related

Pst : *Puccinia striiformis tritici*

PTGS : Post Transcriptional Gene Silencing

PTI : PAMP Triggered Immunity

PTI : PAMP Triggered Immunity

qRT : quantitative Reverse transcriptase

R : Resistance

RAR1 : Required for Mildew LocusA Resistance 1

RISC : RNA Induced Silencing Complex

RNA : Ribonucleic acid

RNAi : RNA interference

ROS : Reactive oxygen species

rpm : Rotation per minute

RT : Reverse transcriptase

SCF : Skp1-Cullin-Fbox

SGS : SGT1 Specific

SGT1 : Suppressor of G2 allele

SiRNA : Small interfering RNA

SOD : Superoxide dismutase

Ss : single stranded

Ta : *Triticum aestivum*

Taq : *Thermus aquaticus*

TIR : Toll Like Interleukine

U : Unit

Ub : Ubiquitin

UBC : Ubiquitin conjugating enzyme**,**

UV : Ultraviolet

VIGS : Virus Induced Gene Silencing

CHAPTER 1

INTRODUCTION

1.1 Plant microRNAs

MicroRNAs (miRNAs) are 19-24 nucleotides long, sequence-specific regulators of eukaryotic genomes. They were unnoticed till their recent discovery in *C. elegans (Ambros and Chen, 2007),* but now known to be important control elements of gene regulatory networks in plants and animals. They are thought to control 30 % of eukaryotic genome (Axtell, 2008). They are chemically and functionally similar to siRNAs (short interfering RNAs) and the distinction between siRNAs and miRNAs are becoming harder as new discoveries are made (Jones-Rhoades et al., 2006) (Voinnet, 2009). miRNAs, like siRNAs control transcription of genes *via* a mechanism known as PTGS (post transcriptional gene silencing).

1.1.1 Biogenesis of plant microRNAs

Formation of a functional miRNA includes four basic steps: (1) induction of miRNA processing elements by double stranded RNA (dsRNA), (2) processing of dsRNA into small RNAs (sRNAs), (3) 3`-O-methylation of sRNA, and (4) incorporation of methylated small RNA into silencing effector complexes. Effector complex incorporated sRNAs interact with their targets in a partial or full complementary fashion.

Plant miRNAs are generally found in genomic regions that are not protein coding and they are thought to be produced from their own genes (Jones-Rhoades et al., 2006). Sometimes as in miR395 cluster, miRNA genes are found as clusters and many miRNAs are transcribed from single primary transcript (Jones-Rhoades and Bartel, 2004; Guddeti et al., 2005). Plant miRNA transcripts are formed by the action of RNA Polymerase II and primary transcripts (pri-miRNA) are characterized by stem-loop structures (Xie et al., 2005). Some of these transcripts are found to be capped, polyadenylated and spliced, and others are thought to be processed in a similar fashion (Aukerman and Sakai, 2003; Xie et al., 2005; Kurihara et al., 2006). Besides RNA Polymerase II transcripts, dsRNA can be produced from viral RNAs or RNA dependant RNA Polymerase 1-6 (RDR1-6). Templates of RDRs include atypical mRNAs or transcripts of plant specific RNA Polymerase IV (Voinnet 2009).

Up to 1 kb long stem-loop containing pri-miRNAs are excised by the activity of RNaseIII type endonucleases such as Dicer. There are four types of Dicer like (DCL) proteins in *Arabidopsis*. The products of each enzyme have different lengths; DCL1 has 18-21 nucleotide long products, DCL2 has 22, DCL3 has 24 and DCL4 has 21 nucleotides long products (Voinnet 2009). The products of DCL proteins are characterized by 3` overhangs, this property is widely used for analyzing deep sequencing data for determination of putative miRNAs (Lee et al., 2003; Lim et al., 2003). In plants DCL1 activity is enough for miRNA accumulation and formation of mature miRNA occurs in nucleus (Park et al., 2002; Kurihara et al., 2006). None of other DCL proteins are required for miRNA biogenesis (Xie et al., 2004). In animals there are two distinct steps of cleavage. First pre-miRNA is formed from pri-miRNA, which is followed by the formation of miRNA/miRNA* in cytoplasm (Lee et al., 2003). In contrast to animals, pre-miRNAs are rarely detected in plants and both cleavage reactions occur in nucleus. The cleavage specificity is mainly depended on the secondary structure of pri-miRNA, which was confirmed by modifications of the pri-miRNA sequence without changing stem-loop structure (Parizotto et al., 2004; Vaucheret et al., 2004). DCL1 interacts with HYL1 (hyponastic leaves 1) and SE

(serrate) in order to perform dicing activity and mutants of these genes are lethal like DCL1 mutants (Kurihara et al., 2006; Fang and Spector, 2007). Finally, DCL1 interacts with DDL (dawdle) protein whose function is not understood completely for now (Yu et al., 2008).

The third step in miRNA biogenesis is 3`-O-methylation of mature miRNA duplex. S-adenosylmethionine-dependant methyltransferase HEN1 (Hua Enhancer 1) catalyzes methylation of all small silencing RNAs in plants. Methylation prevents 3` uridylation and subsequent degradation of small RNAs (Li et al., 2005; Yang et al., 2006).

The last step in miRNA processing is transport of mature miRNA into cytoplasm and association of silencing complex. In order to export miRNA into cytoplasm HST (hasty) protein is required. The complete mechanism of miRNA transport is unknown, but HST is a homolog of animal exportin 5, and some miRNAs are shown to be interacting with HST. However, miRNA accumulation was observed in null mutants of HST, meaning there are some HST-independent transport mechanisms, which are not discovered yet (Poethig et al., 2006).

One strand of the miRNA/miRNA* duplex is incorporated into RISC (RNA induced silencing complex) in order to perform effector function. Strand selection depends on the energetic asymmetry if miRNA/miRNA* duplex (Jones-Rhoades et al., 2006). The 5` ends of miRNA strands are much less stable than miRNA* strand and these strands are incorporated into RISC (Haley and Zamore, 2004). Unassociated miRNA* strand is degraded quickly after loading of miRNA onto RISC. RISCs invariably contain an Argonaute (AGO) protein. Argonoute proteins have a single strand RNA binding PAZ domain and a PIWI domain having RNaseH like activity (Brodersen and Voinnet, 2006; Jones-Rhoades et al., 2006). There are 10 Argonaute proteins identified in *Arabidopsis*, 4 of which are functionally characterized. AGO4 is functioning in methylation of some transposons and inverted repeat genes (Xie et al., 2004). AGO7 and AGO10 is required for normal development of *Arabidopsis*, but the action mechanism is not known yet (Poethig et al., 2006). AGO7 function is related with ta-

siRNA (trans acting small interfering RNA) biogenesis (Vazquez et al., 2004b). AGO6 is functioning in cytosine methylation for epigenetic mechanisms and associated with 24 nucleotide long heterochromatin associated small RNAs (Mallory et al., 2008). The only AGO protein shown to take role in miRNA action is AGO1. AGO1 catalyzes cleavage of miRNA targets and ago1 mutants have higher levels of miRNA targets (Vaucheret et al., 2004). The general scheme of miRNA biogenesis pathway is given in Figure 1.1

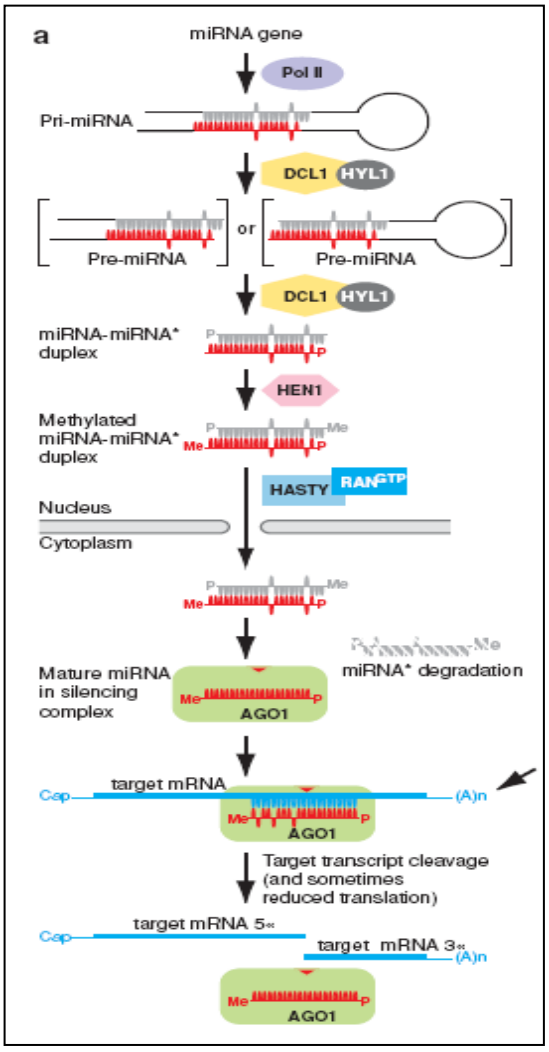

Figure 1.1 Biogenesis of plant miRNAs (Jones-Rhoades et al., 2006). Primary microRNAs are transcribed by RNA Polymerase II and processed by cap and poly-A tail addition. Primary miRNA is processed into miRNA/miRNA* duplex by the action of DCL1. miRNA/miRNA* duplex has 5` phosphates and two nucleotide long 3` overhangs. 3` sugars of miRNA/miRNA* duplex is methylated *via* HEN1. miRNA duplex is transported into cytoplasm by HST and some additional factors, where mature miRNA is incorporated into AGO1 containing RISC. On the other hand, miRNA* is degraded *via* exonucleases. miRNA in silencing complex has the ability to cleave target mRNAs or repress translation.

1.1.2 Mechanisms of plant miRNA action

Plant miRNAs regulate gene expression by three distinct mechanisms: (a) cleavage of complementary target mRNA, (b) repression of translation of target mRNA, and (c) transcriptional silencing of target mRNA. Until recent years cleavage of target mRNA by the aid of AGO1 was the only mechanism that was experimentally verified. Since plant miRNAs show very high complementarities to their target mRNAs, main mode of action of miRNAs was thought to be cleavage. This idea was supported by elevated transcript levels of target mRNAs in ago1, hen1, and hyl1 mutants (Boutet et al., 2003; Vaucheret et al., 2004; Vazquez et al., 2004a); increasing of target mRNAs in cells that are over expressing viral suppressors of RNA silencing (Kasschau et al., 2003; Chapman et al., 2004; Chen et al., 2004; Dunoyer et al., 2004) and reduction of target mRNA levels in cells that are overexpressing miRNAs (Palatnik et al., 2003; Achard et al., 2004; Guo et al., 2005; Kim et al., 2005b; Wang et al., 2005; Williams et al., 2005; Sunkar et al., 2007). Moreover detection of cleavage targets by 5` RACE (rapid amplification of cDNA ends) (Kasschau et al., 2003; Palatnik et al., 2003; Xie et al., 2003; Chen et al., 2004; Jones-Rhoades and Bartel, 2004; Llave, 2004; Mallory et al., 2004; Vazquez et al., 2004a; Allen et al., 2005; Mallory et al., 2005) and Northern blot experiments (Kasschau et al., 2003; Souret et al., 2004; Mallory et al., 2005) further confirmed sequence specific degradation of complementary mRNA targets from 9-11 nucleotides of miRNA. As a further confirming evidence slicing activity of Piwi domain in AGO1 protein is experimentally shown (Vaucheret et al., 2004; Valencia-Sanchez et al., 2006; Diederichs and Haber, 2007). Cleavage of target mRNA resembles switches; when the target is cleaved there is no turning back. Such kind of regulation might be important in regulating developmental processes, which require permanent determination of cell fates.

Second mode of action of plant miRNAs, which was discovered very recently, is translational repression of target mRNA (Brodersen and Voinnet, 2009). Repression of

translation was discovered by analysis of miRNA-action deficient mutants (mad1-6) and the general outcome was many of plant miRNAs are acting *via* both cleavage and repression. The degree of complementarity if miRNA with its target was known to be determining factor for cleavage, but it was discovered that neither the position of complementarity (ORF, 5`UTR or 3`UTR) nor the degree of complementarity is decisive in the mode of action of plant miRNAs. Translational repression of target mRNAs was supported by detection of full length target mRNAs by Northern blot analysis (Dunoyer et al., 2004; Souret et al., 2004). The experimental evidence of the mode of action of plant miRNAs are summarized in Figure 1.2

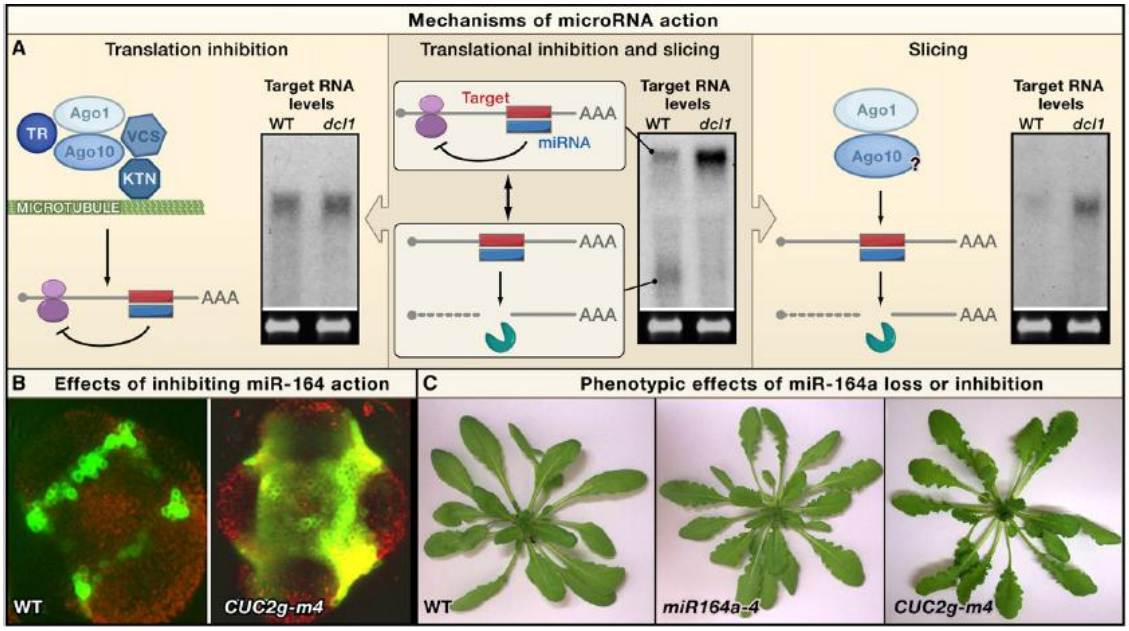

Figure 1.2 Plant miRNA modes of action (Voinnet 2009)**.** (A) The general picture of Northern gels after miRNA action is similar to the one depicted in the center which supports both cleavage and repression occurring at the same time. The mutant dcl1 is used as negative control. WT is the RNA isolated from wild type plants. Occurrence of small fragments leads us to slicing, but occurrence of full length mRNAs in the same lane is an evidence for translational suppression. The left lane shows the northern blots, if only translational repression is acting, and the right lane shows the northern blots if only slicing is acting. Translational repression requires microtubule severing enzyme Katanin (KTN) and P-body component Varicose (VCS). On the other hand, slicing activity might require AGO10. (B) Plant miRNAs restrain the expression of the target. In *Arabidopsis* miR164 controls the expression of Cup Shaped Cotyledon (CUC2). On the left expression of wild type CUC2 is shown which confirms localized expression of CUC2. On the right expression of miRNA resistant CUC2 is shown, whose expression is showing enlarged domains. (C) The phenotypic effects of miR164 target or miR164 mutants are shown.

In contrast to on-off switching of cleavage, this mode of action enables fine tuning of targets, and might be important in regulation of negative regulators of stress responses. By repressing translation of negative regulators, it is guaranteed that expression of the regulators will reappear when the stress is disappeared. This idea was supported by miRNAs controlling phosphate starvation (Sunkar et al., 2007) and basal defence against bacterial infection (Navarro et al., 2008). Reversibility ensures reducing the fitness loss due to prolonged stress response activation (Voinnet 2009).

1.1.3 Regulation of plant miRNA activity

Plant miRNA activity can be controlled at many levels, including controlling expression of miRNA genes, processing of miRNAs and action of miRNAs.

The first level of control of miRNA activity is regulating transcription from miRNA coding MIR genes. Some of the plant miRNA genes have conserved TATA-box like sequences, increasing the possibility that these genes have their independent promoters (Xie et al., 2005). Also tissue or even cell specific expression patterns of these conserved MIR genes suggest precisely controlled expression of these genes (Parizotto et al., 2004; Kawashima et al., 2009). Moreover many MIR genes have binding sites for transcription factors like ARF (activates gene expression without auxin), LFY (activated floral homeobox gene induction), MYC2 (increases resistance to drought) (Megraw et al., 2006). These transcription factors have binding sites for some miRNAs, which indicates the existence of some feedback loops and increases the complexity of the transcriptional control (Megraw et al., 2006). There are paralogues of MIR genes whose mature miRNA products are the same. Until recently, it was thought that these genes are formed by duplication events and have similar expression patterns. However, discovery of spatio-temporal differential expression of nine miR166 genes in maize shoot apex showed that, paralogous genes gained binding sites

for specific control elements and regulated in a distinct manner from each other (Figure 1.3 A)(Nogueira et al., 2007).

Regulation of plant miRNA processing is the second type of control for regulating miRNA activity. For now direct evidence indicating the control of processing is missing, but unequivalency seen in pri/pre-miRNA and miRNA levels in different miRNAs suggests the occurrence of such a control mechanism. In a wide variety of plant species, DCL3 dependant 24 nucleotides long miRNAs are identified (Parizotto et al., 2004; Vazquez et al., 2008). These miRNAs are formed independent of DCL1 and they are generally found in flora tissues, which was also supported by 10 times more abundance of DCL3 in floral tissues, compared to DCL1 (Figure 1.3 B). This organ specific expression manner might constitute a broad control circuit for miRNA expression. In 2008, overexpression of SINEs (short interspaced elements) was found to be similar to miRNA-deficient mutants. Later on it was discovered that, stem loops of SINEs are similar to miRNA precursors and bind to miRNA processing element HYL1 (Figure 1.3 B) (Pouch-Pelissier et al., 2008). Thus, competition between miRNA precursors and SINEs for HYL1 might control tissue or developmental stage specific miRNA expression. Another interesting miRNA activity control is, sequestering of DCL1 by miR162. So spatial or temporal differential expression of miR162 can modulate a global change in miRNA activity (Xie et al., 2003). The same type of control is also valid for AGO1, which is controlled by miR168 (Figure 1.3 C) (Vaucheret et al., 2004).

Another complexity to the miRNA action control mechanism was added by discovery of non-protein coding gene IPS1 (induced by phosphate starvation). IPS1 gene has a complementary region to miR399, but has a loop at cleavage point of miR399. So IPS1 pairing with miR399, prevents inhibitory effect of miR399. Both IPS1 and miR399 expression are induced upon phosphate starvation and IPS1 expression seems to be required for fine tuning of miR399 activity (Figure 1.3 D) (Franco-Zorrilla et al., 2007).

Another miRNA activity control can be achieved by sorting miRNAs onto different AGO complexes. In 2008, it was discovered that 5` last nucleotide of small RNA guide strand determines which AGO complex small RNA will be loaded (Montgomery et al., 2008; Takeda et al., 2008). For example AGO1 prefers uridine at 5` end, whereas AGO2 and AGO4 prefers adenosine and a change of uridine to adenosine abolishes silencing activity. Occurrence of length variants of miRNAs in different tissues support this idea (Vazquez et al., 2008). This type of control lacks supporting evidences for now, but seems to occur for tissue or cell specific miRNA expression.

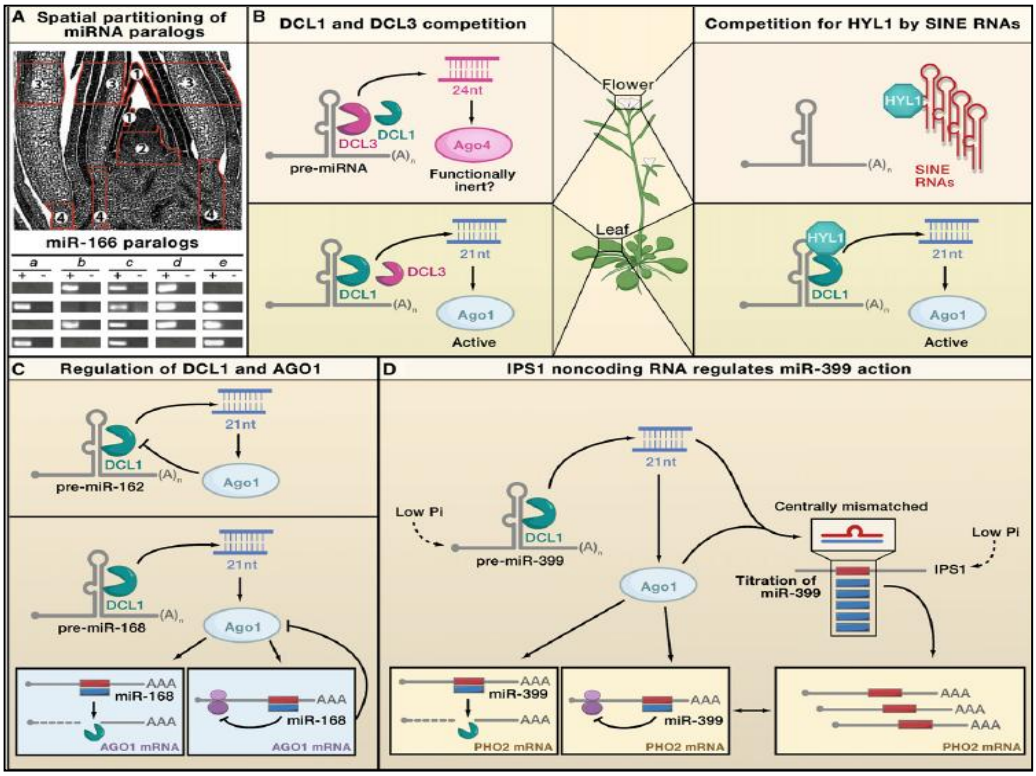

Figure 1.3 Modulation of plant miRNA action (Voinnet 2009). (A) Spatial expression pattern of miR166 isoforms in maize shoot apical meristem is shown by laser dissecting microscopy. Then the results were confirmed by RT-PCR of different miR166 isoforms. (B) Normally miRNAs are produced by DCL1. In flowers DCL3 is much more abundant than DCL1, and DCL3 produces 24 nucleotide long siRNAs. So the competition between DCL1 and DCL3 determines the miRNA activity in flowers. On the right, another competition between miRNA precursors and SINEs are presented. SINEs mimic stem loop precursors of miRNAs and compete for binding to HYL1. So the expression pattern of SINEs might be a determining factor for miRNA activity. (C) DCL1 and AGO1 which are required for miRNA biogenesis and action respectively are controlled by miR162 and miR168 respectively. (D) IPS1, a non-coding RNA, controls the activity of miR399 by binding through complementary regions. Both IPS1 and miR399 are induced upon phosphate starvation and IPS1 seems to be required for fine tuning of miR399 activity.

1.1.4 Functions of Plant miRNAs

1.1.4.1 Functions of plant miRNAs in development

Plant miRNAs are found to have roles in determination of meristem boundaries, meristem maintenance and initiation, leaf morphogenesis, stomatal development, light responses, sex determination, and most likely many yet uncovered processes.

The role of miRNAs in meristem differentiation was discovered by the studying silencing defective mutants. In these mutants, whose RNA silencing machinery is mutated, HD-ZIPIII transcription factor was decreased, and miR166 level was increased. Moreover, when HD-ZIPIII is overexpressed no radial leaves were produced (Nagasaki et al., 2007; Nogueira et al., 2007). So miR166 seems to have roles in determining meristem differentiation. Another striking data came from CUC (cup shaped cotyledon) gene studies. CUC genes normally determine the place of cotyledons in embryo and cuc1 and cuc2 mutants cannot initiate leaf formation (Aida and Tasaka, 2006). CUC genes are controlled by miR164 and mutations in miR164 isoforms, such as miR164a, miR164b, miR164c lead to different numbered floral organ sizes, such as formation of extra sepals, fewer stamens etc. (Nikovics et al., 2006; Sieber et al., 2007). miR164 mutants were also defective in phyllotaxy and had abnormal leaf shapes (Nikovics et al., 2006).

In tomatoes, LA (lanceolate) gene controls leaf morphogenesis. Normal tomato leaves are compound, whereas semidominant La mutant leaves are simple. It was shown that LA gene codes a TCP transcription factor, which has a target site for miR399. Strikingly, the expression domains of LA and miR399 are partially overlapping, meaning LA and miR399 are together determining the leaf shape of tomato (Ori et al., 2007). miRNAs are not only controlling leaf shape, but also controlling stomatal

complex formation. Recently miR824 was found to target a MADS-box gene which is controlling formation of stomatal complexes in meristemoids (Kutter et al., 2007).

Besides leaves miRNAs are found to regulate root formation. In *Medicago*, overexpression of miR166 caused a decrease in lateral root initiation and nodule formation (Boualem et al., 2008).

The functions of miRNAs in flowers were identified by studies on miR172. miR172 targets AP2 (Apetala2) gene and miRNA resistant forms of AP2 results in abnormal floral structure (Aukerman and Sakai, 2003; Chen, 2004). In Petunia and Antirrhinum defects in miR169 genes showed similar phenotypes to AP2 mutants, meaning miR169 replaced the function of AP2 in these plants (Cartolano et al., 2007). miR172 is also involved in determination of flowering time by interacting with photoreceptors. Functions of miR172 are not limited to flowering development. miR172 also controls sex determination in maize (Chuck et al., 2007b).

In *Arabidopsis*, overexpression of miR156 caused extended juvenile stage and late flowering, meaning miRNAs having role in phase change (Wu and Poethig, 2006). In maize miR156 overexpression was observed to decrease miR172 level and miR172 initiated flowering (Chuck et al., 2007a). So, it was suggested that a balance between mir156 and miR172 determines when the phase change will occur (Chuck et al., 2009).

These data shows that miRNAs are playing very definitive roles in plant development and further investigations of mutants having developmental defects will reveal more functions of miRNAs in development.

1.1.4.2 Functions of plant miRNAs in abiotic stress responses

Abiotic stress responses including extreme temperatures, salinity, nutrient deprivation and drought control expression of thousands of genes in plants and some of these genes are found to be regulated by miRNAs.

The role of miRNA in nutrient sensing was found by studying miR399. miR399 was found to be induced under phosphate starvation and the target of miR399, a putative ubiquitin conjugating enzyme (UBC), was decreased. Moreover, transgenic *Arabidopsis* plants overexpressing miR399 accumulated more phosphate than wild type plants and had higher levels of phosphate transporter gene in primary roots (Sunkar et al., 2007). Role of miRNAs in nutrient sensing was extended by studies showing the interaction of miR395 with ATP sulfurylase (APS) proteins. It was shown that miR395 is 100-fold induced upon sulfur starvation and APS1 level was decreases in miR395 inducing conditions (Jones-Rhoades and Bartel, 2004).

Oxidative stress responses are also regulated by miRNAs. Oxidative stress induces formation of reactive oxygen species and some scavengers like superoxide dismutases (SOD) remove these damaging molecules. The targets of miR398 were found to be copper SOD in *Arabidopsis* and rice and overexpression of miR398 reduced levels of Cu-SOD. More interestingly under low level copper conditions the level of Cu-SOD decreased and miR398 level increased, meaning miR398 is an important regulator of copper homeostasis and oxidative stress (Yamasaki et al., 2007).

The interaction of miRNAs with plant hormones was discovered by studying ABA responses. It was shown that miR159 is induced in ABA treated seedlings, and miR159 target MYB3 and MYB101 are decreased. The same situation is observed under drought conditions, meaning miR159 is one of the regulators controlling drought response related ABA functions (Reyes and Chua, 2007). There are more ABA induced miRNAs, which are miR393, miR397b and miR402. On the contrary, ABA

decreases level of miR398 (Sunkar et al., 2007). These results confirm that miRNAs are a part of hormone related stress responses.

One of the most important abiotic stress factors in tree species is mechanical stress. In 2008, it was found that tension and compression downregulates miR156, miR162, miR164, miR475, miR480 and miR481, whereas upregulates miR408 (Lu et al., 2008). So miRNAs are also involved in mechanical stress responses.

In addition to these findings, miR393 was found to be induced upon drought, cold and NaCl treatment, whereas miR319c was induced by cold not dehydration. In addition to miR393, miR169g was upregulated by drought conditions and thought to interact with drought response elements directly (Sunkar et al., 2007; Zhao et al., 2007).

These results show us miRNAs are indispensable elements in response to abiotic stress factors.

1.1.4.3 Functions of plant miRNAs in biotic stress responses

Although the role of miRNAs in development and abiotic stress was studied intensely, functions of miRNAs in biotic stress responses started to be unrevealed very recently. The first report came from *Arabidopsis*. A bacteria derived peptide, flg22, which is a widely known PAMP (pathogen associated molecular pattern) induced miR393 transcription which targets an F-box protein TIR1 (Figure 1.4 A) (Navarro et al., 2006). TIR1 is an auxin receptor, functioning in auxin mediated physiological responses. A similar increase was observed in *Arabidopsis* infected with Pst DC3000 hrcC (*Pseudomanas syringae* lacking functional type III secretion system). Overexpression of miR393 resistant TIR1 in tir1 mutant increased susceptibility to Pst DC3000 (Navarro et al., 2006). These results imply that miRNAs are at a critical place in PTI (PAMP triggered immunity) pathway. Strikingly, miRNA deficient mutants

like dcl1, rescued growth of Pst DC 3000 hrcC, which is normally nonvirulent (Navarro et al., 2008). Furthermore dcl1 mutants allowed growth of bacteria which are normally not infecting *Arabidopsis*, meaning miRNAs are also functioning in nonhost resistance. High throughput sequencing of Pst DC3000 hrcC infected *Arabidopsis* revealed many downregulated miRNAs, one of which is miR825. miR825 targets potential PTI regulators in *Arabidopsis* (Jin, 2008). This result explains why Pst DC3000 hrcC growth was lower than normal, because miRNAs that are downregulated by pathogen infection like miR825 are increased in these mutants. Downregulation of miRNAs upon pathogen infection was also observed in *Cronartium quercuum* infected loblolly pine. 10 miRNA families, including 7 pine specific miRNA families were downregulated by infection. Targets of these downregulated miRNA families were found to be R genes or RLKs (receptor like kinases), suggesting miRNA suppression is required for pathogen infection (Figure 1.4 B) (Lu et al., 2007).

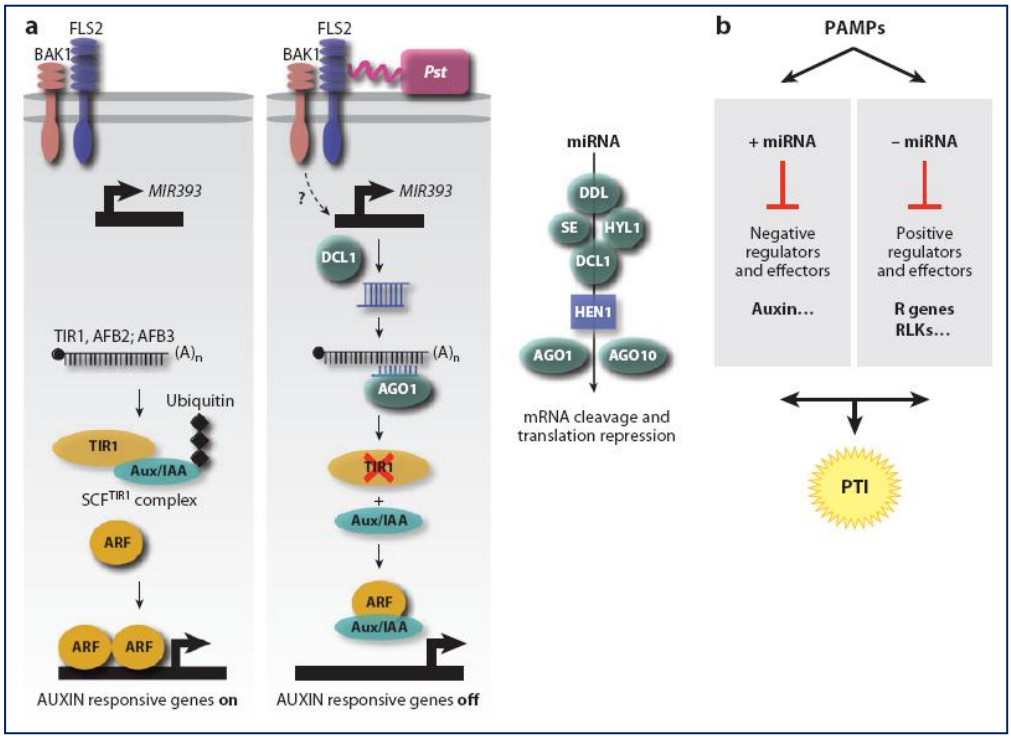

Figure 1.4 Plant miRNAs in biotic stress responses (Voinnet 2009). (A) Under low miR393 levels, TIR1 F-box proteins induce ubiquitin mediated degradation of auxin factors and promote induction of auxin responsive genes, which are suppressing defence responses. On the middle panel, the activation of FLS2 with flg22, leads to cleavage of TIR1 which results in suppression of auxin responsive genes. This reduction enhances PTI. (B) The production of miRNA is maintained in a balance by positive and negative regulators.

These results imply that the regulatory roles of miRNAs at all levels of pathogen response will grow much larger in real soon. In this study, the roles of miRNAs in two fungus-plant pathosystems were studied. Until now there are studies showing the important role of miRNAs in response to phytopathogenic bacteria. To our best knowledge, this study is the first one, investigating the role of miRNAs in plant fungal interactions.

1.2 The role of ubiquitination in plant defence responses

1.2.1 A summary of plant-microbe interaction machinery

There are various types of biotic stress factors trying to invade plant cells, including viruses, bacteria, oomycetes, and fungi. In contrast to animals plants lack mobile immune system cells and they depend on innate immunity, which is harbored by each cell, and signals spreading systematically from the infection site (Ausubel, 2005; Chisholm et al., 2006; Jones and Dangl, 2006). Plants try to prevent pathogen colonization by both constitutive and induced resistance mechanisms. Constitutive barriers include waxy cuticle, antimicrobial enzymes and secondary metabolites, which acts as the first barrier for all pathogens. If these barriers are passed, which is very common in nature, pathogen specific molecules are recognized by host plants and induced resistance occurs. Induced resistance can be divided into two parts depending on the nature of attacking pathogen. It is called non-host resistance if resistance is defined by host range of the pathogen.

The other type of induced resistance is called race-specific resistance, which relies on recognition of cognate avr (avirulence) genes of pathogens by R (resistance) genes (Bonas and Lahaye, 2002). If this interaction is a direct recognition of avr gene by corresponding R gene, this is called “gene-for-gene” interaction and lacking of either R gene or avr gene leads to disease (Flor, 1971). Recognition of avr factor by R gene generally activates a strong local response, namely hypersensitive response (HR), which is followed by cell death in infected area. Avr recognition also immunizes plant by spreading of signal molecules from the infection site which results in a global response (systemic acquired resistance (SAR)) (Heath, 2000; Durrant and Dong, 2004). “Gene-for-gene” interaction is supported by discovery of interaction of Flax R gene “L” with flax rust avr gene “avrL” (Ellis et al., 1999). In addition to direct

interaction, indirect interactions between R genes and avr genes were also discovered. This type of resistance mechanism were explained by "guard hypothesis" (Jones and Dangl, 2006). According to guard hypothesis, R gene recognizes modified Avr proteins such as Avr protein complexed with host proteins such as RIN4 protein of *Arabidopsis* (Van der Hoorn et al., 2002; Mackey et al., 2003). Avr proteins (also known as effectors) interact with host target proteins and this interaction results in susceptibility. In order to have a resistance response, R genes must recognize host target molecules that are modified by Avr molecules (Jones and Dangl, 2006).

1.2.2. Ubiquitin/26S Proteasome Pathway

Post-translational modification is a major determining factor of protein stability and modulation of protein activity. Modifications include phosphorylation, acetylation, methylation, glycosylation, myristoylation, sumoylation and ubiquitination. Ubiquitination can be monoubiquitin addition or linking a polyubiquitin chain onto target proteins which both lead to different responses. Addition of polyubiquitin chain to the target proteins direct the target protein to the 26S proteasome system which degrades proteins (Figure 1.5)

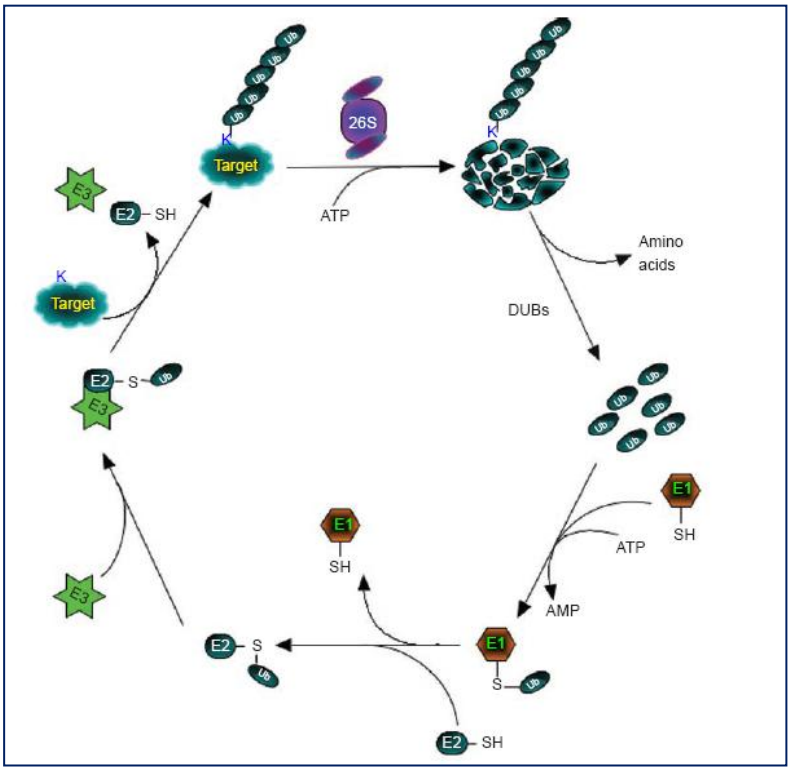

Figure 1.5 The Ubiquitin/26S Proteasome pathway (Zeng et al., 2006). The first step in ubiquitination is activation of ubiquitin molecule with ATP hydrolysis. Activated ubiquitin is then transferred to the active site of ubiquitin conjugating enzyme (E2). Finally, ubiquitin ligase (E3) transfers the ubiquitin from E2 to target protein by forming an isopeptide bond between lysine residue of target protein and ubiquitin. After repeating this cycle for many times, polyubiquitin added protein is directed to 26S proteasome. Here proteins are degraded into their monomers and polyubiquitin is also monomerized for further use, by the action of de-ubiquitination enzymes (DUBs).

Ubiquitination involves three sequential reactions that are acting in concert. Initially ubiquitin activating enzyme (E1) activates ubiquitin molecule, which is a 76 amino acid long highly conserved small peptide (Figure 1.6). Activation occurs by formation of a high energy thiol bond at C-terminal glycine residue of ubiquitin. E2 (ubiquitin

conjugating enzyme) carries this activated ubiquitin to a member of E3 (ubiquitin ligase) family. E3 catalyzes the final step of ubiquitination and transfers the ubiquitin molecule from E2 to the lysine residue of target protein. After addition of first ubiquitin, many more ubiquitins are added to the 48th lysine residue of ubiquitin, by the same process. Added polyubiquitin chain destines the target protein to the 26S proteasome.

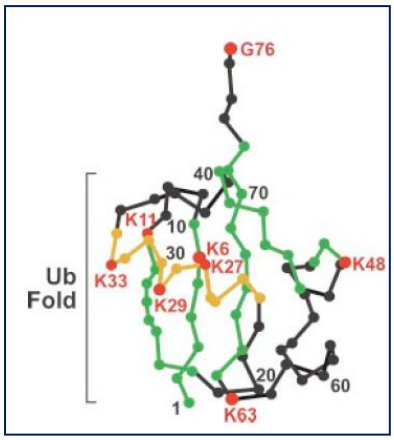

Figure 1.6 Three dimensional structure of ubiquitin.

26S proteasome is comprised of 20S core particle, which has an inner proteolytic chamber, and two 19S regulatory particles at each end, which are functioning in ATP-dependant unfolding and protein recognition (Smalle and Vierstra, 2004). In eukaryotes 20S core particle is composed of α and β subunits which are arranged as $\alpha_{1-7}/\beta_{1-7}/\beta_{1-7}/\alpha_{1-7}$. The two central heptameric β subunits form the catalytic chamber of the proteasome. β 1, β2 and β5 subunits of β rings are postranslationally modified to yield and active protease site. The α subunits form two rings at outer side of β rings and provide a channel which takes in the protein to be cleaved in an unfolded state and takes out the cleaved peptide fragments (Figure 1.7 a) 19S regulatory particle contains a lid and a base. The base part interacts with α-subunit of the 20S core particle and contain 6 AAA-ATPase (RPT1-6) and 3 non-ATPase subunits (RPN1, RPN2 and

RPN10) (Zeng et al., 2006). The lid is composed of eight subunits including RPN3, RPN5, RPN6, RPN7, RPN8, RPN9, RPN11, and RPN12 (Figure 1.7 b) (Gorbea et al., 1999). Some other elements which are required for regulating proteasome activity and localization can bind to these subunits transiently (Ferrell et al., 2000; Glickman and Raveh, 2005). Finally deubiquitinating enzymes (DUBs) that are cleaving ε-amide bond between ubiquitin and lysine residue of target protein, enabling ubiquitin recycling, are found in 19S complex (Figure 1.7 c) (Kurucz et al., 2002).

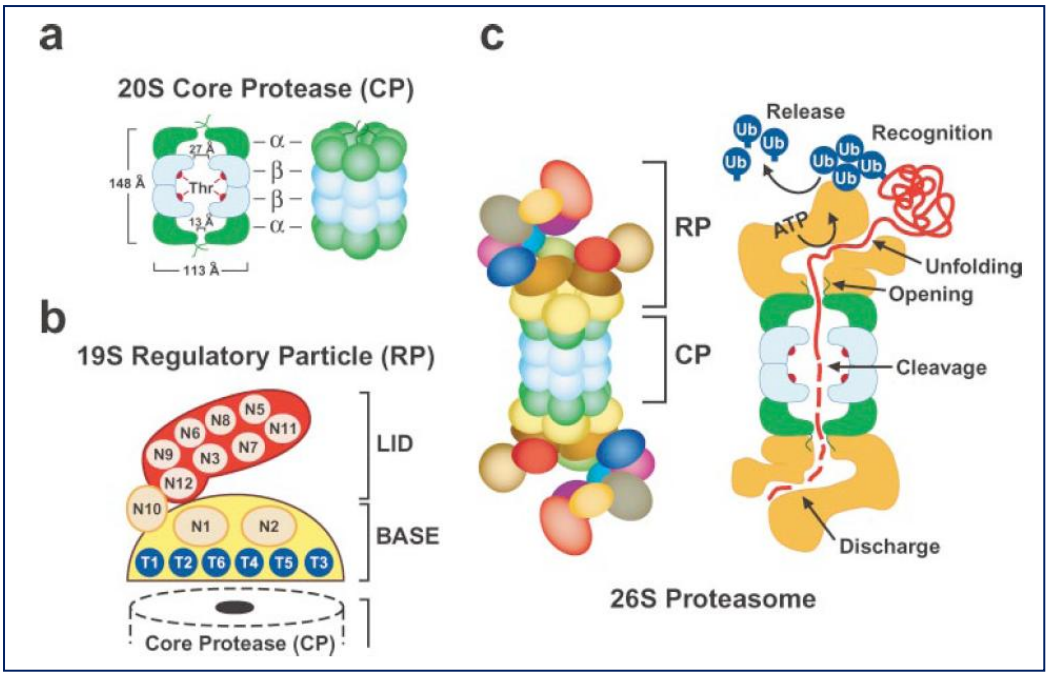

Figure 1.7 Structure of 26S proteasome (Smalle and Vierstra, 2004). (**a**) Organization of 20S core particle. Active site treonines are shown. (**b**) Organization of 19S regulatory particle. (**c**) Diagram showing a functional 26S proteasome.

The ubiquitination pathway is ending with 26S proteasome activity which is arranged in a hierarchical manner. E1, E2 and E3 enzymes` copy numbers within genomes give us insights about the functional divergence of these enzymes. For example there are 2

E1s, 41 E2s and more than 1200 E3 components in *Arabidopsis* genome (Vierstra, 2003). In ubiquitination/26S proteasome pathway, E3s are the elements conferring specificity to the system, meaning E3s are determining the target protein that will be degraded. This is the reason why E3s have such tremendous copy numbers (Smalle and Vierstra, 2004). Till now there are four different E3 families defined according to their mechanism of action and subunit composition. The HECT (homologous to E6-AP COOH terminus) domain is composed of 350 aminoacids and has a cysteine residue at its C-terminus conferring ligase function. HECT type E3 ligase is the only known E3 type that is forming a thiolester bond between ubiquitin and substrate (You and Pickart, 2001). SCF type E3 ligase is composed of four subunits: An adaptor protein Skp1, Cullin1 (CDC53), a RING finger protein RBX1 (or ROC1 and HRT1) that is interacting with Cullin1 and E2 and an F-box protein that is recruiting substrates. Cullin1 acts as a scaffold protein that brings E2s and substrates in proximity. APC type E3 ligases are composed of more than 10 proteins and thought to include a Cullin protein. APC E3 ligase complex is found in very few copies in plant genomes (Shen et al., 2002; Vierstra, 2003). RING-finger motif is characterized by the presence of zinc chelating residues, and acts similar to SCF E3 ligases (Zeng et al., 2006). SCF and RING-finger E3 ligases are found in hundreds of copies in plant genome, whereas there are very few HECT type E3 ligases identified (Mazzucotelli et al., 2006). A newly identified E3 ligase type is U-box domain which is composed of 75 amino acids.

1.2.3 The role of ubiquitination in plant defence signaling

The ubiquitination system can be thought as a housekeeping mechanism that is degrading abnormal proteins. However, besides its housekeeping role ubiquitin pathway plays a regulatory role by degrading key regulators in different pathways (Zeng et al., 2006). The first data for the role of protein degradation in defence signaling came from degradation of R protein RPM1 with the start of HR (Boyes et al.,

1998). After the discovery of RPM1 and its relation with ubiquitination pathway several more members of the defence system is found to be related with ubiquitin system (Table 1.1)

As mentioned before E3 ligases are the most diverse members of the ubiquitination pathway and they are the specificity determining elements. So it is not surprising to find E3 ligase components in defence signaling regulation. ACRE132 (Avr9/Cf9 rapidly elicited), ACRE189, and ACRE276 were determined in cDNA-AFLP analysis of Cf9 tobacco cell cultures treated with Avr9. Silencing of ACRE189 and ACRE276 drastically reduced Cf4 and Cf9 dependent resistance (Rowland et al., 2005). Other components of the E3 ligase system and interactors of E3 ligase (SGT1) are also shown to play critical roles in plant defence (Austin et al., 2002; Liu et al., 2002; Gray et al., 2003).

Table 1.1 Members of the Ubiquitin/26S Proteasome system functioning in plant defence responses (Zeng et al., 2006).

Gene	Protein type	Host	Challenge
ACRE132	RING-H2 (E3)	Tobacco/tomato	*C. fulvum*
ACRE189	F-box (E3)	Tobacco/tomato	*C. fulvum*
ACRE276	U-box (E3)	Tobacco/tomato	*C. fulvum*
At2g35000	RING finger (E3)	*Arabidopsis*	*E. cichoracearum*
AtCMPG1/AtCMPG2	U-box (E3)	*Arabidopsis*	*P. syringae*
ATL2/ATL6	RING-H2 (E3)	*Arabidopsis*	Elicitor chitin
BRH1	RING-H2 (E3)	*Arabidopsis*	Elicitor chitin
COI1	F-box (E3)	*Arabidopsis*	P. mastophorum
LeCOI1	F-box (E3)	Tomato	Spider mites
COP9	19S RP like	Tobacco	T.M.V.
EL5	RING-H2 (E3)	Rice	N-acetylchitooligo-saccharide elicitor
NtE1A and 1B	E1	Tobacco	T.M.V
PcCMPG1 (*ELI17*)	U-box (E3)	Parsley	Oligopeptide elicitor or *P. sojae*
RCE1	RUB-conjugating enzyme	*Arabidopsis*	-
SGT1	TPR domain	*Arabidopsis*	*P. parasitica* or powdery mildew
SKP1	SCF subunit	Tobacco	T.M.V
SON1	F-box (E3)	*Arabidopsis*	*P. parasitica* and *P. syringae*
SPL11	U-box (E3)	Rice	*M. grisea* and *X. oryzae* pv *oryzae*

1.2.4 F-box proteins in defence

Besides huge diversity of E3 ligases, F-box proteins of the E3 ligases are the most diverse member of E3 ligase complex which makes F-box proteins the best candidate as a regulatory element of ubiquitination pathway. F-box motif was named after the discovery of Skp1 interacting Cyclin F protein (Bai C., et al, 1986). After the discovery of 40 amino acid conserved F-box domain, it was found to be highly conserved and widespread among eukaryotes. There are about 700 hundred computationally identified F-box domain containing proteins in *Arabidopsis* (Xu et al., 2009). As mentioned above, F-box protein is a part of SCF type E3 ligase family and it binds to Skp1 which is interacting with scaffold protein Cullin1 (Figure 1.8 A). The function of F-box proteins in SCF complex is thought to be recruiting target proteins, so they are the major determinants of specificity of the system. F-box proteins have multiple functions in SCF complex: (1) it targets phosphorylated substrates for degradation, (2) it can form dimmers, (3) it is involved on neddylation of Cul1 and p53, and (4) itself is a ubiquitination target (Ho et al., 2008) The N-termini of the F-box proteins are interacting with Skp1, whereas C-termini have substrate recognition domains like WD40 repeats (WD40), leucine rich repeats (LRRs), Kelch repeats, etc. (Figure 1.8 B) (Ho et al., 2008).

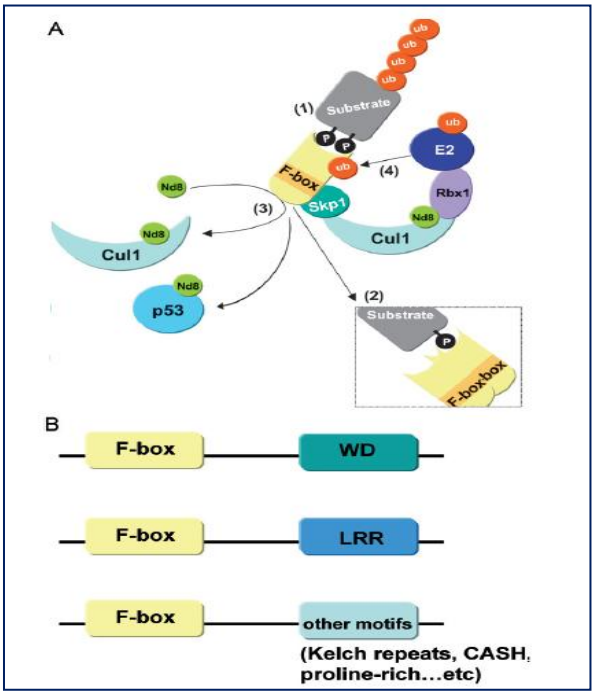

Figure 1.8 F-box protein is a component of SCF E3 ligase complex (Ho et al., 2008). (A) Components of SCF complex. The SCF complex has Cullin1 (Cul1) as a scaffold protein which interacts with Skp1 at its N-terminus and RING domain protein (Rbx) at C-terminus. The interaction of Cul1 with ubiquitin like Nedd8 (Nd8) is important for ligase activity. (B) Typical types of F-box proteins. The F-box domain is located at N terminus and it interacts with Skp1. C-terminus domain contains different domains like WD40, LRR, Kelch repeats etc.

F-box proteins have many diverse functions in plants such as phytohormones responses, organ formation, self incompatibility, floral development, circadian clock and defence responses (Lechner et al., 2006) (Table 1.2)

Table 1.2 Plant and microbial F-box proteins and their functions (Lechner et al., 2006)

F-box proteins	Motif	Substrates	Regulation	Biological Process
TIR1	LRR	Aux/IAA	Auxin binding	Auxin signalling
COI1	LRR	Histone deacetylase?	?	JA signalling
SLY1-SNE-GID2	-	DELLAs	Phosphorylation?	GA signalling
EBF1 and EBF2	LRR	EIN3	?	Ethylene signalling
TLP9	Tubby domains	?	?	ABA signalling?
EID1	Leucine-zipper	?	?	phyA signalling
AFR	Kelch repeats	?	?	
ZTL	LOV/PAS domain & Kelch repeats	TOC1		Circadian clock
FKF1		CDF1	?	
LKP2		?	?	
UFO-FIM	-	?	?	Floral development
MAX2/ORE9	LRR	?	?	Shoot branching, Leaf senescence
ARABIDILLO1 ARABIDILLO2	Arm-repeats	?	?	Lateral root development
CEGENDUO	-	?	?	
SFB/SLF	-	S-RNAses?	?	Self incompatibility
SKP2A	LRR	E2Fc?	Phosphorylation	Cell cycle
SON1	-	?	?	Defence response
CLINK	LxCxE motif	pRB?	?	Host DNA replication
P0	-	?	?	Host RNA silencing

This study adds another ring to the role of F-box proteins in plant defence responses. Until now there are three F-box proteins known to play role in resistance mechanisms. COI1 (CORONATINE INSENSITIVE1) was identified in *Arabidopsis* and coi1 mutants were found to be susceptible to fungal and bacterial pathogens (Penninckx et al., 1998). COI1 homolog in tomato, known as JA1 has a similar function and mutants of ja1 are insensitive to jasmonic acid, which also results in hypersusceptibility (Li et al., 2004). These are F-box proteins that are positive regulators of defence responses. A newly characterized positive regulator F-box protein was identified in rice. Overexpression of OsDRF1 resulted in increased resistance to M. grisea (Cao et al., 2008). F-box proteins also act as a negative regulator in plant pathogen interactions. The mutant of son1 (SUPPRESSOR OF NIM1-1) showed increased resistance to *H. parasitica* (Kim and Delaney, 2002). These results show that F-box proteins can either function as a positive regulator or a negative regulator.

In our studies, gene function analysis of a putative F-box protein in barley against powdery mildew infection was studied, by using BSMV mediated virus induced gene silencing (VIGS). This F-box gene was found to increase in response to yellow rust infection (Bozkurt et al., 2007). We functionally characterized and classified this F-box protein (HvDRF) in this thesis.

1.2.5 BSMV mediated VIGS

VIGS depends on sequence homology and occurs when plants are infected with a virus containing homologous parts to host target gene (Beclin and Vaucheret, 2001). By activating post transcriptional gene silencing (PTGS) machinery, plants normally protect themselves from attacking viruses. This property of plants is utilized as a powerful reverse genetic tool to silence endogenous plant genes and determine their function (Pogue et al., 2002). VIGS studies are highly preferred in gene function studies, because transient silencing of a specific gene *via* VIGS can be achieved in a short time and do not require cell culture, explants formation, testing steps etc. The beauty of this system is that it can be applied to any plants having an efficient infecting virus and it can be applied much easier than obtaining transgenic mutants. VIGS method is also cost effective (Shao et al., 2008).

PTGS mechanism is present in all land plants but it is recently widely understood in monocots. Application of VIGS as reverse genetic tool for monocots was first applied by Holzberg et al., 2001 using barley stripe mosaic virus (BSMV) (Holzberg et al., 2002). Since than BSMV became the virus for silencing in monocots. BSMV is a tripartite RNA containing virus and can infect many agriculturally important monocot species such as barley, wheat etc. BSMV virus has α, β, and γ genome parts. For silencing of endogenous plant genes, the target gene is cloned into γ-genome in either sense or antisense direction and silencing of the target gene can be observed 7-10 days after inoculation of transcripts of each genome part of BSMV to the plant. This technique was applied successfully in gene function studies of powdery mildew resistance genes in barley. They have discovered the roles of genes such as Rar1, Sgt1 and Hsp90, which are known to be critical genes in plant resistance mechanisms (Hein et al., 2005)

1.3 Aim of the study

Pathogens that are infecting agriculturally important plants result in loss of millions of dollars in each year. Understanding the molecular mechanisms underlying resistance mechanisms are very important in order to develop durable resistance mechanisms, which might reduce yield loss.

Powdery mildew and yellow rust are pathogens of barley and wheat, respectively; which are both economically very important crop species. These pathogens are causing dramatic amounts of yield loss in the world and Turkey.

In this study, we aimed to clarify two different branches of plant microbe interactions. In the first part, the role of miRNAs in powdery mildew and yellow rust infection were studied. miRNAs are regulatory elements controlling expression of other genes. As part of the thesis we tried to unravel putative miRNAs having regulatory roles in susceptibility or resistance. In order to perform this, we used compatible (avirulent pathogen race inoculated) and incompatible (virulent pathogen race inoculated) interactions which are resulting disease and resistance phenotypes respectively. By such a strategy we aimed to elucidate the functions of miRNAs in both of these pathways.

In the second part of this thesis, we tried to annotate a function to a putatively identified F-box protein. F-box proteins are known to play important roles in plant physiology and responses to biotic and abiotic stress factors. In our case, we performed a gene level functional study *via* BSMV mediated VIGS to observe the phenotypic changes in powdery mildew infected susceptible and resistance silenced barley cultivars, namely Bulbul and Pallas 01, respectively.

CHAPTER 2

MATERIALS AND METHODS

2.1 Fungal inoculations

2.1.1 Yellow rust infections

The bread wheat cultivar AvoYr1 containing Yr1 resistance gene was used for yellow rust (also known as stripe rust), *Puccinia striiformis f. sp. tritici*, (Pst) infection. The plants were grown for 15 days. These plants were infected with virulent 169E136 (not containing avrYR1) and avirulent 232E137 (containing avrYr1) races of Pst. Infections were made by spreading the spores by using small brushes. The spores that were infected were mixed with 1:3 ratio of talk powder, and spores were heat treated for 5 min at 48 ^{o}C, prior to infections. For each race, mock infections were also performed with talk powder alone treatment. Pathogen treated plants were kept at 10 ^{o}C at extreme humidity for 24 hours without light. Following dark incubation period, plants were kept at 17 ^{o}C, 16 hours day and 8 hours night conditions for infections to take place. The samples were collected at 6, 12, 24, and 48 hours post infection (hpi) and stored at -80 ^{o}C.

2.1.2 Powdery mildew infections

Barley cultivars, Bulbul (universal susceptible), Pallas01 (containingMla1 resistance gene) and Pallas03 (containing Mla6 resistance gene) were used for powdery mildew, *Blumeria graminis f. sp. hordei*, (Bgh) infections. The plants were grown for 10 days, prior to experiments. Bgh103 (containing avrMla1) is used for HvDRF silencing infections. Bgh95 (containing avrMla6) and Bgh103 (containing avrMla1) strains were used for the infections required for miRNA analysis experiments. Plant leaves were plated on 15 % agar plates containing 1% benzimidazole. Agar plates were kept at 60 % humidity for 16 hours light and 8 hours dark period over 10-15 days. For HvDRF silencing experiments, samples were collected and stored 10 days after infection (dai) and 12 dai, and stored at -80 ^{o}C.

On the other hand, for miRNA analysis, time point samples were collected 6, 12, 24 and 48 hpi. and stored at -80 ^{o}C.

Table 2.1 Summary of plants and pathogens used in this thesis.

Plant	Cultivar	Pathogen race used for infection	Time point samples	Experiment
Barley	Bulbul	Bgh103	10,12 dai	HvDRF silencing
	Pallas01	Bgh103	10,12 dai	HvDRF silencing
	Pallas03	Bgh95	6, 12, 24, 48 hpi	miRNA microarray and qRT-PCR analysis
		Bgh103	6, 12, 24, 48 hpi	miRNA microarray and qRT-PCR analysis
Wheat	AvoYr1	232E137	6, 12, 24, 48 hpi	miRNA microarray and qRT-PCR analysis
		169E136	6, 12, 24, 48 hpi	miRNA microarray and qRT-PCR analysis

2.2 RNA isolation from plant leaf tissue

For miRNA expression profiling, expression level determination by qRT-PCR, and HvDRF silencing experiments total RNA isolation was performed.

Total RNAs from wheat and barley were isolated *via* Trizol® reagent (Invitrogen, CA, USA) according to the procedure suggested by the manufacturer. Total RNA samples were isolated from infected and mock treated time point samples of wheat and barley. Firstly, leaf tissues (approximately 100 mg) were powdered in liquid nitrogen in an ice-cold mortar by grinding with a pestle. Powdered tissues were transferred by spatula into 2 mL Eppendorf tubes containing 1 mL Trizol reagent per 100 mg leaf tissue. The collected samples that were homogenized in Trizol, were kept at room temperature for 5-10 minutes. Chloroform (0.2 mL) was added per 1 mL Trizol used, and tubes were shaken vigorously for 15-20 seconds followed by incubation at room temperature for 5 minutes. Then, tubes were centrifuged at 15300 rpm for 15 min at 4 ^{o}C. After centrifugation RNA remains in the upper aqueous phase, which was transferred to a new sterile Eppendorf tube. 0.5 mL ice-cold isopropyl alcohol was used per 1 mL Trizol used for precipitation of RNA. Tubes were incubated for 10 min at room temperature and centrifuged at 15300 rpm for 10 min at 4 ^{o}C. After centrifugation, pellets were visible on the bottom of the tubes. Upper phase was removed and RNA precipitate was washed once with 75 % ice-cold ethanol. The samples were centrifuged at 10000 rpm for 6 min at 4 ^{o}C. The upper phase was decanted and pellets were dried for 5-10 min. Finally the dried pellets were dissolved by adding 30-40 µL PCR grade sterile water and incubating at 50 ^{o}C for 5 min. The suspended RNA samples were either immediately used or stored at -80 ^{o}C

2.3. Characterization of isolated RNA

The isolated RNA sample (1 µL) was used for concentration determination, using NanoDrop ND-1000 spectrophotometer. The integrity of isolated RNA samples was observed on 2 % agarose gels by loading 1-2 µL of the sample. For RNA gel electrophoresis 1X Phosphate Buffer (prepared by combining 13.9 g sodium phosphate monobasic with 500 mL dH_20) were used and renewed at every 20 min during electrophoresis. The sample intactness was analyzed by Agilent 2100 Bioanalyzer using NanoChip system (5067.1511).

2.4 Preparation of isolated RNAs for microarray analysis

The isolated total RNAs (5-8 ug) from time point samples (6, 12, 24 and 48 hpi) of powdery mildew infected and mock treated barley and yellow rust infected and mock treated wheat (Table 2.1) were precipitated with 1/3 volumes of 3M NaOAc (pH 5), and 10 volumes of absolute ethanol. Yellow rust infected wheat total RNAs were bulked by combining equal amount of RNA from each time point for infected and mock treated samples. Powdery mildew infected and mock treated samples were sent separately for miRNA microarray analysis to LC sciences (Control 6, 12, 24, 48 hpi; Bgh95 inf. 6, 12, 24, 48 hpi; Bgh103 inf. 6, 12, 24, 48 hpi).

2.5 miRNA expression profiling

miRNA expression profiling experiments were carried out by LC Sciences, USA. The microarray used for analysis included all the miRNAs found in Sanger miRBase Release 9.2. (http://www.sanger.ac.uk/Software/Rfam/mirna/). Multiple control probes are included in each chip. The control probes are used for quality controls of chip production, sample labeling and assay conditions. Among the control probes, PUC2PM-20B and PUC2MM-20B are the perfect match and single-based match detection probes, respectively, of a 20-mer RNA positive control sequence that is spiked into the RNA samples before labeling. One may assess assay stringency from the intensity ratio of PUC2PM-20B and PUC2MM-20B, which is normally larger than 30. When the option for custom probes is selected, custom probes are also included. The images are displayed in pseudo colors so as to expand visual dynamic range. In the Cy3 and Cy5 intensity images, as signal intensity increases from 1 to 65,535 the corresponding color changes from blue to green, to yellow, and to red. In the Cy3/Cy5 ratio image, when Cy3 level is higher than Cy5 level the color is green; when Cy3 level is equal to Cy5 level the color is yellow; and when Cy5 level is higher than Cy3 level the color is red.

2.6 First strand cDNA synthesis

Prior to first strand cDNA synthesis isolated total RNA samples were DNase treated and purified for qRT-PCR experiments. For DNase treatment 10-15 ug total RNA was mixed with 1 U Turbo DNase (Ambion, USA) and incubated at 37 ^{o}C for 15 min. DNase was heat inactivated by incubation at 65 ^{o}C for 15 min. for purification of total RNA, lithium chloride was used. In order to purify the total RNA samples, 20 µL total RNA, 20 µL sterile water, and 20 µL lithium chloride (7.5 M) was mixed in a sterile

Eppendorf tube and the tubes were incubated at -20 ^{o}C overnight. After overnight incubation, tubes were centrifuged at 15300 rpm at 4 ^{o}C for 15 min. the supernatant was removed by pipetting and the pellets were washed with 70 % ice-cold ethanol. Finally, samples were centrifuged at 15300 rpm at 4 ^{o}C for 10 min and supernatant was decanted. The remaining pellets were dried for 5 min and resuspended in 15 µL sterile water. These cleaned total RNA samples were used for qRT-PCR experiments.

Superscript III reverse transcriptase method was used for first strand cDNA synthesis. For cDNA synthesis 50 pmol oligo dT_{20}, isolated total RNA (500 ng-5µg), 0.1 mM dNTP mix (Fermentas, USA) were mixed in a sterile Eppendorf tube and the volume was completed to 12 µL. The mixture was incubated at 65 ^{o}C for 5 min and quickly transferred to ice for 2 min incubation. 4 µL 5X first strand buffer, 1 µL 0.1M DTT, 1 µL 40 U RNase inhibitor (Invitrogen CA, USA) were added to the mixture on ice. The tubes were mixed and spinned briefly, followed by incubation at 50 ^{o}C for 2 min. Finally 200 U of SuperScript III^{TM} (Invitrogen CA, USA) reverse transcriptase enzyme was added and the tubes were incubated at 50 ^{o}C for 90 min. The enzyme was inactivated by 15 min incubation at 70 ^{o}C.

2.7 Expression level analysis by qRT-PCR

The expression level determination of putative miRNA targets in infected and mock treated samples and HvDRF silenced and empty vector (BSMV:00) and mock treated samples were determined by Stratagene Mx3005p qPCR System using the Brilliant SYBR Green qPCR Master mix (Stratagene, Cat no: 600548) (see Table 2.1). qRT-PCR experiments were carried out as triple replicated for each biological sample. The amount of RNA in each sample was normalized with 18S rRNA primers (X16077.1). The sequences of the primers are 18S Fwd 5'-TTTGACTCAACACGGGGAAA-3' and 18S Rev 5'-CAGACAA ATCGCTCCACCAA-3' targeting 200 base pairs. The

PCR conditions in all q-RT-PCR experiments were 95 ^{o}C 10 min for one cycle; 95 ^{o}C 30 sec, 53 ^{o}C 30 sec and 72 ^{o}C 45 sec for 40 cycles.

2.7.1 Expression level determination of putative miRNA targets

The expression levels of two putative miRNA targets in wheat were determined, MYB3 as the target of miR159/miR319 family microRNAs and WHAP4/WHAP6 as the target of miR169. The primers used for amplification of these targets are given in Table 2.2. The data were analyzed by Pfaffl's model using threshold (Ct) values (Pfaffl and Meyer, 2006). The expression levels were determined by comparing the Ct values of mock treated samples with infected samples (see Table 2.1). According to Pfaffl model Ct value differences between mock treated infected samples correspond to 2^{n} (n = Ct value difference) fold expression level difference.

The expression levels of five putative miRNA targets in barley were determined, Cellulose synthase as the target of miR393, Hsp90 as the target of miR396, GAMYB as the target of miR159, DNAJ like protein as the target of miR1436 and MAP Kinase 2 as the target of miR164. The primers used for amplification of these targets are given in Table 2.2. Ct values of mock treated samples were compared with infected samples for data analysis according to Pfaffl model (see Table 2.1).

Table 2.2 Primers used for miRNA qRT-PCR experiments.

Gene	Accession number	Primer name	Primer Sequence	Product length
Myb transcription factor	TC194473	Myb Fwd Myb Rev	5'-CACCATTTGGGGGTACACTT-3' 5'-TTCACTGACGGAGTTGCTGT-3'	180
WHAP4-WHAP6 transcription factor	TC223902 TC208778	Whap Fwd Whap Rev	5'-AGTGTCCGGGATGAGTGAAG-3' 5'-ATATGGCGAAGGGATGAGTG-3'	193
GAMyb	TC147900	GAMyb Fwd GAMyb Rev	5'-CCTTTTTAAATGGCACCTTC-3' 5'-GACTGCATGTACGGATCAAC-3'	185
Cellulose synthase	TC139386	Cell s. Fwd Cell s. Rev	5'-AGAAAGGTTCCCATTCCTTC-3' 5'-TGTCGAACCTCAATGTCAAC-3'	196
Hsp90	TC131381	Hsp90 Fwd Hsp90 Rev	5'-ACTCCACCAAGAGTGGTGAT-3' 5'-TGACCTCATAGCCCTTCTTC-3'	190
DNA J protein	TC130805	DNA J Fwd DNA J Rev	5'-AGGATGTTGTCCATCCACTT-3' 5'-CACCTGCTGTATCATGGAAG-3'	177
MAP kinase 2	TC139947	MAPK Fwd MAPK Rev	5'-CTGCCTTCGTATCCCTCAT-3' 5'-AGTAGTGCTTGCCATGGTTT-3'	182

2.8 BSMV mediated virus induced gene silencing

BSMV (barley stripe mosaic virus) vectors pα, pβΔβa, pγ and pγ.bPDS4 sense and pγ.bPDS4 anti-sense were obtained from Large Scale Biology Corporation. The maps of the vectors are given in Figure 2.1. The sequences of plasmids are given in Appendix A

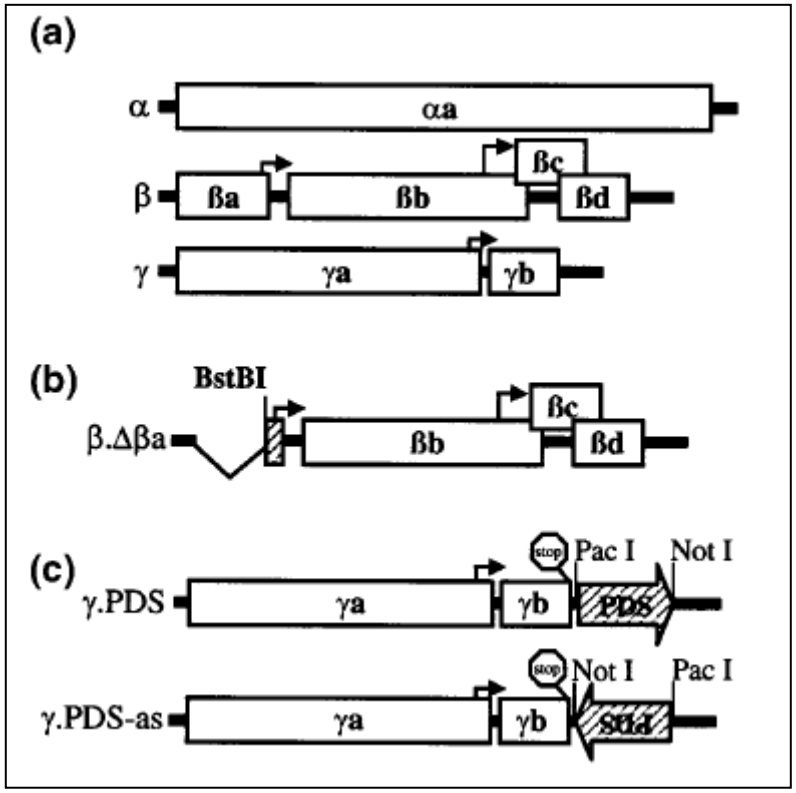

Figure 2.1 Genomic organization of BSMV (Holzberg et al., 2002). Map of tripartite genome of BSMV virus **(a)**. Synthesis of βΔβa by deleting a coat protein from BSMV RNA β, which enables more efficient silencing **(b)**. Genomic organization of BSMV RNA γ, modified top express PDS in sense and antisense direction **(c)**.

2.8.1 Silencing of HvDRF gene in barley

2.8.1.1 Amplification of HvDRF gene from barley cDNA

The full length of HvDRF (FJ913272) gene was obtained in Akkaya laboratory in previous studies. To silence HvDRF gene, a fragment in the 3` UTR (untraslated region) is amplified from barley cDNA. Amplification was performed by forward and reverse primers having NotI and PacI restriction sites at the ends, respectively. The sequences of the primers were HvDRF Fwd 5`- ATAGCGGCCGC CAAATTAGACCTTTCA-3' and HvDRF Rev 5`-ATATTAATTAA GACCCA ACCATATCTCAC-3' (ATA sequence at the beginning of primers are needed for activity of restriction enzymes. The restriction sites are highlighted). For amplifying HvDRF fragment, touchdown extension PCR was performed. The PCR conditions were 94 ^{o}C 2 min for one cycle; 94ºC 1 min, 60ºC 1 min, 72ºC 1 min for 1 cycle; 94ºC 1 min, 59ºC 1 min, 72ºC 1 min for 1 cycle; 94ºC 1 min, 58ºC 1 min, 72ºC 1 min for 1 cycle; 94ºC 1 min, 57ºC 1 min, 72ºC 1 min for 1 cycle and 94ºC 1 min, 56ºC 1 min, 72ºC 1 min for 35 cycles. The PCR components were 2 µL 1/20 diluted barley cDNA, 5 µL 10 X PCR buffer (Fermentas, USA), 1 µL 10 mM dNTP mix (Fermentas, USA), 1,5 mM $MgCl_2$ (Fermentas, USA), 0.4 µL 5 U *Taq* Polymerase (Fermentas, USA), 10 pmol forward primer and 10 pmol reverse primers. Final PCR volume was completed to 50 µL with PCR water.

Amplified products were analyzed on 1 % agarose gel. 185 bp amplification products from several PCRs were gel purified and ligated into pGEMT-Easy vector for further cloning experiments and sequencing.

2.8.1.2 Gel extraction of amplified HvDRF fragments

Gel extraction was made according to Qiagen, Qiaquick Gel Extraction Protocol. The amplified fragments that are in correct length (185 bp) were excised with a clean scalpel and weighed. Buffer QG (3 volumes) were added per one volume gel and the content was incubated at 50 ºC for 10 min, until all the agarose was dissolved. 1 gel volume isopropanol was added to the dissolved agarose mix and the solution was transferred to QIAquick columns which was followed by 1 min centrifugation at 10000 g. flow-through was discarded and 0.75 mL Buffer PE was added. Flow-through was discarded and columns were centrifuged one more time for 1 min at 10000 g. For eluting DNA, 50 µL Buffer EB was added, and centrifuged at 10000 g for 1 min, after 3 min of incubation at room temperature.

2.8.1.3 Ligation of Engineered HvDRF gene fragments into pGEMT-Easy vector

Amplified PCR products having *Not*I and *Pac*I cut sites at the ends were ligated by following reaction components: 5 ng pGEMT-Easy vector (Promega, USA), 1X Ligation Buffer (Promega, USA), 2 U of T_4 DNA Ligase (Promega, USA), 6 µL of PCR product. Ligation mixture was briefly spinned and incubated overnight at 4°C.

2.8.1.4 Transformation of pGEMTe-HvDRF into *E. coli*

Prior to transformation, *E. coli* DH5α cell were made competent. To prepare competent cells a single bacterial colony was incubated in 2 mL LB medium (5 g Tryptone, 2.5 g NaCl, and 2.5 yeast extract dissolved in 500 mL distilled water) and grown overnight at 37°C with shaking at 250 rpm. Overnight grown bacteria were transferred to ice for 30 min. Then the cells were centrifugated at 4000 rpm for 10 min. Supernatant was decanted and the cells were resuspended in 5 mL ice-cold 4 mM $CaCl_2$. After the first resuspension they were again centrifuged at 4000 rpm for 5 min and resuspended in 2 mL ice-cold 4 mM $CaCl_2$. The last step is repeated for one more time. This procedure makes the cells competent and they can be used for transformation up to two weeks.

These competent cells were transformed by the ligation product (pGEMTe-fHvDRF). 10 µL of ligation reaction was mixed with 100 µL of competent cells in a sterile Eppendorf tube. The mixture was incubated on ice for 30 min. then heat shock was applied for 45 sec. at 42 °C. After heat shock the mixture was transferred to ice without shaking and incubated for 2 min. The volume was completed to 200 µL by addition of LB medium. This mixture was spreaded on agar plates containing 1ug/1L ampicilin and grown overnight at 37 °C. A day later, the colonies that grew on the plates were analyzed with colony PCR to confirm transformation.

2.8.1.5 Colony PCR of pGEMTe-HvDRF containing *E. coli* cells

The positive colonies that grew on ampicilin containing LB-agar, were used in colony PCR experiments as templates. Since F-box genes are unique to eukaryotes, F-box primers that were used for constructing silencing vectors were used to confirm transformation. Thermal conditions of colony PCR were: 3 min at 94°C for one cycle; 1 min at 94°C, 1 min at 53°C and 1 min at 72°C for 35 cycles and 5 min at 72°C. The PCR components were 1 loop of colony, 1 µL 10 mM dNTP mix (Fermentas, USA), 5 µL 10X PCR buffer (Fermentas, USA), 1.5 mM $MgCl_2$, 0.4 µL 5 U *Taq* Polymerase (Fermentas, USA), 1 µL forward primer and 1 µL reverse primer. The final volume was completed to 50 µL by adding PCR water. The colony PCR products were analyzed at 1 % agarose gel.

2.8.1.6 Plasmid isolation from selected colonies

Plasmids were isolated using QIAGEN QIAprep Spin Miniprep Kit (Cat no: 27104) according to the manufacturers protocol. The positive colonies were grown in 5 mL LB-ampicilline (1ug/1L) for overnight at 37°C with shaking at 250 rpm. These cultures were harvested by centrifugation for 2 min at 14000 rpm. The supernatant was decanted and 250 µL Buffer P1 (RNase added (100 ug/mL)) was added onto the pellet. The mixture was vortexed until no visible cell debris was observable. Then the mixture in Falcon tubes were transferred to sterile Eppendorf tubes. 250 µL Buffer P2 was added and the content was mixed by inverting 5-10 times. After 5 min of incubation at room temperature Buffer N3 was added and the solution was again mixed by inverting 5-10 times, which followed by centrifugation at 14000rpm for 10 min. The supernatant was transferred to a spin column which was placed in a collection tube. Then the solution was centrifugated for 1 min at 14000 rpm. Flow through was discarded and

spin column were washed with 750 µL Buffer PE. To remove the residual PE buffer, spin column was washed for one more time by centrifugation at 14000 rpm for 1 min. Then the column was transferred to a new sterile Eppendorf tube. To elute the plasmids that were remained in the spin column, 30 µL Elution Buffer was added and the column was incubated at room temperature for 3 min. Then plasmids were collected by centrifugation at 14000 rpm for 1 min, into fresh tubes.

2.8.1.7 Ligation of HvDRF fragment γ vectors in sense and antisense direction

The pGEMTe-fHvDRF, pγ-PDS4 antisense and pγ-PDS4 sense plasmids were double digested with NotI and PacI restriction enzymes. Double digestions were performed by incubation of the digestion mixture at 37°C for 4 hours. The mixture contained 10 U *Not*I and *Pac*I, 1X NEB2 Buffer and 3 ug of plasmids. The digestion products were analyzed by running on 1 % agarose gel. HvDRF fragment and pγ-antisense and pγ-sense vectors were gel purified. Purified HvDRF fragment was ligated with vectors. Ligation was performed as in Section 2.8.1.2. Ligation products were transformed into competent *E. coli* as in Section 2.8.1.3. Positive colonies were selected and confirmed by colony PCR as in 2.8.1.4. pγ-HvDRF sense and pγ-HvDRF antisense plasmids were isolated as in Section 2.8.1.5.

2.8.1.8 Linearization of BSMV vectors

Plasmids pα, pβΔβa, pγ and pγ.fHvDRF were digested with restriction enzymes prior to *in vitro* transcription. For linearization of pα was digested with *Ml*uI enzyme (MBI fermentas), pβΔβa was digested with *SpeI* enzyme (MBI fermentas), and pγ and pγ.fHvDRF were digested with *BssHII* enzyme (New England Biolabs). For each

digestion 10 U restriction enzyme, 1X enzyme buffer, and 10 ug plasmid DNA were mixed in a sterile Eppendorf tube. The volume was completed to 50 µL, by adding sterile water. Then, pα and pβΔβa tubes were incubated at 37 °C and pγ and pγ.fHvDRF tubes were incubated at 50 °C for 3 h. after incubation the linearization products were observed in 1 % agarose gel and the linearized plasmids were gel purified as in 2.8.1.2.

2.8.1.9 *In vitro* Transcription of linearized Vectors

All of the linearized plasmids were *in vitro* transcribed according to the manufacturer`s protocol, mMessage mMachine T7 *in vitro* transcription kit (cat no: 1340, Ambion, Austin, TX). For one reaction, 80 ng linearized plasmid, 1X Buffer (Ambion, USA), 1X nucleotide mix with NTP Cap (Ambion, USA), 0.15 µL T7 RNA polymerase mix (Ambion, USA) were mixed in a sterile Eppendorf tube. The volume was completed to 1.5 µL and the content was incubated at 37 °C for 2 hours.

2.8.1.10 Inoculation of plants with BSMV transcripts

Second leaves of 10-day old Bulbul and Pallas01 barley plants were inoculated with the transcripts. Transcripts of each BSMV RNA were mixed in 1:1:1 ratio (1.5 µg of each transcript). For mock treatment, only FES was spreaded onto leaves. For emptye vector control (BSMV:00) pγ was mixed with other vectors; and for HvDRF silencing pγ:HvDRF was mixed with other vectors. Transcript mix was mixed with 45 µL FES ((50 ml 10X GP (18.77 g Glycine, 26.13 g K_2HPO_4, dd$H_2$0 upto 500 ml, autoclave 20 min), 2.5 g Sodium pyrophosphate, 2.5 g Bentonite, 2.5 g Celite and dd$H_2$0 up to 250 ml (Pogue et al., 1998)), and directly applied to the leaves, starting from the bottom of

the leaves. The viral symptoms (stripes) were apperant 10 days after inoculation. For determination of silencing level by qRT-PCR, silenced leaf samples were collected 14 days after inoculation. Total RNA was isolated from these leaves as in 2.2 and cleaned as in 2.6. 10 days after inoculation of transcripts plant leaves were transferred to agar plates and infected with Bgh103.

2.8.1.11 Trypan blue staining of fungi inoculated silenced and unsilenced plants

Trypan blue staining is used for determination of fungal structures. 10 day after Bgh103 infection silenced and unsilenced Bulbul and Pallas01 plants were observed after trypan blue staining. Trypan blue staining was performed by boiling plant leaf samples in lactophenol typan (20 ml of ethanol, 10 ml of phenol, 10 ml of water, 10 ml of lactic acid (83%), and 10 mg of trypan blue) for 2 min, and decolorization with chloral hydrate (2.5 g chloral hydrate dissolved in 1 L water) by incubating overnight. The stained samples were observed under light microscope, Leica, DFC 280.

2.8.1.12 Expression level determination of HvDRF

The total RNA isolation and first strand cDNA synthesis was performed as in 2.2 and 2.6 respectively. The silencing was quantified by comparing the expression level of HvDRF fragment in silenced and control samples (BSMV:00 treated and FES treated). For HvDRF expression level determination the primers HvDRF Fwd 5'-GACCCAACC ATATCTCAC-3' and OligodT_{20} were used.

CHAPTER 3

RESULTS AND DISCUSSION

3.1 Investigating the role of microRNAs in plant-pathogen interactions

miRNAs are found to be playing important roles in plant-microbe interactions (Figure 1.4). Besides bacterial infections, in order to investigate the role of miRNAs in plant-fungal interactions, microarray expression profiling followed by qRT-PCR analysis of AvoYr1 wheat plants, inoculated with avirulent (232E137) and virulent (169E136) strains of *Puccinia striiformis f. sp. tritici* (Pst) and Pallas01 barley plants, inoculated with avirulent Bgh95 and virulent Bgh103 strains of *Blumeria graminis f. sp. hordei* (Bgh) was performed.

3.1.1 MicroRNAs in yellow rust-wheat pathosystem

For yellow rust-wheat pathosystem AvoYr1 plants were infected with avirulent and virulent Pst strains and time point samples after infection were collected. These time point samples were used for miRNA profiling and expression level determination of putative miRNA targets.

3.1.1.1 Total RNA isolation from AvoYr1 wheat plants infected with virulent and avirulent Pst races.

Total RNA was isolated from time point samples (6, 12, 24, and 48 hours post inoculation (hpi)) of AvoYr1 wheat plants inoculated with avirulent (232E137) and virulent (169E136) strains of Pst. These RNA samples were tested for intactness (Figure 3.1).

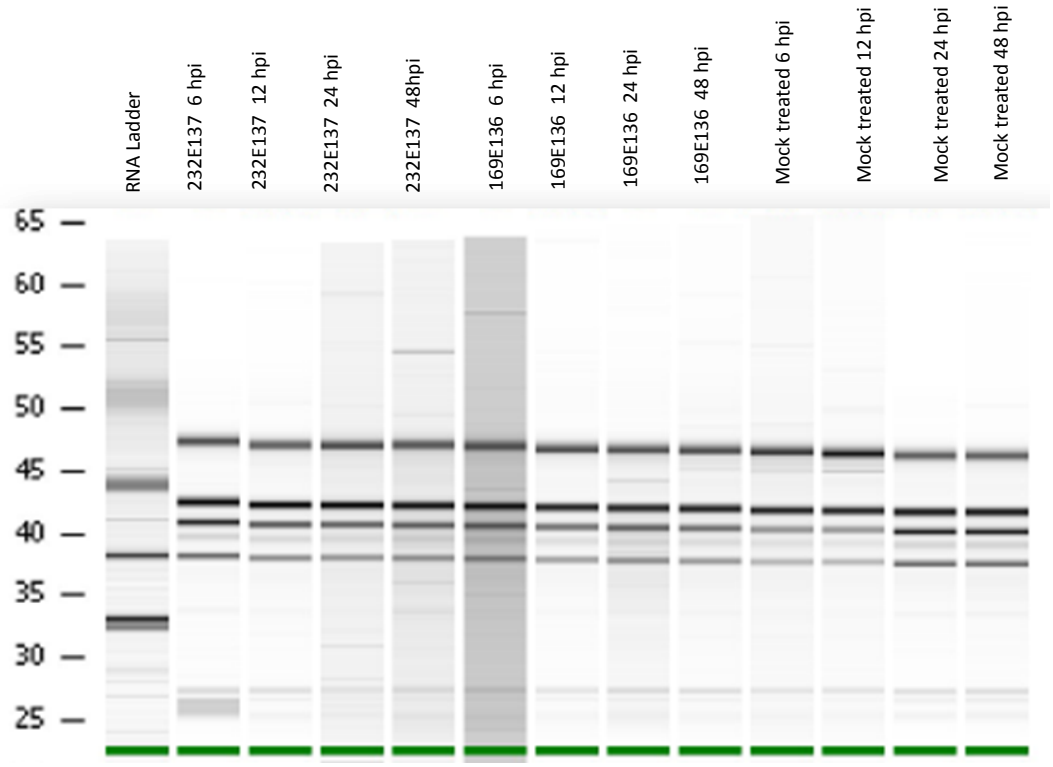

Figure 3.1 Characterization of RNAs isolated from time point samples of Pst infected AvoYr1 plants on Agilent Bioanalyzer 2100.

Isolated total RNA samples have four bands (23 S rRNA, 18 S rRNA, 16 S rRNA, 5 S rRNA) and no smear which are characteristics of an intact plant total RNA, meaning these RNAs can be used for further experiments.

3.1.1.2 miRNA expression profiling of yellow rust infected wheats

After confirming that isolated total RNAs are intact, they were prepared for LC Sciences MicroRNA Expression Profiling Service as described in 2.2. There are only 32 miRNAs annotated in miRBase for wheat. However, since plant miRNAs are highly conserved, performing such a microarray analysis might give us important clues about wheat-yellow rust pathosystem. The samples were labeled with Cy3 and Cy5 and the color was changed with changing intensity (Figure 3.2). The control probes were appearing as the most intense bands on the arrays.

The data was analyzed with student`s t-test for enabling comparison of compatible and incompatible interactions. Student`s t-test resulted in about 80 miRNAs differentially expressed in yellow rust infected wheat plants (Table 3.1) (Appendix C).

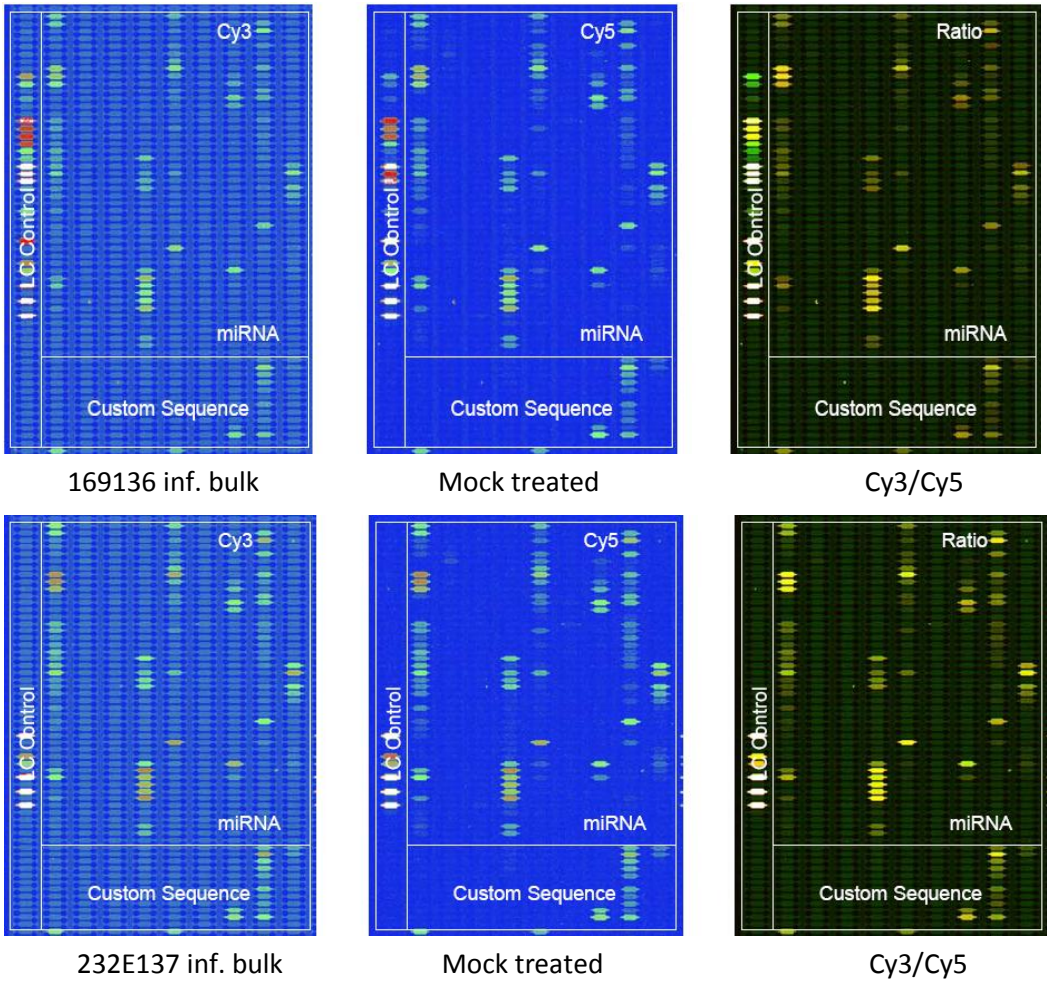

Figure 3.2 miRNA expression profile of in Pst infected AvoYr1 plants. The microarray chip contained all the plant miRNAs found in miRBase 9.2 (http://www.sanger.ac.uk/Software/Rfam/mirna/). In each chip there are multiple control probes and all chips are controlled with these probes for chip quality, sample labeling and assay production. Samples are labeled with Cy3 and Cy5 fluorophores and differential expression can be understood by colour changes in the array images. The colors of the fluorophores change with intensity. When Cy3 labeled sample has higher level than Cy5 labeled sample the color is green, for the reverse case the color is red, when they have equal levels the color is yellow.

Table 3.1 Student`s t-test results of miRNA expression profiling of yellow rust infected wheat. The results are average signal ratios of avirulent (232E137) and virulent (169E136) Pst infected AvoYr1 wheat plants.

miRNA ID	232E137 infected samples`s signal	169E136 infected sample`s signal
Ath-miR169b	1,011	704
Ath-miR169a	888	599
Ppt-miR894	7,189	10,161
Sof-miR159e	3,159	4,690
Zma-miR169e	185	11
Ath-miR169h	1,004	696
Ath-miR167d	2,758	2,270
Ptc-miR169o	952	645
Osa-miR164d	2,040	1,711
Ptc-miR159f	1,684	3,341
Ath-miR167a	2,687	2,301
Osa-miR159f	18,750	17,070
Osa-miR159a	20,777	18,769
Zma-miR162	25	0
Ptc-miR172i	45	13
Osa-miR393b	1,947	1,635
Ppt-miR896	441	655
Sbi-miR164c	2,575	2,156
Osa-miR164c	2,344	2,042
Osa-miR396d	15,672	13,981
Ath-miR167c	1,612	1,347
Ptc-miR395a	18	3
Ptc-miR397b	20	0
Sof-miR168b	13,392	11,805
Ptc-miR167f	2,964	2,469
Ath-miR169d	976	752
Ppt-miR319c	2,290	3,135

Table 3.1 cont`d

Osa-miR395b	114	63
Osa-miR167d	3,086	2,665
Sbi-miR172a	51	22
Ath-miR390a	45	25
Ath-miR823	32	61
Osa-miR164e	3,173	2,856
Ath-miR156h	281	561
Ptc-miR482	32	12
Ppt-miR1219a	35	15
Osa-miR528	73	124
Mtr-miR395a	115	60
Ath-miR828	7	24
Osa-miR169e	942	754
Sbi-miR166a	915	705
Ath-miR826	23	44
Ath-miR399b	75	120
Sof-miR408e	25	4
Sbi-miR171f	74	28
Ppt-miR319a	5,203	6,249
Sbi-miR172b	48	19
Ath-miR834	21	40
Gma-miR319a	3,251	3,724
Ptc-miR166p	225	327
Ath-miR394a	63	41
Osa-miR166k	987	843
Ath-miR867	26	53
Ath-miR157d	195	341
Osa-miR168a	14,876	13,104
Ptc-miR156k	2,579	3,129
Ptc-miR319i	39	17
Ath-miR395a	66	40
Ath-miR160a	102	154

Table 3.1 cont`d

Ptc-miR169s	846	701
Ath-miR825	15	35
Ath-miR827	42	196
Osa-miR395c	70	36
Bna-miR393	2,092	1,901
Ptc-miR169a	49	96
Ath-miR853	12	31
Osa-miR159d	12,474	11,763
Ath-miR157a	279	410
Osa-miR441a	5	28
Ptc-miR474c	54	33
Osa-miR435	28	45
Gma-miR156b	2,882	3,368
Ath-miR400	20	46
Osa-miR169d	41	92
Ath-miR830	27	55
Osa-miR395o	71	32
Ath-miR395b	69	45
Osa-miR807a	20	6

The abbrev*ia*tions at the beginning of each miRNA are suffixes of plants: Ath: *Arabidopsis thaliana*, Osa: *Oryza sativa*, Ptc: *Populus tricocarpa*, Bna: *Brassica napus*, Gma: *Glycine max*, Mtr: *Medicago truncatula*, Sof: *Saccharum officinarum*, Sbi: *Sorghum bicolor*, Ppt: *Physcomitrella patens*, Zma: *Zea mays*

The microarray results showed that miRNA expression levels were changing upon pathogen infection and they may have pivotal roles in plant disease responses. An increase in miRNA level might result in a decrease in its target and that miRNA might play a role in either susceptibility or resistance responses. In order to hypothesize a model the target of differentially expressed miRNAs were investigated. Plant miRNAs show high complementarities to their targets, which enable the identification of

possible miRNA targets using BLAST based bioinformatic tools. For this purpose we used Plant miRNA Target Finder (http://bioinfo3.noble.org/psRNATarget/) and identified the possible targets of these miRNAs in wheat genome (TAGI Release 9). The analysis resulted in at least one target in 27 of 80 miRNAs (Table 3.2), including MAPK proteins, WHAP type transcription factors, MYB3 transcription factor etc. MAP kinases are well known regulatory elements of plant physiology (Mishra et al., 2006; Zhang et al., 2006) and stress responses against abiotic and biotic stress factors (Wrzaczek and Hirt, 2001; Yu and Tang, 2004). MBY transcription factors and WHAP4/6 transcription factors are also playing important regulatory roles especially in biotic stress responses (Eulgem, 2005; Du et al., 2009).

Table 3.2 Identified targets of differentially expressed miRNAs in yellow rust infected AvoYr1 plants. The targets were identified by using "Plant miRNA Target Finder".

miRNA ID	**miRNA Targets**	
Ath-miR169b	CCAAT-box transcription factor complex WHAP4	CCAAT-box transcription factor complex WHAP6
Ath-miR169a	CCAAT-box transcription factor complex WHAP4	CCAAT-box transcription factor complex WHAP6
Sof-miR159e	Cytosolic aldehyde dehydrogenase	
Ath-miR169h	CCAAT-box transcription factor complex WHAP4	CCAAT-box transcription factor complex WHAP6
Ptc-miR169o	CCAAT-box transcription factor complex WHAP4	CCAAT-box transcription factor complex WHAP6
Osa-miR164d	MAP kinase 2	

Ptc-miR159f	Transcription factor Myb3	

Table 3.2 Cont`d

Osa-miR159f	Transcription factor Myb3	
Ptc-miR172i	NL43 Nonspecific lipid-transfer protein 4.3 precursor (LTP 4.3)	
Osa-miR164c	MAP kinase 2	
Ptc-miR397b	Gamma-glutamylcysteine synthetase	
Ath-miR169d	CCAAT-box transcription factor complex WHAP4	CCAAT-box transcription factor complex WHAP6
Ppt-miR319c	Transcription factor Myb3	
Osa-miR164e	MAP kinase 2	
Osa-miR169e	CCAAT-box transcription factor complex WHAP4	CCAAT-box transcription factor complex WHAP6
Ppt-miR319a	Transcription factor Myb3	
Ath-miR834	Alcohol dehydrogenase	BZIP transcription factor ZIP1
Gma-miR319a	Transcription factor Myb3	
Ptc-miR319i	Transcription factor Myb3	PISTILLATA-like MADS box protein
Ath-miR395a	Gamma-gliadin	Ribosomal protein L19
Ptc-miR169s	CCAAT-box transcription factor complex WHAP4	CCAAT-box transcription factor complex WHAP6
Ath-miR827	RAB1Y	
Ptc-miR169a	CCAAT-box transcription factor complex WHAP4	CCAAT-box transcription factor complex WHAP6

Ath-miR853	Glycoprotein	

Table 3.2 Cont`d

Osa-miR159d	Lipid transfer protein	Transcription factor Myb3
Ath-miR157a	Trypsin/alpha-amylase inhibitor CMX1/CMX3 precursor	60S ribosomal protein L18a
Osa-miR169d	CCAAT-box transcription factor complex WHAP4	CCAAT-box transcription factor complex WHAP6

The abbrev*ia*tions at the beginning of each miRNA are suffixes of plants: Ath: *Arabidopsis thaliana*, Osa: *Oryza sativa*, Ptc: *Populus tricocarpa*, Bna: *Brassica napus*, Gma: *Glycine max*, Mtr: *Medicago truncatula*, Sof: *Saccharum officinarum*, Sbi: *Sorghum bicolor*, Ppt: *Physcomitrella patens*, Zma: *Zea mays*

The targets identified by the bioinformatic software are compatible with the general nature of miRNA effect. miRNAs generally control transcription factors which control expression of other genes. So these targets may have important roles in resistance to yellow rust infection. Since miRNAs generally lead to cleavage of their targets, the levels of "in silico" determined targets were analyzed by qRT-PCR.

3.1.1.3 Expression level determination of possible miRNA targets

To determine the levels of targets, first of all, infected and control RNAs are cleaned and treated with DNase to prevent any DNA contamination. Then cDNA is synthesized from mock treated and time point samples of both virulent and avirulent spore inoculated AvoYr1 wheat plants. These cDNAs are normalized by using 18S rRNA gene specific primers and three technical repeats are performed for each biological sample (Figure 3.4). 18S rRNA gene is constitutively expressed in plants and found to be a suitable internal control for qRT-PCR experiments (Bozkurt et al., 2007).

First, the normalization primers are controlled by looking at their dissociation curves. In order to be able to use these primers, they should have only one peak in their dissociation curves, which means primers are not forming dimers with each other and amplify only a unique site in barley or wheat genome (Figure 3.3).

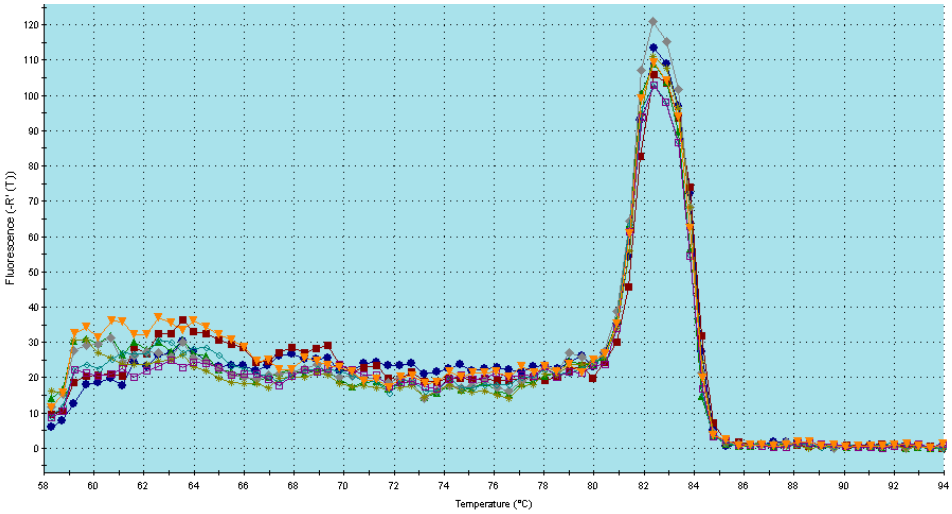

Figure 3.3 The dissociation curve of 18S rRNA primers. Dissociation curves of the primers in time point samples of 232E137 infected, 169E136 infected and mock treated samples.

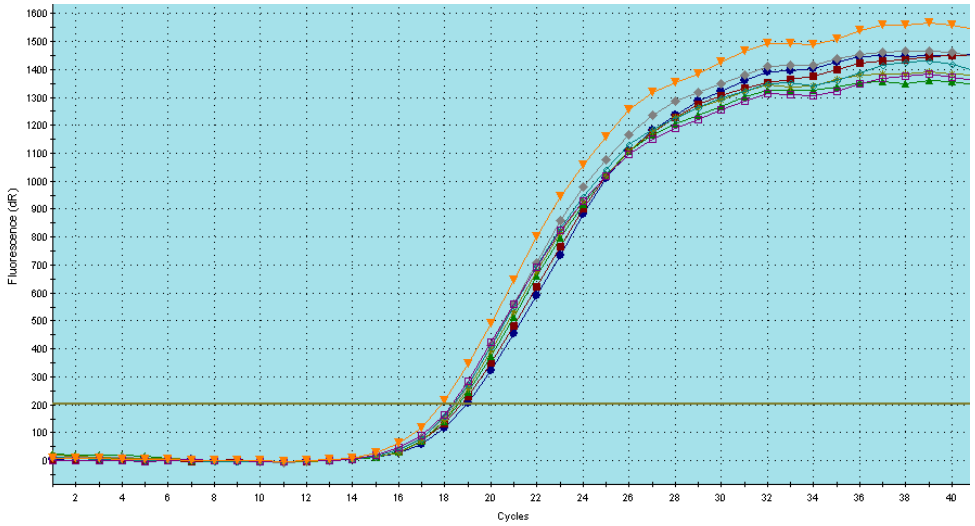

Figure 3.4 Amplification plot of yellow rust infected and mock treated samples. Normalization of 232E137 infected, 169E136 infected and mock treated time point samples (6, 12, 24, 48 hpi) of each group.

The time point samples of 232E137 infected, 169E136 infected and mock treated plants after normalization reactions, the expression levels of putative miRNA target genes were determined. There are 27 targets determined "in silico" by "Plant miRNA Target Finder". The two most important ones were selected for qRT-PCR experiments: MYB3 transcription factor which is the putative target of miR159/miR319 family microRNAs and WHAP4/WHAP6 transcription factor which is the target of miR169 family microRNAs. These genes are found to play important roles in plant pathogen interactions (Asselbergh et al., 2008) and in this study a new control circuit for their expression controlled by miRNAs in wheat-yellow rust interaction. are tried to be investigated.

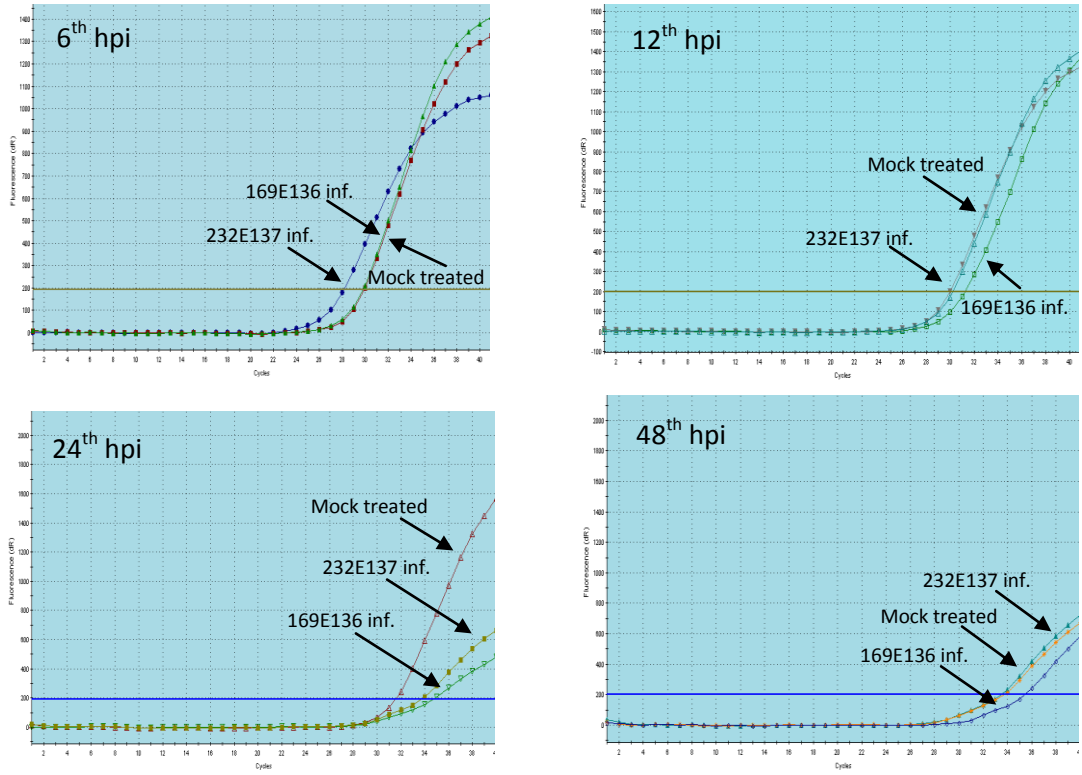

Figure 3.5 Expression level of MYB3 transcription factor at time point samples of 232E137 infected, 169E136 infected and mock treated AvoYr1 wheat plants. Average values of 3 technical repeats were given.

Table 3.3 Expression level changes of MYB3 transcription factor in compatible and incompatible interaction (↓: decrease, ↑: increase, N.C: No change).

Pathogen	**6 hpi**	**12 hpi**	**24 hpi**	**48 hpi**
232E137 (avirulent) infected	3 ↑	N.C	4 ↓	N.C
169E136 (virulent) infected	N. C	2.3 ↓	5↓	3.6 ↓

MYB3 transcription factor level is found to be decreasing after 12 hpi in virulent spore inoculated plants, which might mean that pathogen is suppressing MYB3 transcription factor in order to colonize on the plant. On the other hand there is not such a regular pattern observed in avirulent spore inoculated plants (Figure 3.5) (Table 3.3).

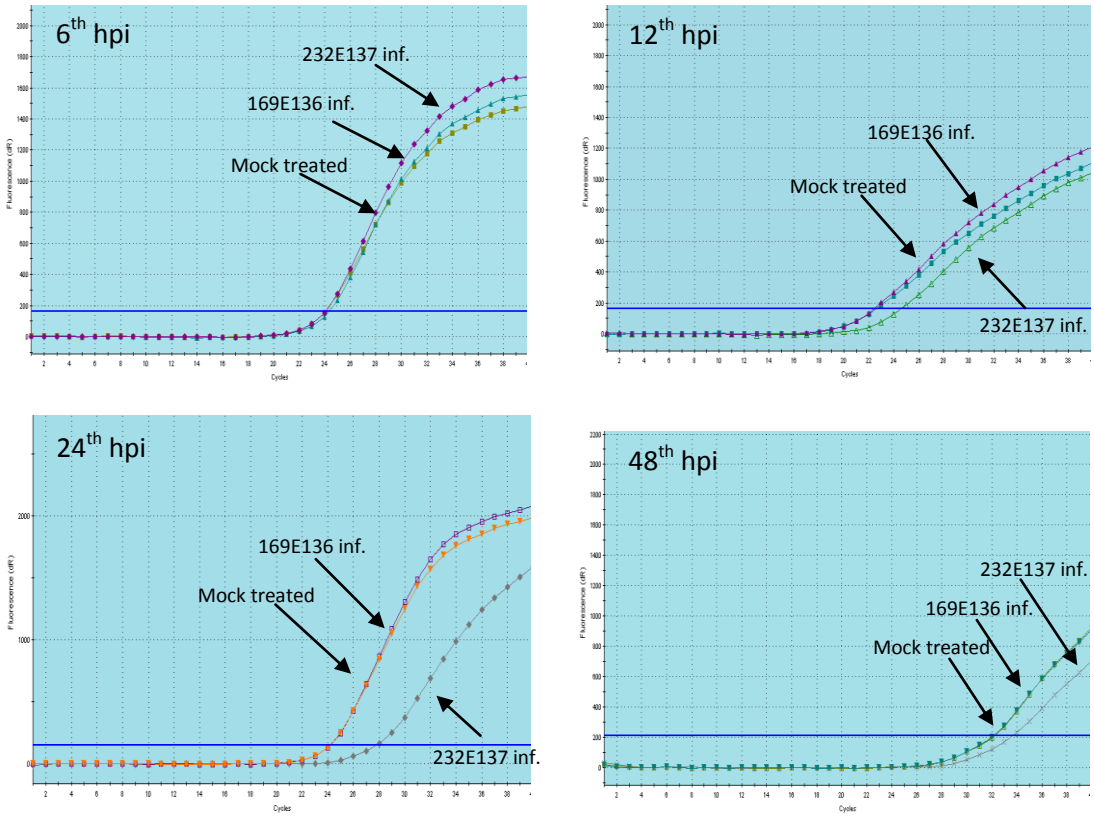

Figure 3.6 Expression level of WHAP4/6 transcription factor in time point samples of 232E137 infected, 169E136 infected and mock treated AvoYr1 wheat plants. Average values of 3 technical repeats were given.

Table 3.4 Expression level changes of WHAP4/6 transcription factor in compatible and incompatible interaction (↓: decrease, ↑: increase, N.C: No change).

Pathogen	6 hpi	12 hpi	24 hpi	48 hpi
232E137 (avirulent) infected	N.C	4 ↓	8 ↓	2 ↓
169E136 (virulent) infected	N.C	N.C	N.C	N.C

WHAP4/6 transcription factor does not change in susceptible condition. However it is decreasing in resistance condition after 6^{th} hpi. It seems that WHAP4/6 transcription factor is suppressed for activating disease resistance responses (Figure 3.6) (Table 3.4).

3.1.1.4 Identification of putative miRNAs *via* expression profiling in yellow rust

To search for possible miRNAs in pathogen itself, total RNAs of two different spores were isolated; quality checked and sent for miRNA microarray analysis. Interestingly there were some miRNAs giving hybridization signals in yellow rust spores (Table 3.5) (Appendix C).

Table 3.5 miRNA microarray analysis results of yellow rust spores. The analysis in spores R41 and R67 gave 7 miRNAs belonging to two families. Ath: *Arabidopsis thaliana*, Ptc: *Populus tricocarpa*.

miRNA ID	R41	R67
Ath-miR854a	1153.12	2452.53
Ath-miR854b	1228	2564.68
Ath-miR854c	1193.21	2664.11
Ath-miR854d	1301.77	2599.15
Ptc-miR474a	10930.07	7394.63
Ptc-miR474b	10788.46	6435.4
Ptc-miR474c	10895.23	6830.56

In plants resistance pathways are discovered to have quite similar players between different plant species. So, in order to generalize the hypothesis that is established in yellow rust-wheat interaction, another pathosystem, powdery mildew-barley, was investigated.

3.1.2 MicroRNAs in powdery mildew-barley pathosystem

3.1.2.1 Total RNA isolation from Pallas03 barley plants infected with virulent and avirulent Bgh races.

As in the yellow rust-wheat system, Pallas03 barley plants were infected with avirulent (Bgh95), and virulent (Bgh103) strains of *Blumeria graminis*. Total RNAs were

isolated from time point samples (6, 12, 24, and 48 hpi) of both compatible and incompatible interactions and checked for integrity and quality (Figure 3.7).

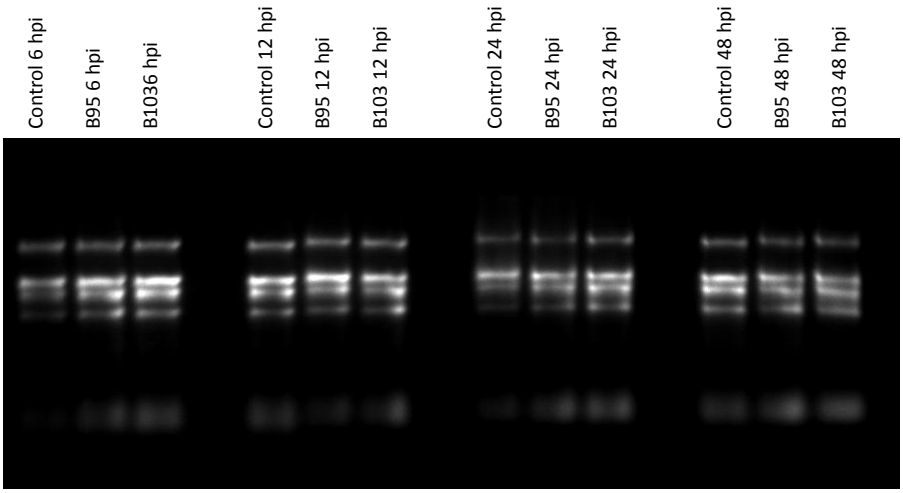

Figure 3.7 Characterization of RNAs isolated from mock treated, and infected Pallas01 plants.

3.1.2.2 miRNA expression profiling of powdery mildew infected barleys

After being satisfied by the quality of RNAs isolated from time points of both infected and mock treated barley samples, they were sent to LC Sciences Company for miRNA Expression profiling. Each time points were sent to analysis separately, meaning there were 8 chips analyzed (Control 6 hpi vs B95 hpi; Control 6 hpi vs B103 6 hpi and so on). By this strategy, the roles of miRNAs at different stages of both susceptibility and resistance mechanisms were attempted to be investigated. Also, in order to increase the reliability, three biological replicates were analyzed for differential miRNA expression (Table 3.6) (Appendix C).

Table 3.6 Paired t-test results of miRNA expression profiling of powdery mildew infected barley.

6 hpi

miRNA ID	Bgh103 infected	Bgh95 infected
Pta-miR319	587	437
Ath-miR167a	297	243
Tae-miR1125	28	23

12 hpi

miRNA ID	Bgh103 infected	Bgh95 infected
Vvi-miR166c	1153.12	2452.53
Ppt-miR1041	1228	2564.68
Osa-miR168b	1193.21	2664.11
Ptc-miR166n	1301.77	2599.15
Ptc-miR167h	10930.07	7394.63
Osa-miR319a	10788.46	6435.4

24 hpi

miRNA ID	Bgh103 infected	Bgh95 infected
Sbi-miR156e	795	542
Osa-miR159d	4,322	4,025
Ath-miR156g	945	699
Osa-miR168a	797	1,217
Osa-miR396d	478	769
Osa-miR156l	612	356
Ath-miR156a	938	704
Bna-miR156a	837	622
Ath-miR159b	7,590	6,445
Osa-miR159f	7,375	6,365
Ath-miR159a	7,608	6,377
Osa-miR159e	3,825	3,638
Osa-miR166m	80	149
Ptc-miR166n	41	87
Ppt-miR166j	31	49
Zma-miR171c	24	32
Osa-miR166k	63	109
Vvi-miR166d	56	110
Vvi-miR166b	62	125
Sbi-miR166a	79	130
Osa-miR408	23	40
Ptc-miR167h	231	209
Ppt-miR896	25	80

48 hpi

miRNA ID	Bgh103 infected	Bgh95 infected
Ppt-miR894	930	1,227
Pta-miR159b	509	802
Osa-miR166m	65	105
Ptc-miR166n	43	65
Sbi-miR166a	74	100
Ptc-miR166p	29	36
Vvi-miR166d	72	89
Osa-miR393b	94	146
Ppt-miR166j	28	41
Sof-miR408e	13	31
Osa-miR166k	55	84

The abbrev*ia*tions at the beginning of each miRNA are suffixes of plants: Ath: *Arabidopsis thaliana*, Osa: *Oryza sativa*, Ptc: *Populus tricocarpa*, Bna: *Brassica napus*, Gma: *Glycine max*, Mtr: *Medicago truncatula*, Sof: *Saccharum officinarum*, Sbi: *Sorghum bicolor*, Ppt: *Physcomitrella patens*, Zma: *Zea mays*, Pta: *Pinus taeda*, Tae: *Triticum aestivum*, Vvi: *Vitis vinifera.*

As in the yellow rust-wheat pathosystem, targets of the differentially expressed miRNAs in powdery mildew-barley pathosystem were detected by using "Plant miRNA Target Finder" programme in barley. The blast analysis identified putative targets for 7 of 35 differentially expressed miRNAs which were generally GAMyb transcription factor (Table 3.7).

Table 3.7 Identified targets of differentially expressed miRNAs in powdery mildew infected Pallas03 barley plants.

miRNA ID	miRNA Targets	
Sbi-miR156e	ribosomal protein L39	
Osa-miR159d	GAMyb protein	
Ath-miR159b	GAMyb protein	
Osa-miR159f	GAMyb protein	
Ath-miR159a	GAMyb protein	
Osa-miR159e	GAMyb protein	
Pta-miR159b	Oxalate oxidase	Myb4 transcription factor

3.1.2.3 Expression level determination of putative miRNA targets with qRT-PCR

The microarray analysis results confirmed that putative target of miR159, GAMyb transcription factor, is an important regulatory element in powdery mildew infection response of barley. In order to understand the role of GAMyb in more detail, qRT-PCR profiling was performed on time point samples of both Bgh103 and Bgh95 infected Pallas03 barley plants (Figure 3.8) (Table 3.8). Prior to qRT-PCR of putative miRNA targets, the normalization experiments were performed as in 3.1.1.3.

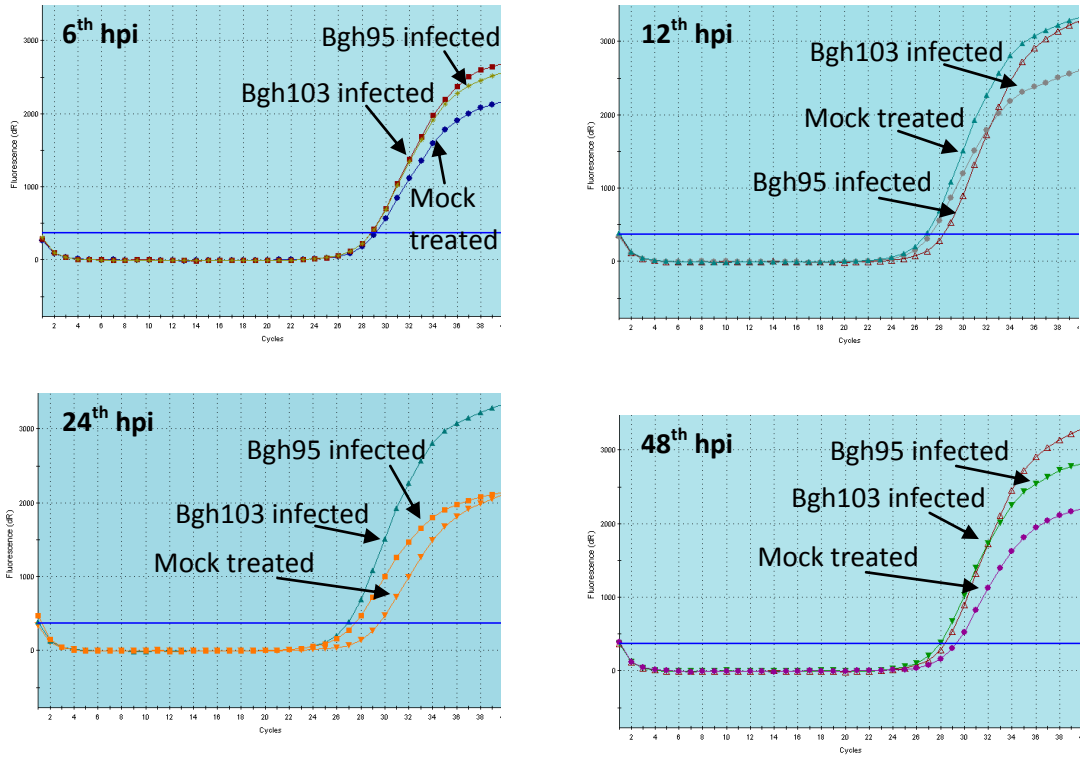

Figure 3.8 qRT-PCR profiling of GAMyb in Bgh103 infected, Bgh95 infected, and mock treated Pallas03 plants. Expression levels at each time point are shown and average values of 3 technical repeats were given.

Table 3.8 Expression level changes of GAMyb transcription factor in compatible and incompatible interaction (↑: decrease, ↑: increase, N.C: No change).

	6 hpi	**12 hpi**	**24 hpi**	**48 hpi**
Bgh95 infected	1.1 ↑	3 ↑	1.8 ↑	1.2 ↑
Bgh 103 infected	1.1 ↑	3.4 ↑	2.8 ↑	1.1 ↓

These results apparently confirm that GAMyb transcription factor is responding to pathogen attacks and generally do not show a race specific expression pattern. Although the level of increase in compatible interaction is higher, there is a general increasing pattern till 48th hpi. GAMyb level is decreased at 48th hpi in Bgh103 infected barley plant.

Unfortunately there were not too many differentially expressed miRNAs that resulted in different targets than Myb transcription factor in blast analysis. Nevertheless, putative miRNA targets that are found to be important in plant microbe interactions by other studies are also confirmed with qRT-PCR experiments. These putative targets were, miR393 target Cellulose synthase (Figure 3.9) (Table 3.9), miR1436 target DNA J (Figure 3.19) (Table 3.10), miR396 target Hsp90 (Figure 3.11) (Table 3.11), and miR164 target MAP Kinase 2 (Figure 3.12) (Table 3.12) (Appendix B).

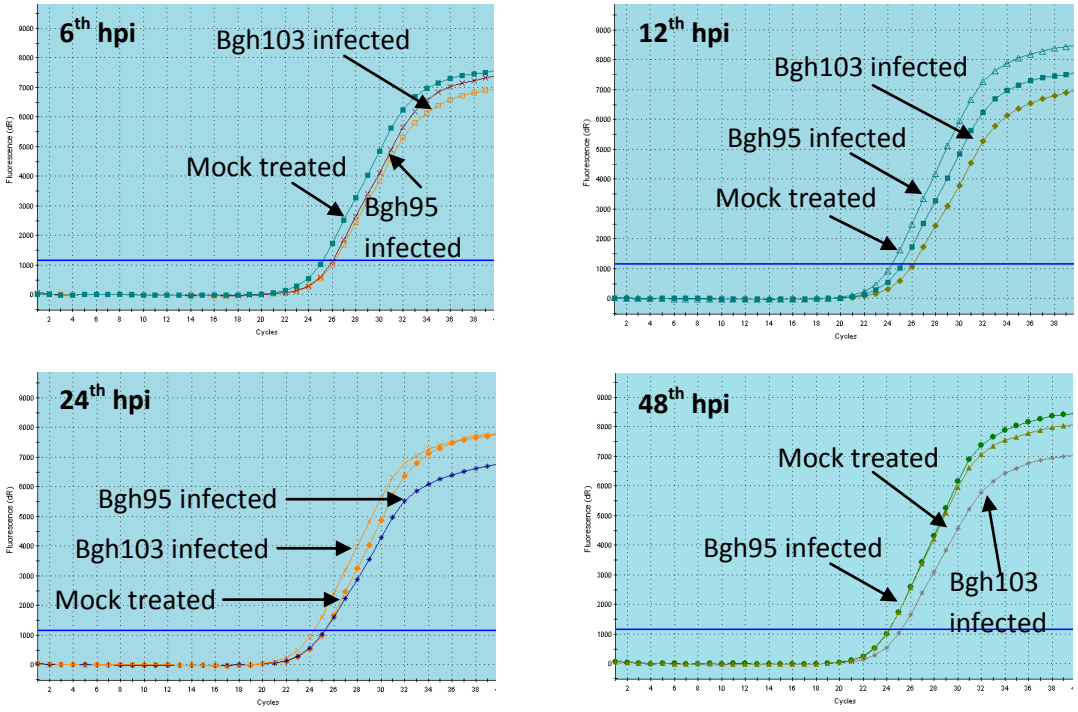

Figure 3.9 qRT-PCR profiling of Cellulose synthase in Bgh103 infected, Bgh95 infected, and mock treated Pallas03 plants. Expression levels at each time point are shown and average values of 3 technical repeats were given.

Table 3.9 Expression level changes of Cellulose synthase in compatible and incompatible interaction (↑: decrease, ↑: increase, N.C: No change).

	6 hpi	**12 hpi**	**24 hpi**	**48 hpi**
Bgh95 infected	1.5 ↓	2 ↑	N.C	N.C
Bgh 103 infected	1.7 ↓	3 ↑	1.5 ↑	1.7 ↓

The decrease in level of cellulose synthase might be explained by PTI response which is not race specific immunity. The increase in 12th and 24th hpi in Bgh103 infected samples might give a clue about the development of resistance against powdery mildew. Increasing the thickness of cell wall might be a general defence mechanism against pathogens.

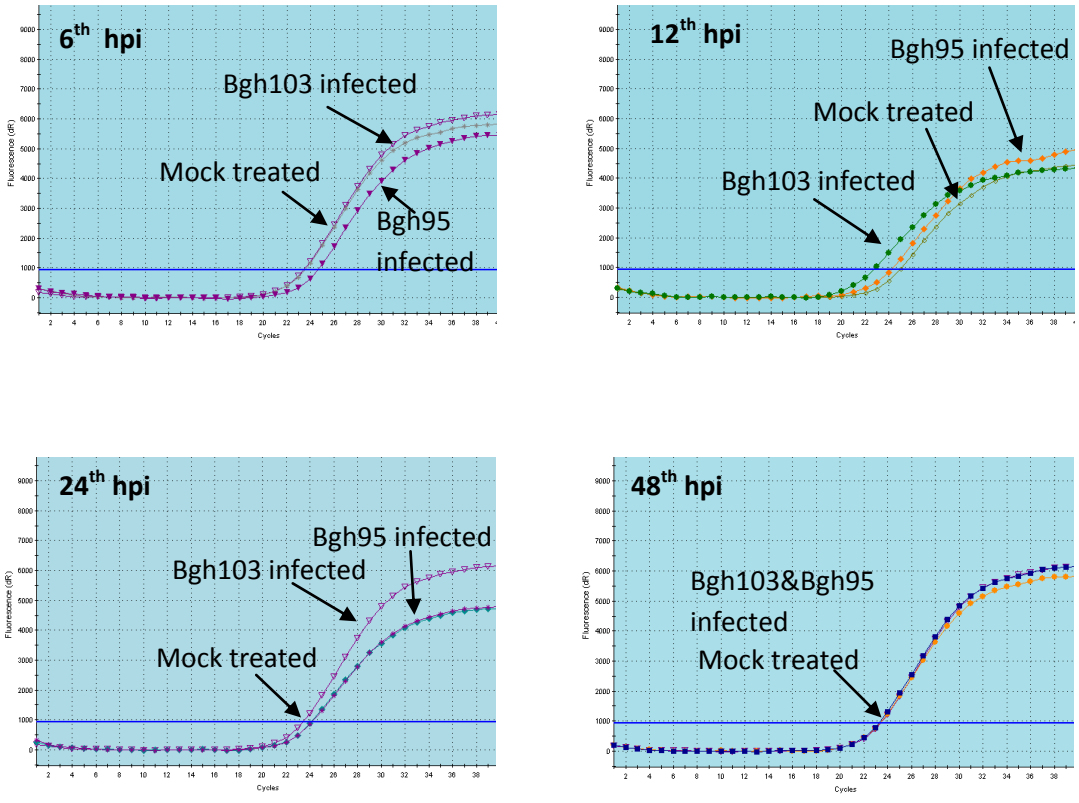

Figure 3.10 qRT-PCR profiling of DNA J in Bgh103 infected, Bgh95 infected, and mock treated Pallas03 plants. Expression levels at each time point are shown and average values of 3 technical repeats were given.

Table 3.10 Expression level changes of DNA J in compatible and incompatible interaction (↑: decrease, ↑: increase, N.C: No change).

	6 hpi	**12 hpi**	**24 hpi**	**48 hpi**
Bgh95 infected	1.8 ↓	1.2 ↑	N.C	N.C
Bgh 103 infected	N.C	3.8 ↑	1.4 ↑	N.C

The decrease in Bgh103 infected 12th hpi samples might enable colonization of pathogen, because DNA J protein is a part of ubiquitination pathway and upregulation of the elements of proteasome system might be important for infection.

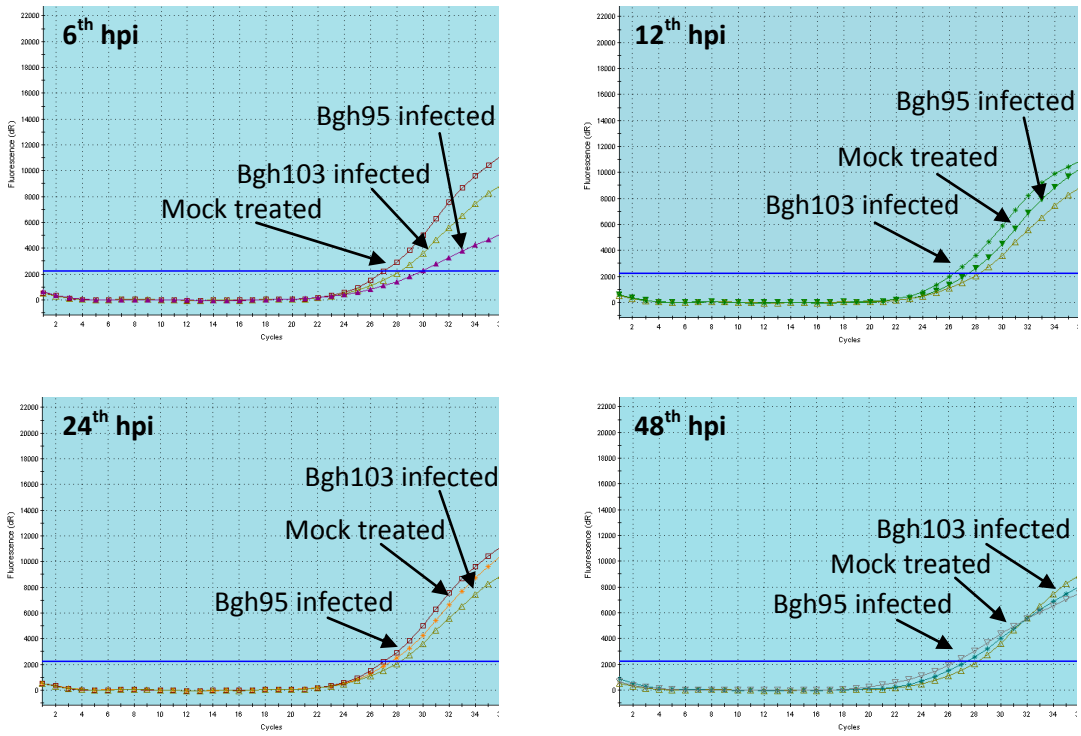

Figure 3.11 qRT-PCR profiling of Hsp90 in Bgh103 infected, Bgh95 infected, and mock treated Pallas03 plants. Expression levels at each time point are shown and average values of 3 technical repeats were given.

Table 3.11 Expression level changes of Hsp 90 in compatible and incompatible interaction (↑: decrease, ↑: increase, N.C: No change).

	6 hpi	**12 hpi**	**24 hpi**	**48 hpi**
Bgh95 infected	4.1 ↓	1.8 ↓	1.1 ↓	1.8 ↑
Bgh 103 infected	2.6 ↓	2.5 ↑	1.5 ↑	1.1 ↓

Hsp90 level is decreased in incompatible interaction, whereas it is increased in compatible interactions` 12th and 24th hpi. Hsp90 functions as a regulatory element in protein folding and suppression of Hsp90 might enable pathogen to infect plant.

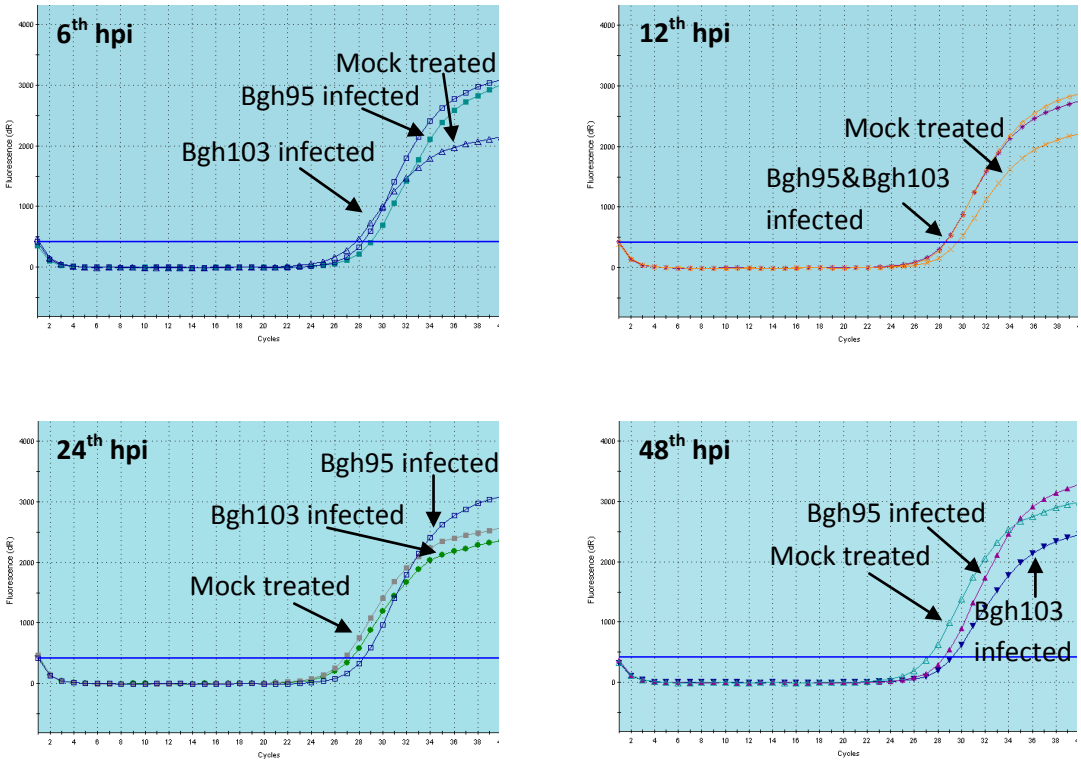

Figure 3.12 qRT-PCR profiling of MAP kinase in Bgh103 infected, Bgh95 infected, and mock treated Pallas03 plants. Expression levels at each time point are shown.

Table 3.12 Expression level changes of MAP kinase in compatible and incompatible interaction (↑: decrease, ↑: increase, N.C: No change).

	6 hpi	**12 hpi**	**24 hpi**	**48 hpi**
Bgh95 infected	2.3 ↓	1.7 ↑	1.9 ↓	1.3 ↓
Bgh 103 infected	1.2 ↓	1.7 ↑	1.1 ↑	2.2 ↑

MAP kinase do not have a regular pattern of increase or decrease in its expression level. MAP kinase pathway is known to one of the most complex pathways in plants and might function in both susceptibility and resistance.

3.2 Functional Analysis of a novel F-box protein (HvDRF) *via* BSMV mediated Virus Induced Gene Silencing

3.2.1 Characterization of HvDRF protein

In previous studies of Akkaya lab many genes were found to be differentially expressed in wheat upon yellow rust inoculation such as pathogen related proteins, antifungal proteins, disease related proteins, and ubiquitin mediated protein degradation proteins. One of the ubiquitin mediated degradation protein was an F-box protein (Bozkurt et al., 2007). The same researchers identified the full length of this F-box protein.

In this study, functional analysis of this specific F-box protein was investigated. The F-box gene is named as HvDRF (*Hordeum vulgare* Disease Related F-box). For characterizing this F-box gene, sequence homology studies were conducted. HvDRF showed higher than 80 % homology to ZEITLUPE Type F-box proteins (Figure 3.13).

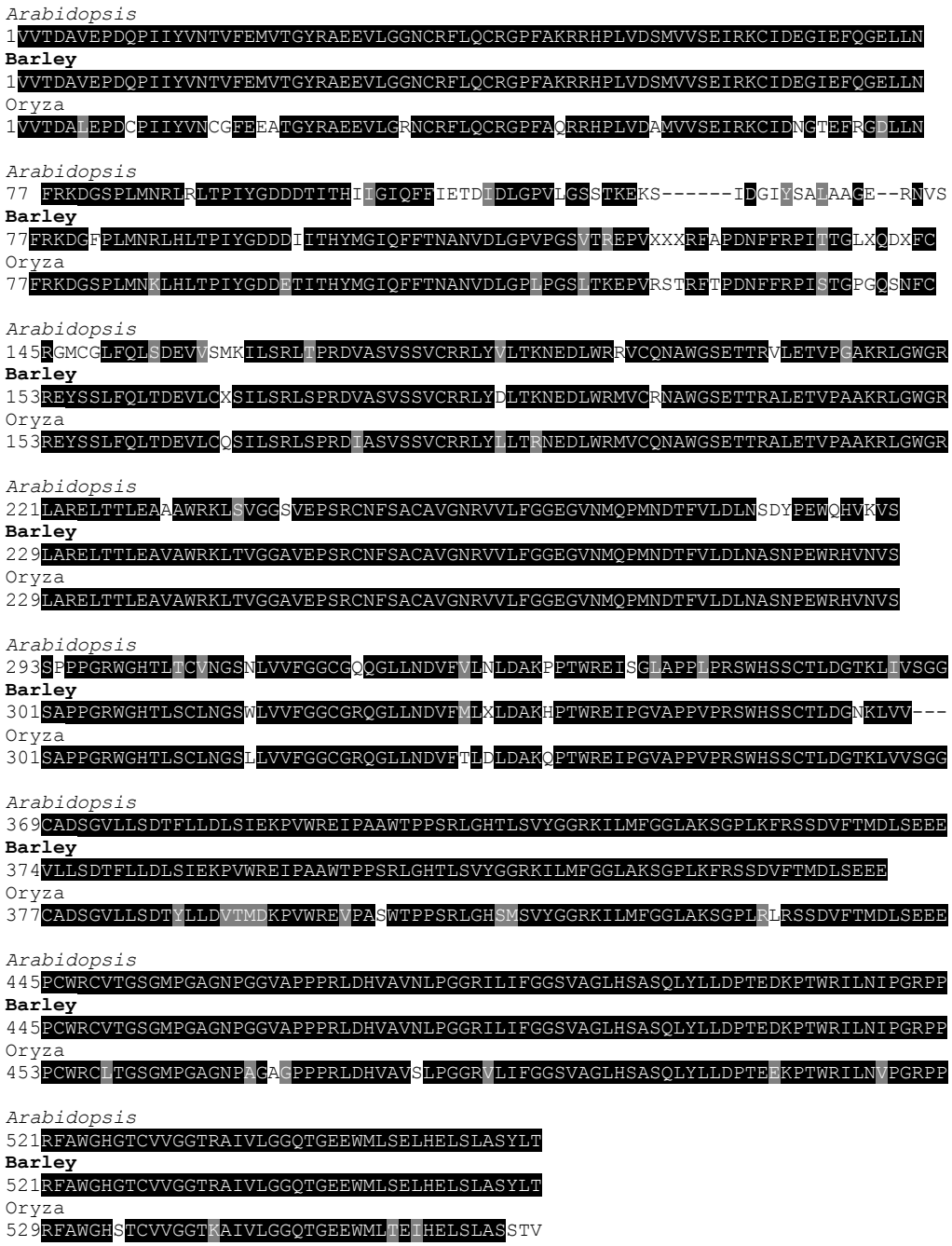

Figure 3.13 Alignment of HvDRF with its homologues genes in *Oryza* and *Arabidopsis*.

3.2.2 Functional analysis of HvDRF

After classification of HvDRF as a ZEITLUPE type F-box protein, the function of HvDRF in response to powdery mildew infection was studied. For this purpose BSMV mediated virus induced gene silencing (VIGS) was performed, which enables the silencing of specific genes within the host.

3.2.2.1 Cloning of 3` UTR part of HvDRF

There are more than 700 F-box genes present in *Arabidopsis* and they show high level of similarity within each other. Widespread occurrence of F-box domain containing proteins are also found in plant species whose genome is fully sequenced (Lechner et al., 2006). For virus induced gene silencing a part of the gene is cloned into the genome of the virus which has infection ability to its host, barley. When the virus infects the plant, the transcripts of the viral genome form siRNAs (small interfering RNAs) which activates sequence specific degradation of the gene of interest (Dinesh-Kumar et al., 2007). So the fragment cloned into the viral genome should be designed to be very specific for that gene of interest to mediate the silencing of only the gene of interest. In this case, since F-box proteins are frequently found in plant genome and they are well conserved, cloning of 3` UTR (untranslated region) was aimed, which is known to be the least conserved part of a functional gene. To clone the 3` UTR, the correct open reading frame was identified by a DNA-Protein translation software (Fr33 translator; http://www.fr33.net/translator.php) (Figure 3.14).

ATGGAGTGGGACAGTGGTTCCGATCTAAGCGCCGATGATGCTTCGTCACTGGCGGATGATGAAGAGGGA
GGTCTTTTTCCCGGAGGTGGACCAATTCCATATCCCGTTGGGAATTTGCTTCACACGGCGCCTTGTGGA
TTCGTTGTTACTGATGCCGTTGAGCCGGACCAACCTATTATATATGTCAACACCGTCTTCGAAATGGTT
ACAGGGTATCGTGCTGAGGAAGTTCTCGGAGGAAATTGCCGCTTCTTGCAATGTAGAGGACCGTTTGCT
AAAAGAAGGCATCCATTAGTTGACTCTATGGTTGTTTCCGAGATAAGAAAATGTATTGATGAGGGCATT
GAATTTCAAGGCGAGTTGTTGAATTTCAGAAAAGACGGATTTCCNTTGATGAATAGGTTGCACCTGACC
CCTATATATGGAGATGATGATATCATCACCCATTATATGGGCATTCAGTTCTTCACCAATGCTAATGTT
GATTTGGGACCAGTACCTGGTTCAGTTACNAGGGAACCTGTGANATNTNCNCGGTTTGCTCCGGATAAC
TTTTTCCGGCCCATAACCACCGGACTANAGCAGGACANCTTCTGCCGGGAGTATTCCAGTCTCTTCCAG
CTAACTGATGAAGTACTTTGCCANAGTATTTTGTCAAGGTTGTCTCCAAGAGATGTCGCATCTGTGAGC
TCTGTATGTCGACGGTTGTATGACTTGACAAAAAATGAAGATCTTTGGAGAATGGTTTGTCGTAATGCA
TGGGGTAGTGAGACTACTCGAGCTCTTGAGACTGTGCCTGCTGCGAAAAGATTGGGCTGGGGTCGTCTG
GCCAGAGAACTAACCACCCTGGAAGCTGTTGCCTGGAGGAAATTGACTGTTGGAGGTGCAGTGGAGCCA
TCTCGATGCAACTTCAGTGCTTGTGCTGTAGGGAATCGTGTCGTTCTCTTTGGCGGGGAAGGTGTTAAC
ATGCAACCGATGAATGACACATTTGTGTTGGATTTGAATGCTAGCAATCCGGAGTGGAGACATGTCAAT
GTGAGCTCAGCTCCTCCAGGCCGCTGGGGCCATACACTATCGTGCCTAAATGGATCTTGGTTAGTTGTG
TTCGGGGGATGTGGAAGGCAGGGCCTTCTTAATGATGTATTCATGTTGGANTTGGATGCGAAACACCCA
ACTTGGCGGGAGATCCCTGGTGTTGCACCGCCGGTTCCGCGTTCATGGCACAGCTCCTGCACTTTGGAT
GGGAATAAGTTGGTGGTTGTTCTTCTAAGTGACACGTTCCTCCTCGACCTTTCAATAGAGAAACCAGTG
TGGAGAGAGATTCCAGCTGCCTGGACTCCGCCTTCCCGGTTAGGCCACACACTATCGGTTTATGGAGGA
AGAAAGATCTTGATGTTTGGTGGTCTTGCTAAGAGCGGGCCTTTGAAATTCCGTTCGAGTGATGTCTTC
ACAATGGATCTAAGCGAAGAGGAGCCTTGTTGGAGGTGTGTGACCGGTAGCGGAATGCCTGGAGCAGGA
AACCCAGGAGGAGTAGCACCACCACCAAGGCTAGATCACGTTGCAGTTAACCTCCCTGGAGGCAGAATC
TTGATATTTGGCGGCTCAGTGGCAGGGCTTCACTCAGCGTCTCAGCTTTATCTACTTGACCCAACGGAG
GACAAACCGACTTGGAGAATACTAAACATTCCAGGAAGACCGCCTCGGTTTGCTTGGGGACATGGCACT
TGTGTTGTGGGAGGAACACGAGCGATAGTGCTAGGTGGTCAGACCGGAGAAGAATGGATGCTAAGTGAG
CTACACGAATTATCACTAGCGAGCTATCTCACGTAACCAAAGCTTCCATGAAAACAAATTAGACCCTTC
AAGTGGCGTTAAGCTTGATTGTCTTCACCACCGGGCCAGAGCACTGAATGGATGTATTTGCTTGGAAGT
GAGATATGGTTGGGTCTCGAGTAAAGATTAAACCTCTTAGACTGCGGCCGCTCAAAGTCTATATAAAGG
TCTTTCAACCAAAGCTTCCATGAAAACAAATTAGACCTTTCAAGTGGCGTTAAGCTTGATTGTCTTCAC
CACCGGGCCAGAGCACTGAATGGATGTATTTGCTTGGAAGTGAGATATGGTTGGGTCTCGAGTAAAGAT
TAAACCTCTTAGACTGCGGCCGCTCAA

Figure 3.14 Full sequence of HvDRF. The start and stop codons are highlighted. The 3` UTR is underlined.

Then the 3 `UTRs is amplified by extension touchdown PCR, by added *Not*I and *Pac*I restriction sites to the ends of the amplified region (Figure 3.15 a, b). Amplified fragment of 3` UTR of HvDRF is cloned into pGEMT-Easy. Cloning the correct fragment was confirmed by colony PCR using F-box primers and sequencing of the recombinant plasmid (pGEMTe-HvDRF) (Figure 3.15 c).

(a)CCAAAGCTTCCATGAA**AACAAATTAGACCCTTCAA**GTGGCGTTAAGCTTGATTGTCTTCACCACCGG
GCCAGAGCACTGAATGGATGTATTTGCTTGGAAGTGAGATATGGTTGGGTCTCGAGTAAAGATTAAACC
TCTTAGACTGCGGCCGCTCAAAGTCTATATAAAGGTCTTTCAACCAAAGCTTCCATGAAAACAAATTAG
ACCTTTCAAGTGGCGTTAAGCTTGATTGTCTTCACCACCGGGCCAGAGCACTGAATGGATGTATTTGCT
TGGAA**GTGAGATATGGTTGGGTC**TCGAGTAAAGATTAAACCTCTTAGACTGCGGCCGCTCAA 336 bp

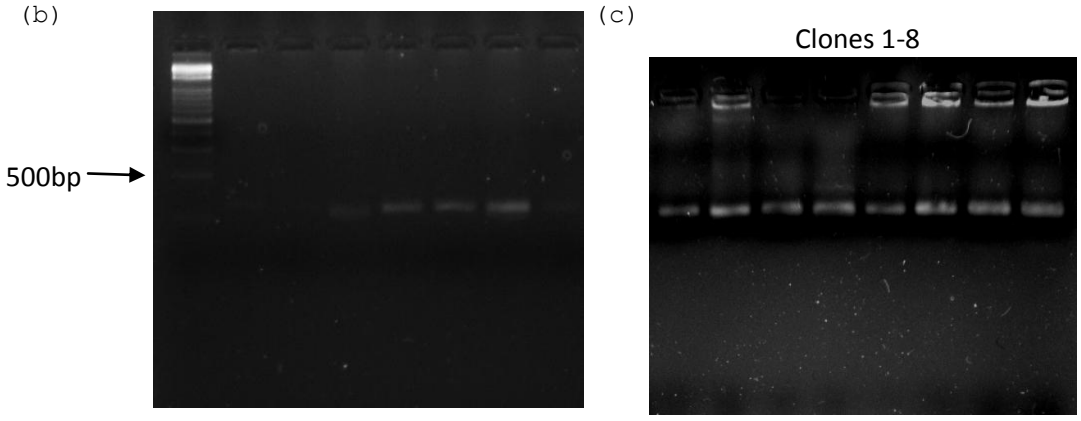

Figure 3.15 Cloning of 3`UTR fragment of HvDRF into pGEMT-Easy. (a) 3` UTR of HvDRF. Forward and reverse primer regions are shown in bold. The sequences of the primers are 5`-ATAGCGGCCGCCAAATTAGACCTTTCA-3′ and 5`-ATATTAATTAAGACCCAACCATATCTCAC. Highlighted parts of the primers are *Not*I and *Pac*I restriction sites respevtively. Extra 3 nucleotides (ATA) were added to the primers for efficient cleavage of restriction enzymes. Total amplification product is 302 bp. (b) Agarose gel image showing the amplification products, that are amplified from various samples of barley cDNA. (c) Agarose gel image showing the colony PCR results of the cloned HvDRF 3`UTR fragment into pGEMT-Easy.

After confirming that HvDRF fragment was cloned into pGEMT-Easy, this fragment was cloned into pγ. For this purpose, the cloned region is cleaved from pGEMT-Easy by double digestion with NotI and PacI (Figure 3.16). The fragment is gel purified and ligated into pγ (pγ:HvDRF-3`UTR). The cloning was again verified by colony PCR.

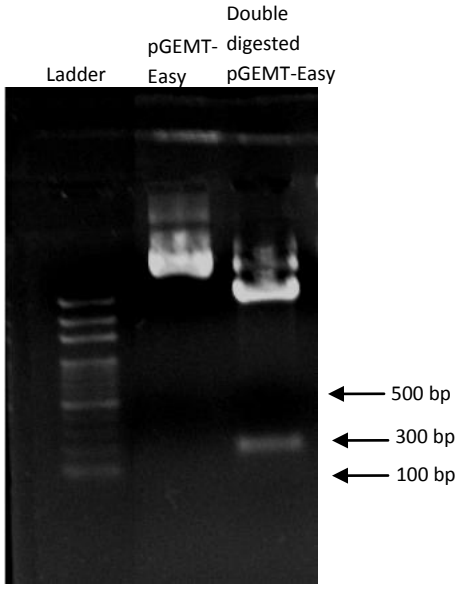

Figure 3.16 Double digestion of BSMV γ genome. Plasmid is cut with *Not*I and *Pac*I restriction enzymes. The fragment of HvDRF is at the expected size.

3.2.2.2 BSMV Mediated Silencing of HvDRF

BSMV is an RNA virus having tripartite genome (α, β, γ). In order to perform VIGS experiments, HvDRF was cloned into γ plasmid. Then all the plasmids containing the other genomes were linearized using appropriate restriction enzymes (Figure 3.17 a) and subjected to *in vitro* transcription (Figure 3.17 b, c). These transcripts were

purified and used at equal amounts to infect barley. To mediate infection FES was used which contains cellite to wound plant cell walls.

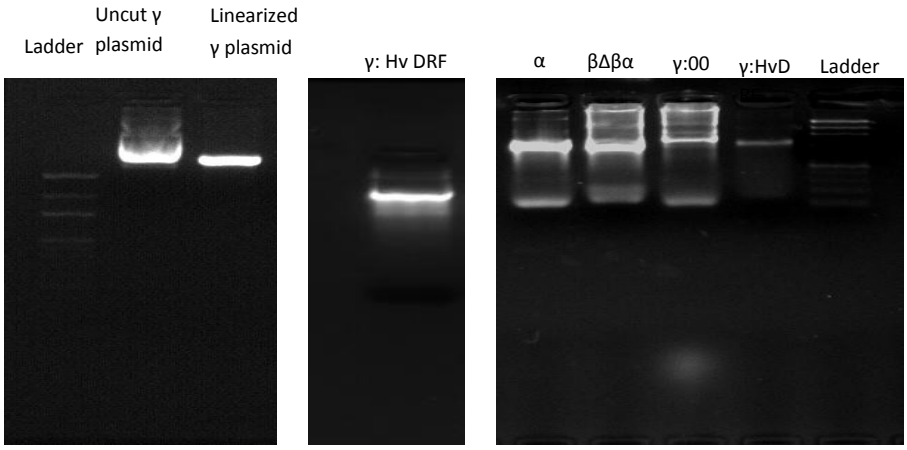

Figure 3.17 Linearization and *in vitro* transcription of BSMV genomes. (a) HvDRF fragment containing γ plasmid (γ:HvDRF) is linearized with BssHII restriction enzyme. As expected, uncut plasmid migrated a little bit less than linearized plasmid. (b) The transcript product of γ:HvDRF was separated in RNA agarose gel. (c) *In vitro* transcription products of BSMV genome parts (Ambion mMessage-mMachine Kit).

Ten day old Pallas01 and Bulbul barley cultivars, whose third leaves were just emerging were used for BSMV infection. The transcripts were applied onto leaves with FES. BSMV:00 is used as negative control and for mock treatment plants were wounded with FES only. After observation of the silencing phenotype (stripes due to viral infection) silenced and mock treated leaves were transferred to agar plates for pathogen inoculation. Bulbul is the universal susceptible cultivar of barley. Pallas01 cultivar contains *Mla1* and is resistant to *AvrMla1* containing Bgh103 strain of powdery mildew. So normally Bgh103 is virulent to Bulbul, but avirulent to Pallas01. 10 days after pathogen infection the results of the silencing on both HvDRF silenced and unsilenced (BSMV:00) plants were examined in comparison to the mock treated

samples under light microscopy, after trypan blue staining (Figure 3.19). Plant leaves were also imaged under dissecting light microscope (Figure 3.18).

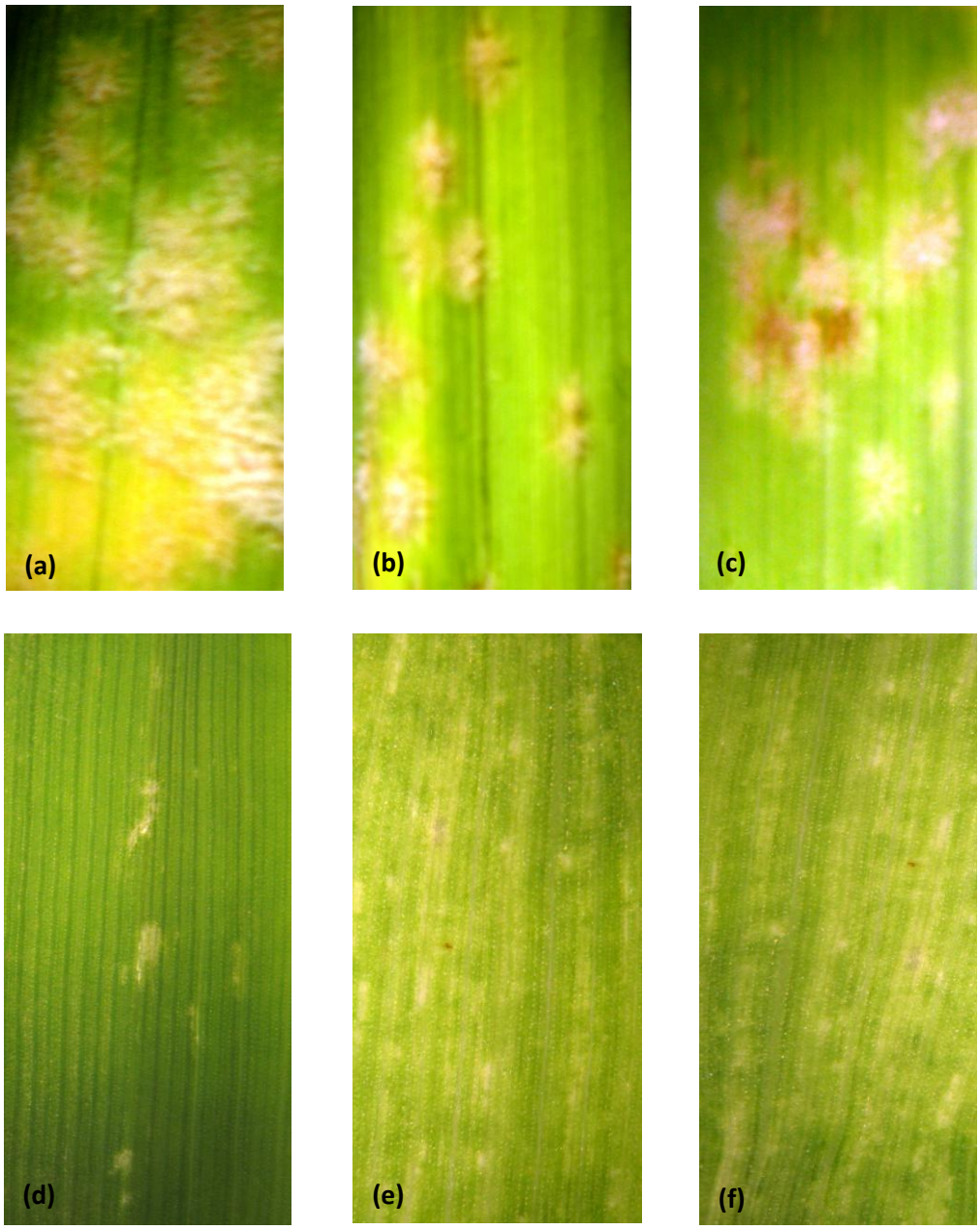

Figure 3.18 Dissecting microscope analysis of 10 day after Bgh 103 infection of (**a**) FES treated Bulbul, (**b**) BSMV:00 treated Bulbul, (**c**) BSMV:HvDRF treated Bulbul, (**d**) FES treated Pallas01, (**e**) BSMV:00 treated Pallas01; (**f**) BSMV:HvDRF treated Pallas01.

Under dissecting light microscope, the viral spreading can be observed (Figure 3.19, (e) and (f)). These stripes meant BSMV infection was successful; hence HvDRF was silenced using BSMV. There were powdery mildew colonies on both mock treated and BSMV:00 (Figure 3.19 a1, a2, a3) and BSMV:HvDRF treated (Figure 3.19 b1, b2, b3) Bulbul plants. So silencing of HvDRF did not cause any secondary changes in susceptible cultivar. All the observations were as expected for susceptibility response. For resistance barley cultivar silencing, although viral stripes were apparent on BSMV:00 treated (Figure 3.18 e) and BSMV:HvDRF treated (Figure 3.18 f) plants, no visible colonies were formed on the leaves.

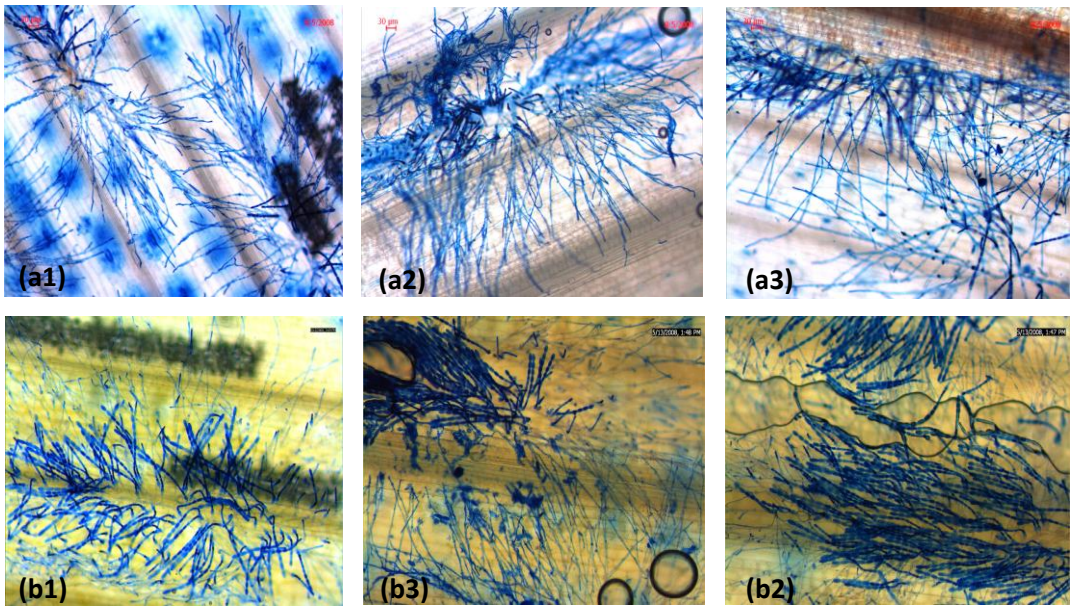

Figure 3.19 Light microscopy of silenced and unsilenced plants. Light microscope images of BSMV:00 treated Bulbul ((a1), (a2), (a3)); BSMV:HvDRF treated Bulbul ((b1), (b2), (b3)); BSMV:00 treated Pallas01 ((c1), (c2), (c3)); BSMV:HvDRF treated Pallas01 ((d1), (d2), (d3)) plants after Trypan blue staining. Arrows ((c2), (c3)) show ungerminated powdery mildew spores on BSMV:00 treated Pallas plants.

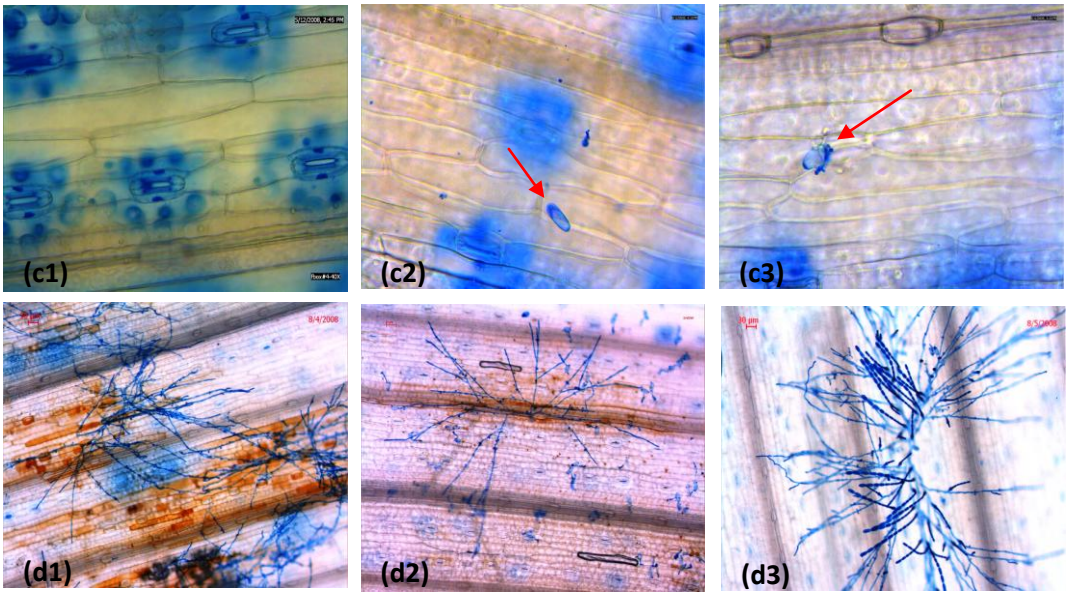

Figure 3.19 cont`d Light microscopy of silenced and unsilenced plants. Light microscope images of BSMV:00 treated Bulbul ((a1), (a2), (a3)); BSMV:HvDRF treated Bulbul ((b1), (b2), (b3)); BSMV:00 treated Pallas01 ((c1), (c2), (c3)); BSMV:HvDRF treated Pallas01 ((d1), (d2), (d3)) plants after Trypan blue staining. Arrows ((c2), (c3)) show ungerminated powdery mildew spores on BSMV:00 treated Pallas plants.

Microscopic analysis revealed that, although there were not any visible colonies on silenced Pallas01 plants, resistance was lost and pathogen now was able to infect plant. Since, no fungal growth were observed on BSMV:00 treated Pallas01 plants (Figure 3.19 c1, c2, c3), the hyphaeal structures observed on silenced plants were not due to viral infection, but due to the silencing of HvDRF (Figure 3.19 d1, d2, d3).

To confirm and assess the level of HvDRF silencing on the plants, qRT-PCR experiments were conducted on BSMV:00 treated, BSMV:HvDRF treated and mock treated samples.

(a)

CCAAAGCTTCCATGAAAACAAATTAGACCCTTCAAGTGGCGTTAAGCTTGATTGTCTTCACCACCG
GGCCAGAGCACTGAATGGATGTATTTGCTTGGAAGTGAGATATGGTTGGGTCTCGAGTAAAGATTA
AACCTCTTAGACTGCGGCCGCTCAAAGTCTATATAAAGGTCTTTCAACCAAAGCTTCCATGAAAAC
AAATTAGACCTTTCAAGTGGCGTTAAGCTTGATTGTCTTCACCACCGGGCCAGAGCAC**TGAATGGA**
TGTATTTGCTTGGAAGTGAGATATGGTTGGGTCTCGAGTAAAGATTAAACCTCTTAGACTGCGGCC
GCTCAA**.....AAA**

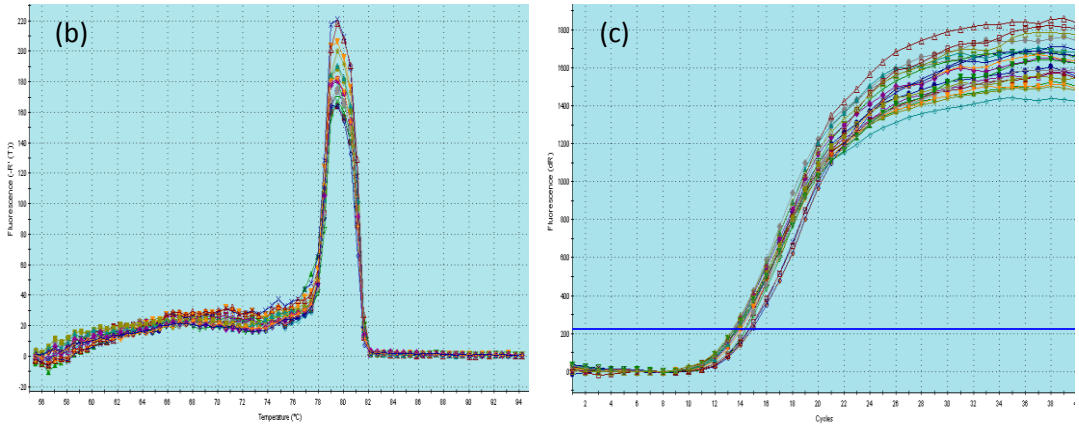

Figure 3.20 qRT-PCR analysis of silencing. For determining the level of silencing the primers (5'-TGAATGGATGTATTTGC-3') and Oligo(dT)$_{20}$ are used. The region amplified is shown in bold (a). The quality of this primer couple is checked by observing the dissociation curve (b). One peak in dissociation curve confirms the compatibility of the primer couple for qRT-PCR experiments. The samples are normalized by using 18 S rRNA gene specific primers (c).

After normalizing the samples (Figure 3.29 c), qRT-PCR were performed, which showed four-fold silencing in BSMV:HvDRF treated plants in comparison to BSMV:00 treated and mock treated plants, which means 25% silencing in comparison to empty vector control (Figure 3.21).

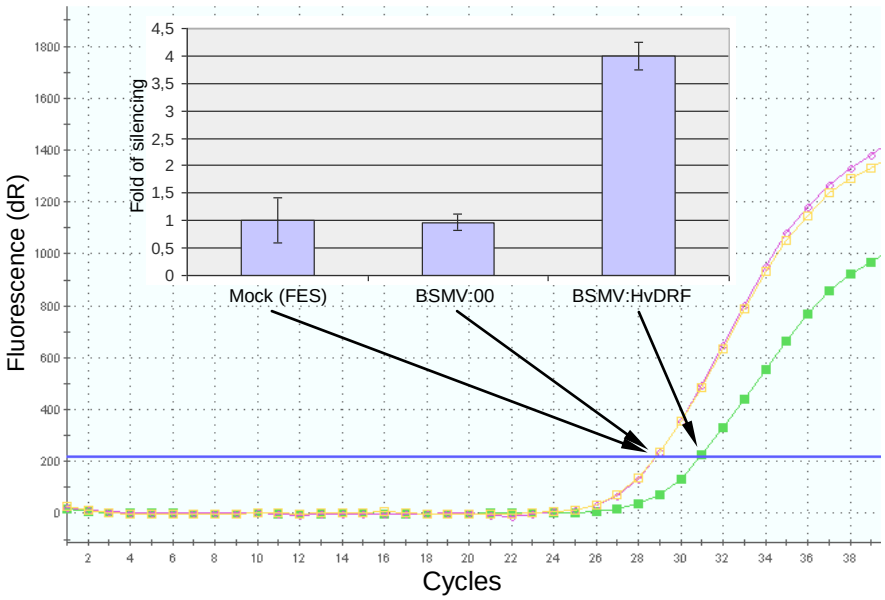

Figure 3.21 The level of HvDRF silencing in Pallas01. On the three biological samples of each treatment, three qRT-PCR technical repeats were performed (Stratagene Mx3500P), which gave four-fold silencing. An average value of three technical repeats for two biological samples was given in the amplification plots.

The effect of silencing was quantified by counting the number of hyphae in unit area for eight different biological samples (Figure 3.22).

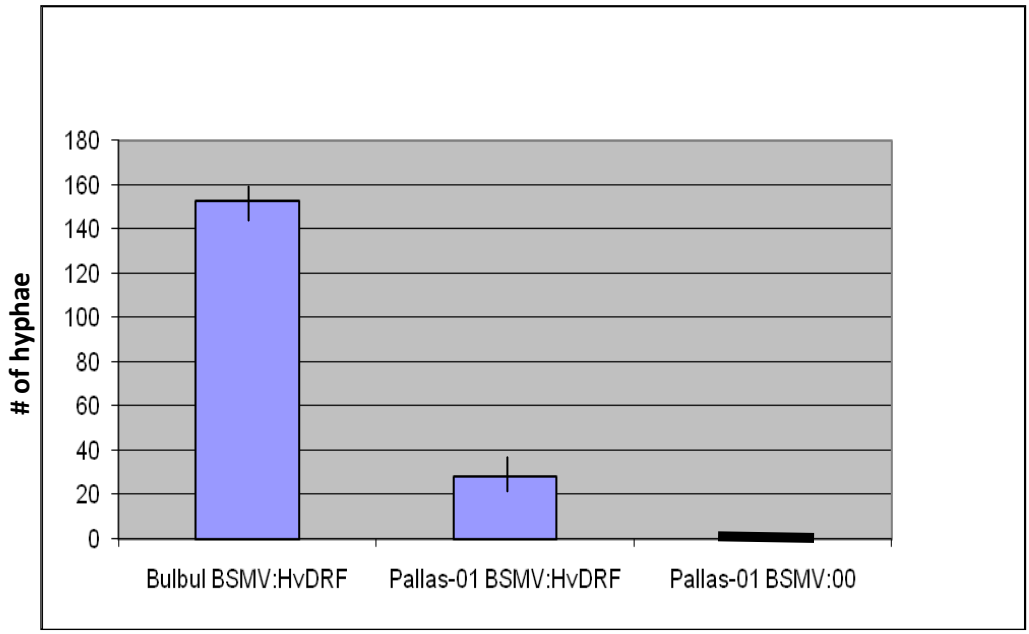

Figure 3.22 Quantification of decrease in resistance upon silencing of HvDRF.

There were not any hyphae on BSMV:00 treated plants, but on the average 28 hyphae were present in BSMV:HvDRF treated plants. The resistance was not totally compromised, since there was fewer numbers of hyphae in HvDRF silenced Pallas01 then HvDRF silenced Bulbul (152 hyphae on the average) (Figure 3.22).

These results have shown that silencing of HvDRF resulted in decreased resistance to powdery mildew and confirmed this novel F-box gene as a positive regulator of plant defence.

3.3 Discussion

3.3.1 MicroRNAs play important roles in shaping plant responses to pathogen attacks

The results of microarray analysis of yellow rust infected wheat and powdery mildew infected barley showed that infecting wheat and barley with race specific pathogens definitely resulted in differential miRNA expression. Since plants miRNAs show high complementarity to their targets and either cleave or repress translation of corresponding targets, the potential targets of differentially expressed miRNAs can be found by computational alignment analysis. Therefore, computational identification of putative miRNA targets and qRT-PCR profiling of previously identified pathogen response related "in silico" determined targets might enable understanding the molecular mechanisms underlying pathogen infection.

3.3.1.2 A new model, for explaining yellow rust-wheat and powdery mildew-barley pathosystem

miRNA microarray analysis of yellow rust infected wheat and powdery mildew infected barley had two common miRNAs that are differentially expressed upon pathogen infections.

Targets of miRNAs that are differentially expressed include CCAAT-box transcription factors, MAP Kinase 2 and Myb transcription factors. Transcription factors and Map Kinases are regulatory elements controlling expression of many genes, which makes

them very important checkpoints of plant metabolism. So, controlling the expression of these genes with miRNAs, enable plants fine-tuning of many metabolic pathways.

CCAAT-box transcription factors are one of the most common elements in eukaryotes and is present in 30 % of the genes (Combier et al., 2006). miR169 family miRNAs are found to control expression of CCAAT-box transcription factors in *Arabidopsis* and rice (Combier et al., 2006; Qiu et al., 2009). Moreover miR169 family miRNAs are shown to play roles in nodule development, drought response, and elicitor response (Combier et al., 2006). In elicitor response, methyl jasmonate, which is a taxoid elicitor, downregulated miR169 level. In our data, miR169 level is higher in the plants having resistance to the pathogen than that of the susceptible plants (see Table 3.1) which is a new and interesting finding. A similar result was observed in qRT-PCR profiling of miR169 target, in which the expression level is consistently decreasing in resistance. This relationship between the miRNA and its target definitely proves that miR169 is controlling gene expression *via* cleavage and should be maintained at higher amounts for resistance response (Combier et al., 2006). CCAAT-box transcription factors might be controlling expression of some genes that are required for effector triggered susceptibility and downregulation of these genes might result in susceptibility. This hypothesis can be tested by using silencing miR169 genes and infecting the silenced plants. If miR169 silenced plants become susceptible, this will mean that miR169 is a required miRNA for resistance against pathogens. Also in order to identify the targets those are controlled by miR169, a microarray analysis can be performed in miR169 silenced plants. The genes whose levels are changing in comparison to controls might give us clues about the specific targets of miR169.

Another differentially expressed miRNA family was miR159, whose computationally identified target was found to be Myb transcription factors. Control of Myb transcription factors with miR159 family miRNAs were shown in previous studies (Allen et al., 2007; Reyes and Chua, 2007). Also the mechanism of action of miR159 was proved to be the cleavage of its target (Zilberstein et al., 2006). miR159 was shown to be induced by ABA (absisic acid) in germinating seedlings (Reyes and Chua,

2007), and repressed by GA (gibberellic acid) in floral development (Achard et al., 2004). Moreover miR159 was proved to be a marker in viral resistance (Simon-Mateo and Garcia, 2006). In our case, miR159 level was increased in susceptibility (see Table 3.1 and Table 3.7) and qRT-PCR profiling of the target resulted in a decreased MYB level in susceptibility (see Table 3.3). The role of MYB transcription factors in fungal resistance is not studied extensively, but from these findings it can be speculated that, MYB transcription factors might be required for effector triggered immunity, hence suppression of MYB might be required for infecting plant tissues. These data should be further confirmed in *Arabidopsis* using *Arabidopsis* pathogens and mutants that are deficient in miRNA action (Brodersen et al., 2008).

Besides miR159 and miR169 targets, the computationally identified targets of miR393, miR396, miR164, and miR1436 were profiled with qRT-PCR.

Cellulose synthase, which was determined to be the putative target of miR393 was analyzed with qRT-PCR. In early studies, impairment of cellulose synthase was resulted in enhanced resistance in other pathogens (Hernandez-Blanco et al., 2007). Cell wall is an element of basal defence; decrease of cellulose synthase in both Bgh103 and Bgh95 infections in this study might be an indicator of PAMP triggered susceptibility (see Table 3.9). It is considered that the basal defence mechanisms are not in action after 6^{th} hpi, so the expression level of cellulose synthase might be under the control of other factors than fungal infection.

The computationally identified target of miR396 is Hsp90. The role of Hsp90, in disease resistance was shown before (Seo et al., 2008; Zhang et al., 2008; Swiderski et al., 2009). It forms a complex with Rar1 and Sgt1 and functions as a core modulator of innate immunity in plants (Seo et al., 2008). However, controlling the expression level of Hsp90 with miR396 is not shown yet. In our studies, we show that both miR396 levels and Hsp90 levels are changing upon pathogen infection (see Table 3.7 and Table 3.11). Although these data do not explain an inverse relationship between miR396 and Hsp90, the differential expression of both might be an indicator of a putative control

mechanism for Hsp90 expression. Also inverse level of Hsp90 in resistance and susceptibility after 6^{th} hpi, supports the role of Hsp90 in pathogen response. This preliminary data can be assessed by designing reporter assays such as luciferase assay or GFP assay by cotransforming miR396 and Hsp90 into a common host and observing the GFP expression. If the GFP expression level decreases in comparison to only GFP:target containing host, Hsp90 would be proved to be the target of miR396.

The putative target of miR1436 was found to be DNA J like protein. DNA J like proteins are involved in a variety of processes including protein folding, protein partitioning into organelles, signal transduction, and targeted protein degradation (Thao et al., 2007). They are also found to be induced in wheat upon *Fusarium* infection (Ulrich et al., 2006; Bolton et al., 2008). In our case, DNA J protein is increasing in both infection types at 12^{th} and 24^{th} hpi (see Table 3.10), so DNA J might have a role in PTI (PAMP triggered immunity responses).

The last gene was MAP kinase 2 which is found to be the target of miR164. MAP kinase 2 was identified in rice and found to be induced upon BTH treatment, which is a disease resistance inducing salisilic acid analog (Song et al., 2006). qRT-PCR profiling resulted in increase and decrease in both resistance and susceptible plants. There was not a consistent expression pattern. Since MAP kinase pathways are very complicated, the qRT-PCR profiling results (see Table 3.12) need further dissection.

3.3.2 HvDRF is a novel ZTL-type F-box protein functioning as a positive regulator of plant defense

3.3.2.1 Virus induced gene silencing, an efficient tool for gene function analysis in barley powdery mildew pathosystem

Barley powdery mildew ranks among the highly risky pathogens since durable resistance mechanism are not known for now (McDonald and Linde, 2002). So dissecting the molecular mechanisms that may lead to foundation of durable resistance mechanisms is very important for countries like Turkey, in which agriculture is a mean of main economic property. Studying gene function in barley is problematic, since gene mutants are hard to obtain and time consuming. Therefore transient silencing mechanisms are tried to be applied for gene level studies. Virus induced gene silencing *via* BSMV is one of the transient silencing methods, which was established in 2002 for barley (Holzberg et al., 2002). Afterwards, it was used to analyze the role of Hsp90-Rar1-SGT1 system in barley powdery mildew resistance. It was shown that VIGS is a robust method to dissect resistance mechanisms in barley (Hein et al., 2005). In this study BSMV mediated VIGS is used to unravel the role of a new player in the resistance mechanism of barley against powdery mildew. One of the major drawbacks of VIGS is silencing specificity. Since it depends on the sequence information of that gene and the genome sequence of many plant species is not known for today, the silencing may be problematic if there are multiple copies or conserved domains in the gene of interest. To increase specificity of the VIGS system, generally 3` UTR (untranslated region) is preferred (Burch-Smith et al., 2004). For silencing of HvDRF, the same methodology was used, the full length of the gene is obtained and 3` UTR is cloned into viral genome. Since F-box proteins are one of the largest multigene families in plants, choosing 3` UTR conferred specificity required in our experiments. Otherwise many of the uncharacterized F-box proteins might had been silenced and

this would not have given information for the function of HvDRF specifically. BLAST analysis confirmed that the UTR of HvDRF does not show significant similarity to any other genes identified in barley. Hence the results of HvDRF silencing *via* VIGS gave reliable information about the role of HvDRF in barley powdery mildew interaction.

3.3.2.2 HvDRF, a positive regulator of plant defense in response to powdery mildew infection

The phylogeny analysis confirmed HvDRF as a ZEITLUPE (ZTL) type F-box protein. It showed very high homology to *Arabidopsis* (NP_568855), rice (NP_001058438), poplar (XP_002329665), Glycine (ABD28285), ZEITLUPE type F-box proteins. The known functions of ZTL-type F-box proteins include plant circadian rhythm control, photomorphogenesis, and phytochrome signaling (Somers, 2001; Kim et al., 2005c; Kim et al., 2007; Zoltowski et al., 2007; Harmon et al., 2008). So, HvDRF explicitly expands the functions of ZTL type F-box proteins to plant-pathogen interactions. In circadian clock controlling the F-box protein interacts with pseudo-response regulator (PRR) proteins which were found to have important roles in cold stress responses (Calderon-Villalobos et al., 2007). Moreover, there are some reports confirming the convergence of abiotic and biotic stress resistance mechanisms (Achuo et al., 2006; Chen et al., 2006). So HvDRF may be at the central point of such a convergent mechanism. To understand this, transcript profiling experiments in silenced barley plants should be done. Differentially expressed genes might give us a clue about the position of HvDRF in both biotic and abiotic stress responses.

The role of HvDRF in barley powdery mildew interaction is unequivocally shown by silencing. There were no hyphae formations in BSMV:00 treated resistant plants (Figure 3.14 c1, c2, c3); whereas there were on the average 28 hyphae per unit area formed on BSMV:HvDRF treated plants. The average number of hyphae on unit area

is calculated by the data obtained from eight biological samples. When 28 hyphae are compared to 152 hyphae in susceptible barley cultivars, there is a 20% difference in susceptible silenced and resistance silenced barley plants. This number should be evaluated with the level of silencing. There is fivefold difference in number of hyphae and the level of silencing is fourfold. So if the silencing efficiency can be increased, the susceptibility might be increased in silenced resistant barleys. Also absence of visible colonies on silenced resistant plants (Figure 3.13, d) might be a result of transient silencing.

Why silencing of HvDRF led to a decrease in resistance? This is the main question that will illuminate the role of HvDRF in powdery mildew resistance response and determine the position of ubiquitination in barley powdery mildew pathosystem. HvDRF is a part of ubiquitin ligase (E3) complex, meaning it transfers polyubiquitin to the target that will be degraded. Thus, the target of HvDRF is the key that will explain the role of HvDRF in resistance responses. There are two possible mechanisms inferring the role of protein degradation in disease resistance mechanisms (Nirmala et al., 2007). The first one is related with negative regulation of HR. This hypothesis was supported by *Arabidopsis* RMP1 (R protein) degradation (Boyes et al., 1998). Degradation of RPM1 results in HR response by which means plants restrict the HR to only infection site. This confinement is vital for necrothrophic pathogens, but since powdery mildew is biotrophic and silencing of HvDRF does not result is HR, this hypothesis seem not to be valid for our study. Second hypothesis involves degradation of a negative regulator of R protein complex. The degradation product might be the signal activating the disease resistance response. The supporting evidence came from *Arabidopsis*. Degradation of RIN4 is activated by *Pseudomanas syringae* effector AvrRpt2 (Kim et al., 2005a) and knockdown of RIN4 led to constitutive activation of defense response (Mackey et al., 2002). This hypothesis is also supported by a very close relative of barley-powdery mildew pathosystem: barley-stem rust pathosystem. In stem rust infected barley plants RPG1 protein is found to be polyubiqutinated upon avirulent pathogen inoculation. The degradation of RGP1 releases a signal peptide

which activates downstream defense responses (Nirmala et al., 2007). This alternative seems more likely for HvDRF silencing case. HvDRF might be the E3 ligase component carrying polyubiquitin chain to the RPG1 like target which activates resistance responses. So in that sense, HvDRF functions as a positive regulator of defense responses. To validate this hypothesis the target that is interacting with HvDRF must be identified by assays like coimmunoprecipitation or yeast two hybrid. If the target of HvDRF is the protein that is interacting with powdery mildew effectors, or it is an R-protein itself, identification of the target of HvDRF becomes much more important. Because if that target is not vital for barley to develop normally, cultivars that lack HvDRF target might convey us to durable resistance for powdery mildew.

CHAPTER 4

CONCLUSION

Wheat and barley are two most important agricultural crop species of Turkey, which makes functional genomics studies of these crops very important. Albeit, Turkey is one of the largest producers of these crops in the world, functional genomics studies of these plants are very poorly performed in our country.

In this thesis two fundamental issues of functional genomics were performed. In the first part a very novel and promising issue of plant functional genomics, the role of miRNAs in biotic stress responses, were studied. The results confirmed that miRNAs are important regulators of defence responses in yellow rust and powdery mildew infections. Also, this study proved the existence of miRNAs in barley, in which no miRNAs are experimentally verified yet, and targets of two miRNAs (miR159 and miR169) in the same plant species. Moreover, in this thesis, existence of miRNAs in yellow rust was shown for the first time. Until now no fungal miRNAs were submitted to miRBase and the identified miRNA in yellow rust could be the first ones after biological function assays. These results are a good source for further investigation of miRNAs in yellow rust and powdery mildew infection and establishing durable resistance mechanisms.

In the second part of this thesis, gene functional analysis of a novel F-box gene (HvDRF) in barley *via* VIGS was performed. HvDRF is a ZTL-type F-box protein, and ZTL-type F-boxes are known to function in flowering. The silencing of this gene resulted in collapse of resistance to powdery mildew, which assigns a critical role to HvDRF in powdery mildew resistance responses. Hence our data, implies a novel function for ZTL-type F-box proteins which is regulating race specific immunity against biotrophic pathogens.

REFERENCES

Achard, P., Herr, A., Baulcombe, D.C., and Harberd, N.P. (2004). Modulation of floral development by a gibberellin-regulated microRNA. Development **131,** 3357-3365.

Achuo, E.A., Prinsen, E., and Hofte, M. (2006). Influence of drought, salt stress and abscisic acid on the resistance of tomato to Botrytis cinerea and Oidium neolycopersici. Plant Pathology **55,** 178-186.

Aida, M., and Tasaka, M. (2006). Genetic control of shoot organ boundaries. Current Opinion in Plant Biology **9,** 72-77.

Allen, E., Xie, Z.X., Gustafson, A.M., and Carrington, J.C. (2005). microRNA-directed phasing during trans-acting siRNA biogenesis in plants. Cell **121,** 207-221.

Allen, R.S., Li, J.Y., Stahle, M.I., Dubroue, A., Gluber, F., and Millar, A.A. (2007). Genetic analysis reveals functional redundancy and the major target genes of the Arabidopsis miR159 family. Proceedings of the National Academy of Sciences of the United States of America **104,** 16371-16376.

Ambros, V., and Chen, X.M. (2007). The regulation of genes and genomes by small RNAs. Development **134,** 1635-1641.

Asselbergh, B., De Vleesschauwer, D., and Hofte, M. (2008). Global switches and fine-tuning - ABA modulates plant pathogen defense. Molecular Plant-Microbe Interactions **21,** 709-719.

Aukerman, M.J., and Sakai, H. (2003). Regulation of flowering time and floral organ identity by a microRNA and its APETALA2-like target genes. Plant Cell **15,** 2730-2741.

Austin, M.J., Muskett, P., Kahn, K., Feys, B.J., Jones, J.D.G., and Parker, J.E. (2002). Regulatory role of SGT1 in early R gene-mediated plant defenses. Science **295,** 2077-2080.

Ausubel, F.M. (2005). Are innate immune signaling pathways in plants and animals conserved? Nature Immunology **6,** 973-979.

Axtell, M.J. (2008). Evolution of microRNAs and their targets: Are all microRNAs biologically relevant? Biochimica Et Biophysica Acta-Gene Regulatory Mechanisms **1779,** 725-734.

Beclin, C., and Vaucheret, H. (2001). PTGS in plants, a virus resistance mechanism. M S-Medecine Sciences **17,** 845-855.

Bolton, M.D., Kolmer, J.A., Xu, W.W., and Garvin, D.F. (2008). Lr34-Mediated Leaf Rust Resistance in Wheat: Transcript Profiling Reveals a High Energetic Demand Supported by Transient Recruitment of Multiple Metabolic Pathways. Molecular Plant-Microbe Interactions **21,** 1515-1527.

Bonas, U., and Lahaye, T. (2002). Plant disease resistance triggered by pathogen-derived molecules: refined models of specific recognition. Current Opinion in Microbiology **5,** 44-50.

Boualem, A., Laporte, P., Jovanovic, M., Laffont, C., Plet, J., Combier, J.P., Niebel, A., Crespi, M., and Frugier, F. (2008). MicroRNA166 controls root and nodule development in Medicago truncatula. Plant Journal **54,** 876-887.

Boutet, S., Vazquez, F., Liu, J., Beclin, C., Fagard, M., Gratias, A., Morel, J.B., Crete, P., Chen, X.M., and Vaucheret, H. (2003). Arabidopsis HEN1: A genetic link between endogenous miRNA controlling development and siRNA controlling transgene silencing and virus resistance. Current Biology **13,** 843-848.

Boyes, D.C., Nam, J., and Dangl, J.L. (1998). The Arabidopsis thaliana RPM1 disease resistance gene product is a peripheral plasma membrane protein that is degraded coincident with the hypersensitive response. Proceedings of the National Academy of Sciences of the United States of America **95,** 15849-15854.

Bozkurt, O., Unver, T., and Akkaya, M.S. (2007). Genes associated with resistance to wheat yellow rust disease identified by differential display analysis. Physiological and Molecular Plant Pathology **71,** 251-259.

Brodersen, P., and Voinnet, O. (2006). The diversity of RNA silencing pathways in plants. Trends in Genetics **22,** 268-280.

Brodersen, P., and Voinnet, O. (2009). Revisiting the principles of microRNA target recognition and mode of action. Nature Reviews Molecular Cell Biology **10,** 141-148.

Brodersen, P., Sakvarelidze-Achard, L., Bruun-Rasmussen, M., Dunoyer, P., Yamamoto, Y.Y., Sieburth, L., and Voinnet, O. (2008). Widespread translational inhibition by plant miRNAs and siRNAs. Science **320,** 1185-1190.

Burch-Smith, T.M., Anderson, J.C., Martin, G.B., and Dinesh-Kumar, S.P. (2004). Applications and advantages of virus-induced gene silencing for gene function studies in plants. Plant Journal **39,** 734-746.

Calderon-Villalobos, L.I.A., Nill, C., Marrocco, K., Kretsch, T., and Schwechheimer, C. (2007). The evolutionarily conserved Arabidopsis thaliana F-box protein AtFBP7 is required for efficient translation during temperature stress. Gene **392,** 106-116.

Cao, Y.F., Yang, Y.Y., Zhang, H.J., Li, D.Y., Zheng, Z., and Song, F.M. (2008). Overexpression of a rice defense-related F-box protein gene OsDRF1 in tobacco improves disease resistance through potentiation of defense gene expression. Physiologia Plantarum **134,** 440-452.

Cartolano, M., Castillo, R., Efremova, N., Kuckenberg, M., Zethof, J., Gerats, T., Schwarz-Sommer, Z., and Vandenbussche, M. (2007). A conserved microRNA module exerts homeotic control over Petunia hybrida and Antirrhinum majus floral organ identity. Nature Genetics **39,** 901-905.

Chapman, E.J., Prokhnevsky, A.I., Gopinath, K., Dolja, V.V., and Carrington, J.C. (2004). Viral RNA silencing suppressors inhibit the microRNA pathway at an intermediate step. Genes & Development **18,** 1179-1186.

Chen, F., Li, Q., Sun, L.X., and He, Z.H. (2006). The rice 14-3-3 gene family and its involvement in responses to biotic and abiotic stress. DNA Research **13,** 53-63.

Chen, J., Li, W.X., Xie, D.X., Peng, J.R., and Ding, S.W. (2004). Viral virulence protein suppresses RNA silencing-mediated defense but upregulates the role of MicroRNA in host gene expression. Plant Cell **16,** 1302-1313.

Chen, X.M. (2004). A microRNA as a translational repressor of APETALA2 in Arabidopsis flower development. Science **303,** 2022-2025.

Chisholm, S.T., Coaker, G., Day, B., and Staskawicz, B.J. (2006). Host-microbe interactions: Shaping the evolution of the plant immune response. Cell **124,** 803-814.

Chuck, G., Candela, H., and Hake, S. (2009). Big impacts by small RNAs in plant development. Current Opinion in Plant Biology **12,** 81-86.

Chuck, G., Cigan, A.M., Saeteurn, K., and Hake, S. (2007a). The heterochronic maize mutant Corngrass1 results from overexpression of a tandem microRNA. Nature Genetics **39,** 544-549.

Chuck, G., Meeley, R., Irish, E., Sakai, H., and Hake, S. (2007b). The maize tasselseed4 microRNA controls sex determination and meristem cell fate by targeting Tasselseed6/indeterminate spikelet1. Nature Genetics **39,** 1517-1521.

Combier, J.P., Frugier, F., de Billy, F., Boualem, A., El-Yahyaoui, F., Moreau, S., Vernie, T., Ott, T., Gamas, P., Crespi, M., and Niebel, A. (2006). MtHAP2-1 is a key transcriptional regulator of symbiotic nodule development regulated by microRNA169 in Medicago truncatula. Genes & Development **20,** 3084-3088.

Diederichs, S., and Haber, D.A. (2007). Dual role for argonautes in MicroRNA processing and Posttranscriptional regulation of MicroRNA expression. Cell **131,** 1097-1108.

Dinesh-Kumar, S.P., Burch-Smith, T., Liu, Y., Schiff, M., Dong, Y., Zhu, X., and Mamillapalli, P. (2007). Virus-induced gene silencing (VIGS) for gene function studies in plants. Phytopathology **97,** S145-S145.

Du, H., Zhang, L., Liu, L., Tang, X.F., Yang, W.J., Wu, Y.M., Huang, Y.B., and Tang, Y.X. (2009). Biochemical and molecular characterization of plant MYB transcription factor family. Biochemistry-Moscow **74,** 1-11.

Dunoyer, P., Lecellier, C.H., Parizotto, E.A., Himber, C., and Voinnet, O. (2004). Probing the microRNA and small interfering RNA pathways with virus-encoded suppressors of RNA silencing. Plant Cell **16,** 1235-1250.

Durrant, W.E., and Dong, X. (2004). Systemic acquired resistance. Annual Review of Phytopathology **42,** 185-209.

Ellis, J.G., Lawrence, G.J., Luck, J.E., and Dodds, P.N. (1999). Identification of regions in alleles of the flax rust resistance gene L that determine differences in gene-for-gene specificity. Plant Cell **11,** 495-506.

Eulgem, T. (2005). Regulation of the Arabidopsis defense transcriptome. Trends in Plant Science **10,** 71-78.

Fang, Y.D., and Spector, D.L. (2007). Identification of nuclear dicing bodies containing proteins for microRNA biogenesis in living Arabidopsis plants. Current Biology **17,** 818-823.

Ferrell, K., Wilkinson, C.R.M., Dubiel, W., and Gordon, C. (2000). Regulatory subunit interactions of the 26S proteasome, a complex problem. Trends in Biochemical Sciences **25,** 83-88.

Franco-Zorrilla, J.M., Valli, A., Todesco, M., Mateos, I., Puga, M.I., Rubio-Somoza, I., Leyva, A., Weigel, D., Garcia, J.A., and Paz-Ares, J. (2007). Target mimicry provides a new mechanism for regulation of microRNA activity. Nature Genetics **39,** 1033-1037.

Glickman, M.H., and Raveh, D. (2005). Proteasome plasticity. Febs Letters **579,** 3214-3223.

Gorbea, C., Taillandier, D., and Rechsteiner, M. (1999). Assembly of the regulatory complex of the 26S proteasome. Molecular Biology Reports **26,** 15-19.

Gray, W.M., Muskett, P.R., Chuang, H.W., and Parker, J.E. (2003). Arabidopsis SGT1b is required for SCFTIR1-mediated auxin response. Plant Cell **15,** 1310-1319.

Guddeti, S., Zhang, D.C., Li, A.L., Leseberg, C.H., Kang, H., Li, X.G., Zhai, W.X., Johns, M.A., and Mao, L. (2005). Molecular evolution of the rice miR395 gene family. Cell Research **15,** 631-638.

Guo, H.S., Xie, Q., Fei, J.F., and Chua, N.H. (2005). MicroRNA directs mRNA cleavage of the transcription factor NAC1 to downregulate auxin signals for Arabidopsis lateral root development. Plant Cell **17,** 1376-1386.

Haley, B., and Zamore, P.D. (2004). Kinetic analysis of the RNAi enzyme complex. Nature Structural & Molecular Biology **11,** 599-606.

Harmon, F., Imaizumi, T., and Gray, W.M. (2008). CUL1 regulates TOC1 protein stability in the Arabidopsis circadian clock. Plant Journal **55,** 568-579.

Heath, M.C. (2000). Hypersensitive response-related death. Plant Molecular Biology **44,** 321-334.

Hein, I., Pacak, M.B., Hrubikova, K., Williamson, S., Dinesen, M., Soenderby, I.E., Sundar, S., Jarmolowski, A., Shirasu, K., and Lacomme, C. (2005). Virus-induced gene silencing-based functional characterization of genes associated with powdery mildew resistance in barley. Plant Physiology **138,** 2155-2164.

Hernandez-Blanco, C., Feng, D.X., Hu, J., Sanchez-Vallet, A., Deslandes, L., Llorente, F., Berrocal-Lobo, M., Keller, H., Barlet, X., Sanchez-Rodriguez, C., Anderson, L.K., Somerville, S., Marco, Y., and Molina, A. (2007). Impairment of cellulose synthases required for Arabidopsis secondary cell wall formation enhances disease resistance. Plant Cell **19,** 890-903.

Ho, M.S., Ou, C., Chan, Y.R., Chien, C.T., and Pi, H. (2008). The utility F-box for protein destruction. Cellular and Molecular Life Sciences **65,** 1977-2000.

Holzberg, S., Brosio, P., Gross, C., and Pogue, G.P. (2002). Barley stripe mosaic virus-induced gene silencing in a monocot plant. Plant Journal **30,** 315-327.

Jin, H.L. (2008). Endogenous small RNAs and antibacterial immunity in plants. Febs Letters **582,** 2679-2684.

Jones-Rhoades, M.W., and Bartel, D.P. (2004). Computational identification of plant MicroRNAs and their targets, including a stress-induced miRNA. Molecular Cell **14,** 787-799.

Jones-Rhoades, M.W., Bartel, D.P., and Bartel, B. (2006). MicroRNAs and their regulatory roles in plants. Annual Review of Plant Biology **57,** 19-53.

Jones, J.D.G., and Dangl, J.L. (2006). The plant immune system. Nature **444,** 323-329.

Kasschau, K.D., Xie, Z.X., Allen, E., Llave, C., Chapman, E.J., Krizan, K.A., and Carrington, J.C. (2003). P1/HC-Pro, a viral suppressor of RNA silencing, interferes with Arabidopsis development and miRNA function. Developmental Cell **4,** 205-217.

Kawashima, C.G., Yoshimoto, N., Maruyama-Nakashita, A., Tsuchiya, Y.N., Saito, K., Takahashi, H., and Dalmay, T. (2009). Sulphur starvation induces the expression of microRNA-395 and one of its target genes but in different cell types. Plant Journal **57,** 313-321.

Kim, H.S., and Delaney, T.P. (2002). Arabidopsis SON1 is an F-box protein that regulates a novel induced defense response independent of both salicylic acid and systemic acquired resistance. Plant Cell **14,** 1469-1482.

Kim, H.S., Desveaux, D., Singer, A.U., Patel, P., Sondek, J., and Dangl, J.L. (2005a). The Pseudomonas syringae effector AvrRpt2 cleaves its C-terminally acylated target, RIN4, from Arabidopsis membranes to block RPM1 activation. Proceedings of the National Academy of Sciences of the United States of America **102,** 6496-6501.

Kim, J., Jung, J.H., Reyes, J.L., Kim, Y.S., Kim, S.Y., Chung, K.S., Kim, J.A., Lee, M., Lee, Y., Kim, V.N., Chua, N.H., and Park, C.M. (2005b). microRNA-directed cleavage of ATHB15 mRNA regulates vascular development in Arabidopsis inflorescence stems. Plant Journal **42,** 84-94.

Kim, W.Y., Hicks, K.A., and Somers, D.E. (2005c). Independent roles for EARLY FLOWERING 3 and ZEITLUPE in the control of circadian timing, hypocotyl length, and flowering time. Plant Physiology **139,** 1557-1569.

Kim, W.Y., Fujiwara, S., Suh, S.S., Kim, J., Kim, Y., Han, L.Q., David, K., Putterill, J., Nam, H.G., and Somers, D.E. (2007). ZEITLUPE is a circadian photoreceptor stabilized by GIGANTEA in blue light. Nature **449,** 356-+.

Kurihara, Y., Takashi, Y., and Watanabe, Y. (2006). The interaction between DCL1 and HYL1 is important for efficient and precise processing of pri-miRNA in plant microRNA biogenesis. Rna-a Publication of the Rna Society **12,** 206-212.

Kurucz, E., Ando, I., Sumegi, M., Holzl, H., Kapelari, B., Baumeister, W., and Udvardy, A. (2002). Assembly of the Drosophila 26 S proteasome is accompanied by extensive subunit rearrangements. Biochemical Journal **365,** 527-536.

Kutter, C., Schob, H., Stadler, M., Meins, F., and Si-Ammour, A. (2007). MicroRNA-mediated regulation of stomatal development in Arabidopsis. Plant Cell **19,** 2417-2429.

Lechner, E., Achard, P., Vansiri, A., Potuschak, T., and Genschik, P. (2006). F-box proteins everywhere. Current Opinion in Plant Biology **9,** 631-638.

Lee, Y., Ahn, C., Han, J.J., Choi, H., Kim, J., Yim, J., Lee, J., Provost, P., Radmark, O., Kim, S., and Kim, V.N. (2003). The nuclear RNase III Drosha initiates microRNA processing. Nature **425,** 415-419.

Li, J.J., Yang, Z.Y., Yu, B., Liu, J., and Chen, X.M. (2005). Methylation protects miRNAs and siRNAs from a 3 '-end uridylation activity in Arabildopsis. Current Biology **15,** 1501-1507.

Li, L., Zhao, Y.F., McCaig, B.C., Wingerd, B.A., Wang, J.H., Whalon, M.E., Pichersky, E., and Howe, G.A. (2004). The tomato homolog of CORONATINE-INSENSITIVE1 is required for the maternal control of seed maturation, jasmonate-signaled defense responses, and glandular trichome development. Plant Cell **16,** 126-143.

Lim, L.P., Glasner, M.E., Yekta, S., Burge, C.B., and Bartel, D.P. (2003). Vertebrate MicroRNA genes. Science **299,** 1540-1540.

Liu, Y., Schiff, M., Serino, G., Deng, X.W., and Dinesh-Kumar, S.P. (2002). Role of SCF ubiquitin-ligase and the COP9 signalosome in the N gene-mediated resistance response to Tobacco mosaic virus. Plant Cell **14,** 1483-1496.

Llave, C. (2004). MicroRNAs: more than a role in plant development? Molecular Plant Pathology **5,** 361-366.

Lu, S.F., Sun, Y.H., and Chiang, V.L. (2008). Stress-responsive microRNAs in Populus. Plant Journal **55,** 131-151.

Lu, S.F., Sun, Y.H., Amerson, H., and Chiang, V.L. (2007). MicroRNAs in loblolly pine (Pinus taeda L.) and their association with fusiform rust gall development. Plant Journal **51,** 1077-1098.

Mackey, D., Holt, B.F., Wiig, A., and Dangl, J.L. (2002). RIN4 interacts with Pseudomonas syringae type III effector molecules and is required for RPM1-mediated resistance in Arabidopsis. Cell **108,** 743-754.

Mackey, D., Belkhadir, Y., Alonso, J.M., Ecker, J.R., and Dangl, J.L. (2003). Arabidopsis RIN4 is a target of the type III virulence effector AvrRpt2 and modulates RPS2-mediated resistance. Cell **112,** 379-389.

Mallory, A.C., Bartel, D.P., and Bartel, B. (2005). MicroRNA-directed regulation of Arabidopsis AUXIN RESPONSE FACTOR17 is essential for proper development and modulates expression of early auxin response genes. Plant Cell **17,** 1360-1375.

Mallory, A.C., Elmayan, T., and Vaucheret, H. (2008). MicroRNA maturation and action - the expanding roles of ARGONAUTEs. Current Opinion in Plant Biology **11,** 560-566.

Mallory, A.C., Reinhart, B.J., Jones-Rhoades, M.W., Tang, G.L., Zamore, P.D., Barton, M.K., and Bartel, D.P. (2004). MicroRNA control of PHABULOSA in leaf development: importance of pairing to the microRNA 5 ' region. Embo Journal **23,** 3356-3364.

Mazzucotelli, E., Belloni, S., Marone, D., De Leonardis, A.M., Guerra, D., Fonzo, N., Cattivelli, L., and Mastrangelo, A.M. (2006). The E3 ubiquitin ligase gene family in plants: Regulation by degradation. Current Genomics **7,** 509-522.

McDonald, B.A., and Linde, C. (2002). The population genetics of plant pathogens and breeding strategies for durable resistance. Euphytica **124,** 163-180.

Megraw, M., Baev, V., Rusinov, V., Jensen, S.T., Kalantidis, K., and Hatzigeorgiou, A.G. (2006). MicroRNA promoter element discovery in Arabidopsis. Rna-a Publication of the Rna Society **12,** 1612-1619.

Mishra, N.S., Tuteja, R., and Tuteja, N. (2006). Signaling through MAP kinase networks in plants. Archives of Biochemistry and Biophysics **452,** 55-68.

Montgomery, T.A., Yoo, S.J., Fahlgren, N., Gilbert, S.D., Howell, M.D., Sullivan, C.M., Alexander, A., Nguyen, G., Allen, E., Ahn, J.H., and Carrington, J.C. (2008). AGO1-miR173 complex initiates phased siRNA formation in plants. Proceedings of the National Academy of Sciences of the United States of America **105,** 20055-20062.

Nagasaki, H., Itoh, J.I., Hayashi, K., Hibara, K.I., Satoh-Nagasawa, N., Nosaka, M., Mukouhata, M., Ashikari, M., Kitano, H., Matsuoka, M., Nagato, Y., and Sato, Y. (2007). The small interfering RNA production pathway is required for shoot meristern initiation in rice. Proceedings of the National Academy of Sciences of the United States of America **104,** 14867-14871.

Navarro, L., Jay, F., Nomura, K., He, S.Y., and Voinnet, O. (2008). Suppression of the microRNA pathway by bacterial effector proteins. Science **321,** 964-967.

Navarro, L., Dunoyer, P., Jay, F., Arnold, B., Dharmasiri, N., Estelle, M., Voinnet, O., and Jones, J.D.G. (2006). A plant miRNA contributes to antibacterial resistance by repressing auxin signaling. Science **312,** 436-439.

Nikovics, K., Blein, T., Peaucelle, A., Ishida, T., Morin, H., Aida, M., and Laufs, P. (2006). The balance between the MIR164A and CUC2 genes controls leaf margin serration in Arabidopsis. Plant Cell **18,** 2929-2945.

Nirmala, J., Dahl, S., Steffenson, B.J., Kannangara, C.G., von Wettstein, D., Chen, X.M., and Kleinhofs, A. (2007). Proteolysis of the barley receptor-like protein kinase RPG1 by a proteasome pathway is correlated with Rpg1-mediated stem rust resistance. Proceedings of the National Academy of Sciences of the United States of America **104,** 10276-10281.

Nogueira, F.T.S., Madi, S., Chitwood, D.H., Juarez, M.T., and Timmermans, M.C.P. (2007). Two small regulatory RNAs establish opposing fates of a developmental axis. Genes & Development **21,** 750-755.

Ori, N., Cohen, A.R., Etzioni, A., Brand, A., Yanai, O., Shleizer, S., Menda, N., Amsellem, Z., Efroni, I., Pekker, I., Alvarez, J.P., Blum, E., Zamir, D., and Eshed, Y. (2007). Regulation of LANCEOLATE by miR319 is required for compound-leaf development in tomato. Nature Genetics **39,** 787-791.

Palatnik, J.F., Allen, E., Wu, X.L., Schommer, C., Schwab, R., Carrington, J.C., and Weigel, D. (2003). Control of leaf morphogenesis by microRNAs. Nature **425,** 257-263.

Parizotto, E.A., Dunoyer, P., Rahm, N., Himber, C., and Voinnet, O. (2004). In vivo investigation of the transcription, processing, endonucleolytic activity, and functional relevance of the spatial distribution of a plant miRNA. Genes & Development **18,** 2237-2242.

Park, W., Li, J.J., Song, R.T., Messing, J., and Chen, X.M. (2002). CARPEL FACTORY, a Dicer homolog, and HEN1, a novel protein, act in microRNA metabolism in Arabidopsis thaliana. Current Biology **12,** 1484-1495.

Penninckx, I.A.M.A., Thomma, B.P.H.J., Buchala, A., Metraux, J.P., and Broekaert, W.F. (1998). Concomitant activation of jasmonate and ethylene response pathways is required for induction of a plant defensin gene in Arabidopsis. Plant Cell **10,** 2103-2113.

Pfaffl, M.W., and Meyer, H.H.D. (2006). Quantification of candidate gene mRNA expression in food producing animals using qRT-PCR. Zuchtungskunde **78,** 440-450.

Poethig, R.S., Peragine, A., Yoshikawa, M., Hunter, C., Willmann, M., and Wu, G. (2006). The function of RNAi in plant development. Cold Spring Harbor Symposia on Quantitative Biology **71,** 165-17060 4.

Pogue, G.P., Lindbo, J.A., Garger, S.J., and Fitzmaurice, W.P. (2002). Making an ally from an enemy: Plant virology and the new agriculture. Annual Review of Phytopathology **40,** 45-74.

Pouch-Pelissier, M.N., Pelissier, T., Elmayan, T., Vaucheret, H., Boko, D., Jantsch, M.F., and Deragon, J.M. (2008). SINE RNA Induces Severe Developmental Defects in Arabidopsis thaliana and Interacts with HYL1 (DRB1), a Key Member of the DCL1 Complex. Plos Genetics **4,** -.

Qiu, D.Y., Pan, X.P., Wilson, I.W., Li, F.L., Liu, M., Teng, W.J., and Zhang, B.H. (2009). High throughput sequencing technology reveals that the taxoid elicitor methyl jasmonate regulates microRNA expression in Chinese yew (Taxus chinensis). Gene **436,** 37-44.

Reyes, J.L., and Chua, N.H. (2007). ABA induction of miR159 controls transcript levels of two MYB factors during Arabidopsis seed germination. Plant Journal **49,** 592-606.

Rowland, O., Ludwig, A.A., Merrick, C.J., Baillieul, F., Tracy, F.E., Durrant, W.E., Fritz-Laylin, L., Nekrasov, V., Sjolander, K., Yoshioka, H., and Jones, J.D.G. (2005). Functional analysis of Avr9/Cf-9 rapidly elicited genes identifies a protein kinase, ACIK1, that is essential for full Cf-9-dependent disease resistance in tomato. Plant Cell **17,** 295-310.

Seo, N.S., Lee, S.K., Song, M.Y., Suh, J.P., Hahn, T.R., Ronald, P., and Jeon, J.S. (2008). The HSP90-SGT1-RAR1 molecular chaperone complex: a core modulator in plant immunity. Journal of Plant Biology **51,** 1-10.

Shao, Y., Zhu, H.L., Tian, H.Q., Wang, X.G., Lin, X.J., Zhu, B.Z., Xie, Y.H., and Luo, Y.B. (2008). Virus-induced gene silencing in plant species. Russian Journal of Plant Physiology **55,** 168-174.

Shen, W.H., Parmentier, Y., Hellmann, H., Lechner, E., Dong, A.W., Masson, J., Granier, F., Lepiniec, L., Estelle, M., and Genschik, P. (2002). Null mutation of AtCUL1 causes arrest in early embryogenesis in Arabidopsis. Molecular Biology of the Cell **13,** 1916-1928.

Sieber, P., Wellmer, F., Gheyselinck, J., Riechmann, J.L., and Meyerowitz, E.M. (2007). Redundancy and specialization among plant microRNAs: role of the MIR164 family in developmental robustness. Development **134,** 1051-1060.

Simon-Mateo, C., and Garcia, J.A. (2006). MicroRNA-Guided processing impairs Plum pox virus replication, but the virus readily evolves to escape this silencing mechanism. Journal of Virology **80,** 2429-2436.

Smalle, J., and Vierstra, R.D. (2004). The ubiquitin 26S proteasome proteolytic pathway. Annual Review of Plant Biology **55,** 555-590.

Somers, D.E. (2001). Clock-associated genes in Arabidopsis: a family affair. Philosophical Transactions of the Royal Society of London Series B-Biological Sciences **356,** 1745-1753.

Song, D., Chen, J., Song, F., and Zheng, Z. (2006). A novel rice MAPK gene, OsBIMK2, is involved in disease-resistance responses. Plant Biology **8,** 587-596.

Souret, F.F., Kastenmayer, J.P., and Green, P.J. (2004). AtXRN4 degrades mRNA in Arabidopsis and its substrates include selected miRNA targets. Molecular Cell **15,** 173-183.

Sunkar, R., Chinnusamy, V., Zhu, J.H., and Zhu, J.K. (2007). Small RNAs as big players in plant abiotic stress responses and nutrient deprivation. Trends in Plant Science **12,** 301-309.

Swiderski, M.R., Birker, D., and Jones, J.D.G. (2009). The TIR Domain of TIR-NB-LRR Resistance Proteins Is a Signaling Domain Involved in Cell Death Induction. Molecular Plant-Microbe Interactions **22,** 157-165.

Takeda, A., Iwasaki, S., Watanabe, T., Utsumi, M., and Watanabe, Y. (2008). The mechanism selecting the guide strand from small RNA duplexes is different among Argonaute proteins. Plant and Cell Physiology **49,** 493-500.

Thao, N.P., Chen, L., Nakashima, A., Hara, S.I., Umemura, K., Takahashi, A., Shirasu, K., Kawasaki, T., and Shimamoto, K. (2007). RAR1 and HSP90 form a complex with Rac/Rop GTPase and function in innate-immune responses in rice. Plant Cell **19,** 4035-4045.

Ulrich, G., Seong, K.Y., Boddu, J., Cho, S.H., Trail, F., Xu, J.R., Adam, G., Mewes, H.W., Muehlbauer, G.J., and Kistler, H.C. (2006). Development of a Fusarium graminearum Affymetrix GeneChip for profiling fungal gene expression in vitro and in planta. Fungal Genetics and Biology **43,** 316-325.

Valencia-Sanchez, M.A., Liu, J.D., Hannon, G.J., and Parker, R. (2006). Control of translation and mRNA degradation by miRNAs and siRNAs. Genes & Development **20,** 515-524.

Van der Hoorn, R.A.L., De Wit, P.J.G.M., and Joosten, M.H.A.J. (2002). Balancing selection favors guarding resistance proteins. Trends in Plant Science **7,** 67-71.

Vaucheret, H., Vazquez, F., Crete, P., and Bartel, D.P. (2004). The action of ARGONAUTE1 in the miRNA pathway and its regulation by the miRNA pathway are crucial for plant development. Genes & Development **18,** 1187-1197.

Vazquez, F., Gasciolli, V., Crete, P., and Vaucheret, H. (2004a). The nuclear dsRNA binding protein HYL1 is required for MicroRNA accumulation and plant development, but not posttranscriptional transgene silencing. Current Biology **14,** 346-351.

Vazquez, F., Blevins, T., Ailhas, J., Boller, T., and Meins, F. (2008). Evolution of Arabidopsis MIR genes generates novel microRNA classes. Nucleic Acids Research **36,** 6429-6438.

Vazquez, F., Vaucheret, H., Rajagopalan, R., Lepers, C., Gasciolli, V., Mallory, A.C., Hilbert, J.L., Bartel, D.P., and Crete, P. (2004b). Endogenous trans-acting siRNAs regulate the accumulation of Arabidopsis mRNAs. Molecular Cell **16,** 69-79.

Vierstra, R.D. (2003). The ubiquitin/26S proteasome pathway, the complex last chapter in the life of many plant proteins. Trends in Plant Science **8,** 135-142.

Voinnet, O. (2009). Origin, Biogenesis, and Activity of Plant MicroRNAs. Cell **136,** 669-687.

Wang, J.W., Wang, L.J., Mao, Y.B., Cai, W.J., Xue, H.W., and Chen, X.Y. (2005). Control of root cap formation by microRNA-targeted auxin response factors in Arabidopsis. Plant Cell **17,** 2204-2216.

Williams, L., Grigg, S.P., Xie, M.T., Christensen, S., and Fletcher, J.C. (2005). Regulation of Arabidopsis shoot apical meristem and lateral organ formation by microRNA miR166g and its AtHD-ZIP target genes. Development **132,** 3657-3668.

Wrzaczek, M., and Hirt, H. (2001). Plant MAP kinase pathways: how many and what for? Biology of the Cell **93,** 81-87.

Wu, G., and Poethig, R.S. (2006). Temporal regulation of shoot development in Arabidopsis thaliana by miR156 and its target SPL3. Development **133,** 3539-3547.

Xie, Z.X., Kasschau, K.D., and Carrington, J.C. (2003). Negative feedback regulation of Dicer-Like1 in Arabidopsis by microRNA-guided mRNA degradation. Current Biology **13,** 784-789.

Xie, Z.X., Allen, E., Fahlgren, N., Calamar, A., Givan, S.A., and Carrington, J.C. (2005). Expression of Arabidopsis MIRNA genes. Plant Physiology **138,** 2145-2154.

Xie, Z.X., Johansen, L.K., Gustafson, A.M., Kasschau, K.D., Lellis, A.D., Zilberman, D., Jacobsen, S.E., and Carrington, J.C. (2004). Genetic and functional diversification of small RNA pathways in plants. Plos Biology **2,** 642-652.

Xu, G.X., Ma, H., Nei, M., and Kong, H.Z. (2009). Evolution of F-box genes in plants: Different modes of sequence divergence and their relationships with functional diversification. Proceedings of the National Academy of Sciences of the United States of America **106,** 835-840.

Yamasaki, H., Abdel-Ghany, S.E., Cohu, C.M., Kobayashi, Y., Pilon, M., and Shikanai, T. (2007). The mechanism of adaptation to copper deficient conditions via microRNA in Arabidopsis. Plant and Cell Physiology **48,** S106-S106.

Yang, Z.Y., Ebright, Y.W., Yu, B., and Chen, X.M. (2006). HEN1 recognizes 21-24 nt small RNA duplexes and deposits a methyl group onto the 2 ' OH of the 3 ' terminal nucleotide. Nucleic Acids Research **34,** 667-675.

You, J.X., and Pickart, C.M. (2001). A HECT domain E3 enzyme assembles novel polyubiquitin chains. Journal of Biological Chemistry **276,** 19871-19878.

Yu, B., Bi, L., Zheng, B.L., Ji, L.J., Chevalier, D., Agarwal, M., Ramachandran, V., Li, W.X., Lagrange, T., Walker, J.C., and Chen, X.M. (2008). The FHA domain proteins DAWDLE in Arabidopsis and SNIP1 in humans act in small RNA biogenesis. Proceedings of the National Academy of Sciences of the United States of America **105,** 10073-10078.

Yu, S.W., and Tang, K.X. (2004). MAP kinase cascades responding to environmental stress in plants. Acta Botanica Sinica **46,** 127-136.

Zeng, L.R., Vega-Sanchez, M.E., Zhu, T., and Wang, G.L. (2006). Ubiquitination-mediated protein degradation and modification: an emerging theme in plant-microbe interactions. Cell Research **16,** 413-426.

Zhang, M.H., Boter, M., Li, K.Y., Kadota, Y., Panaretou, B., Prodromou, C., Shirasu, K., and Pearl, L.H. (2008). Structural and functional coupling of Hsp90-and Sgt1-centred multi-protein complexes. Embo Journal **27,** 2789-2798.

Zhang, T., Liu, Y., Yang, T., Zhang, L., Xu, S., Xue, L., and An, L. (2006). Diverse signals converge at MAPK cascades in plant. Plant Physiology and Biochemistry **44,** 274-283.

Zhao, B.T., Liang, R.Q., Ge, L.F., Li, W., Xiao, H.S., Lin, H.X., Ruan, K.C., and Jin, Y.X. (2007). Identification of drought-induced microRNAs in rice. Biochemical and Biophysical Research Communications **354,** 585-590.

Zilberstein, C.B.Z., Ziv-Ukelson, M., Pinter, R.Y., and Yakhini, Z. (2006). A high-throughput approach for associating MicroRNAs with their activity conditions. Journal of Computational Biology **13,** 245-266.

Zoltowski, B.D., Schwerdtfeger, C., Widom, J., Loros, J.J., Bilwes, A.M., Dunlap, J.C., and Crane, B.R. (2007). Conformational switching in the fungal light sensor vivid. Science **316,** 1054-1057.

APPENDIX A

SEQUENCES OF BSMV GENOMES

1) BSMV α genome sequence:

GTATGTAAGTTGCCTTTGGGTGTAAAATTTCTTGCATGCACATAATCGTAATCGATTCTTCTTGATCTCTAAACAACACTTTCCCGT
TAGCATGGCTAGCGATGAGATTGTCCGCAATCTGATCTCCCGTGAGGAGGTGATGGGTAATTTGATTAGCACAGCTTCTAGCTCAGT
AAGGTCACCCTTACATGACGTACTGTGCTCGCACGTAAGGACCATCGTCGATTCCGTGGATAAGAAAGCGGTCAGTCGCAAGCATGT
TGATGTACGGCGCAACATCTCCTCTGAAGAGTTACAGATGTTGATAAATGCATATCCTGAATATGCCGTTTCATCCTCAGCTTGTGA
ATCTGGTACTCATAGCATGGCGGCTTGTTTTCGATTTCTGGAGACAGAATACCTCTTAGATATGGTTCCAATGAAAGAGACTTTTGT
TTATGACATTGGTGGTAACTGGTTTTCTCATATGAAGTTTCGTGCTGATAGAGAAATTCATTGTTGCTGTCCGATCTTATCTATGAG
AGATTCTGAAAGACTGGAAACACGCATGATGGCAATGCAAAAATATATGCGTGGATCGAAAGACAAACCGTTACGCTTGTTAAGCCG
TTATCAAAATATCCTGCGTGAACAAGCGGCGAGAACAACTGCCTTTATGGCAGGTGAGGTGAATGCGGGTGTTCTCGATGGAGATGT
GTTTTGTGAGAACACTTTTCAAGACTGTGTGAGACAGGTGCCCGAAGGTTTTTTGAAGACAGCTATAGCAGTTCATAGCATCTACGA
TATCAAAGTGGAAGAATTTGCGTCTGCATTGAAAAGAAAAGGTATAACACAGGCTTATGGGTGCTTCCTGTTTCCTCCTGCTGTATT
GATAGGTCAGAAGGAAGGTATTTTACCTTCCGTGGACGGTCATTACTTGGTGGAGAATGGCAGGATTAAGTTCTTCTTTGCGAATGA
TCCGAATGCCGGTTACTCTCATGACCTTAAGGATTATCTGAAGTATGTGGAAAAAACCTACGTGGATATAAAGGATGGAGTGTTTGC
TATTGAGCTGATGCAAATGCGAGGTGATACCATGTTCTTTAAGATCACGGATGTCACCGCAGCAATGTATCATATGAAATACAGAGG
TATGAAACGTGATGAAACATTCAAATGCATTCCGTTGCTAAAAAATTCATCCGTTGTCGTACCTCTATTTTCGTGGGACAACCGTTC
TTTAAAGATCACAAGTGGTTTATTACCACGAACTTTGGTCGAGCAAGGTGCGGCGTTTATTATGAAAAACAAGGAGAAGGACTTGAA
CGTTGCTGTGTTGAAGAACTATCTTTCCGCTGTGAACAACTCATACATTTTCAACGGATCCCAGGTTAGAGATGGTGTGAAAATTGC
CCCGGATTTAATCTCCAAATTGGCAGTGACTCTGTACCTGAGAGAAAAGGTCTATCGACAAAGAGAAAATTCAATCATAAGTTATTT
CGAGCAAGAAATGCTTCACGATCCCAACTTGAAAGCCATGTTTGGAGACTTTCTGTGGTTTGTTCCAAATACTCTCTCGAGTGTCTG
GAAGAACATGCGAAAATCACTGATGGAATGGTTTGGCTACGCAGAATTTGACTTGACTACTTTTGATATTTGCGATCCCGTTCTCTA
CGTAGAGATAGTGGATCGGTATAAGATCATTCAAAAAGGGCGAATTCCACTTGGTGAGTTTTTTGATTGTCATGAAGAATGCGAGAA
TTACGAACTGCGTGAGAAGGAGAAAAATGACCTAGCGGTGAAAATGGCCCAGAAGGTAACAGGGACGGTGACCGAATGCGAGAAGGA
CCTGGGACCTCTTGTTCAACCGATAAAACAGATATTGGTTCAACTTGTGATGCCCAATTTGGTCAGAGCGCTGTGTAGACCTCGTAG
CCCAACGTCTCCTTTGGACTTAAATATCCCAGGGTCAACTCCATCACACTCAAGTTCAGATTCTGAACAATCTATGACTGAAGAAGC
GAGCTGCGCCATTGCGGGTAGCGTACCAACATGGGAAATTGCGACTAAGAAAGATCTAACCTTTCAGCGAATTGATGAAGATATGTC
TCGACGAACTGGTATGCCTCCAAGACCAAAAGTAACTTCTAGTTACAACATGAATGCCAGAGCTGAGTTTCTCTACTATCAACTGTG
TAGCGTGATTTGTGAAAGGGCTCAGATTTTGAGTGTCATCGAAGACTTTCGTCAGAATTTGATATTCTCAGATAAAGTGGCCGTTCC
ATTGAACGCTAGATTCTACAGTTTTCAGTCATTGCAACCCGGATGGGTGTTCAAGACTCCATCGCATAGTGAAGTAGGCCACAGTTA
TGCAGTACATTTTGACTTCAAGACAGTTGGAACCGATTTGGAAGAGAGCCTAGCTTTTTGCCGAATGGTACCGATTTCATGGGATAA
AAGCGGCAAATACATCGCGACAACTCCTCATTTTCCCGAGAGACATGGTTACTACGTGATTTGTGACAACACTAAATTGTGTAACAA
TTGGCTTATTTACAATAAGTTAGTTGATGTCTACGCACGAGTGGCTGATAGACCTCTGAGATTTGAGTTGATTGACGGAGTTCCTGG
CTGCGGAAAGTCAACCATGATTTTAAACAGCTGTGATATTCGACGCGAAGTTGTTGTTGGTGAAGGAAGGAATGCAACTGATGACTT
AAGGGAGAGGTTCAAGCGTAAGAAAAATTTGAATAGTAAGACTGCTAATCATAGAGTTCGAACGCTTGACAGCTTATTACTTGCTGA
AGGACCTTGTGTACCGCAAGCTGATAGGTTTCATTTTGATGAAGCTCTAAAAGTTCATTACGGCGCCATAATGTTCTGTGCTGATAA
GCTTGGTGCCTCAGAAATTCTCGCTCAGGGAGATAGGGCTCAACTGCCGATGATCTGTCGTGTAGAAGGTATTGAACTTCAATTTCA
ATCTCCTGATTACACGAAGACGATCATAAATCCTAAGCTACGATCATACCGTATCCCTGGAGATGTTGCCTTCTATTTGAGTGCTAA
GGAATTTTACAAAGTTAAAGGAATACCTCAAAAGGTTACAACTTCTAACAGTGTGAAACGTTCCCTGTACGCTAGAGGCGAAACAAC
TCCGGAAAGATTCGTGAGTTTGCTTGATGTTCCGGTGAGAAAAAACACCCATTATCTAACCTTCTTACAAGCTGAGAAGGAAAGTTT
GATGAGTCATTTGATTCCAAAGGGTGTGAAGAAAGAGTCTATTTCAACGATTCATGAGGCGCAGGGTGGTACCTATGAAAATGTGAT
TCTGGTCCGTTTGCAACGGACGCCCAATGAAATTTATCCGGGTGGACCTAGGTCCGCCCCTTACATTGTGGTTGGGACTTCAAGGCA
TACAAAAACTTTCACTTATTGTAGTGTTACGGACGATAAGTTGCTTTTAGATATCGCCGACGTCGGTGGTATTGCACATACACCTAT
TCGTACTTTTGAATCTCATATAGTTTAAAAAAAAAAAAAAAAAAAAAAAAAAAAAAAAAAAAAAAAAAAAATGTTTGATCAGATCATTC
AAATCTGATGGTGCCCATCAACCATATGATGGGAGTGTTTGCAAGTCCACTATAATCGAACTTGAAAACGATGCCTGAATTGGAAAC
CATGAATCTTAACGGATTCTGGAGAGAAAATTTAGGAATTGGTATGTAAGCTACAACTTCCGGTAGCTGCGTCACACTTTAAGAGTG
TGCATACTGAGCCGAAGCTCAGCTTCGGTCCCCCAAGGGAAGACCA

2) BSMV β genome sequence:

CTTCCGCTTCCTCGCTCACTGACTCGCTGCGCTCGGTCGTTCGGCTGCGGCGAGCGGTATCAGCTCACTCAAAGGCGGTAATACGGT
TATCCACAGAATCAGGGGATAACGCAGGAAAGAACATGTGAGCAAAAGGCCAGCAAAAGGCCAGGAACCGTAAAAAGGCCGCGTTGC
TGGCGTTTTTCCATAGGCTCCGCCCCCCTGACGAGCATCACAAAAATCGACGCTCAAGTCAGAGGTGGCGAAACCCGACAGGACTAT
AAAGATACCAGGCGTTTCCCCCTGGAAGCTCCCTCGTGCGCTCTCCTGTTCCGACCCTGCCGCTTACCGGATACCTGTCCGCCTTTC
TCCCTTCGGGAAGCGTGGCGCTTTCTCATAGCTCACGCTGTAGGTATCTCAGTTCGGTGTAGGTCGTTCGCTCCAAGCTGGGCTGTG
TGCACGAACCCCCCGTTCAGCCCGACCGCTGCGCCTTATCCGGTAACTATCGTCTTGAGTCCAACCCGGTAAGACACGACTTATCGC
CACTGGCAGCAGCCACTGGTAACAGGATTAGCAGAGCGAGGTATGTAGGCGGTGCTACAGAGTTCTTGAAGTGGTGGCCTAACTACG
GCTACACTAGAAGGACAGTATTTGGTATCTGCGCTCTGCTGAAGCCAGTTACCTTCGGAAAAAGAGTTGGTAGCTCTTGATCCGGCA
AACAAACCACCGCTGGTAGCGGTGGTTTTTTTGTTTGCAAGCAGCAGATTACGCGCAGAAAAAAAGGATCTCAAGAAGATCCTTTGA
TCTTTTCTACGGGGTCTGACGCTCAGTGGAACGAAAACTCACGTTAAGGGATTTTGGTCATGAGATTATCAAAAAGGATCTTCACCT
AGATCCTTTTAAATTAAAAATGAAGTTTTAAATCAATCTAAAGTATATATGAGTAAACTTGGTCTGACAGTTACCAATGCTTAATCA
GTGAGGCACCTATCTCAGCGATCTGTCTATTTCGTTCATCCATAGTTGCCTGACTCCCCGTCGTGTAGATAACTACGATACGGGAGG
GCTTACCATCTGGCCCCAGTGCTGCAATGATACCGCGAGACCCACGCTCACCGGCTCCAGATTTATCAGCAATAAACCAGCCAGCCG
GAAGGGCCGAGCGCAGAAGTGGTCCTGCAACTTTATCCGCCTCCATCCAGTCTATTAATTGTTGCCGGGAAGCTAGAGTAAGTAGTT
CGCCAGTTAATAGTTTGCGCAACGTTGTTGCCATTGCTACAGGCATCGTGGTGTCACGCTCGTCGTTTGGTATGGCTTCATTCAGCT
CCGGTTCCCAACGATCAAGGCGAGTTACATGATCCCCCATGTTGTGCAAAAAAGCGGTTAGCTCCTTCGGTCCTCCGATCGTTGTCA
GAAGTAAGTTGGCCGCAGTGTTATCACTCATGGTTATGGCAGCACTGCATAATTCTCTTACTGTCATGCCATCCGTAAGATGCTTTT
CTGTGACTGGTGAGTACTCAACCAAGTCATTCTGAGAATAGTGTATGCGGCGACCGAGTTGCTCTTGCCCGGCGTCAATACGGGATA
ATACCGCGCCACATAGCAGAACTTTAAAAGTGCTCATCATTGGAAAACGTTCTTCGGGGCGAAAACTCTCAAGGATCTTACCGCTGT
TGAGATCCAGTTCGATGTAACCCACTCGTGCACCCAACTGATCTTCAGCATCTTTTACTTTCACCAGCGTTTCTGGGTGAGCAAAAA
CAGGAAGGCAAAATGCCGCAAAAAAGGGAATAAGGGCGACACGGAAATGTTGAATACTCATACTCTTCCTTTTTCAATATTATTGAA
GCATTTATCAGGGTTATTGTCTCATGAGCGGATACATATTTGAATGTATTTAGAAAAATAAACAAATAGGGGTTCCGCGCACATTTC
CCCGAAAAGTGCCACCTGAAATTGTAAACGTTAATATTTTGTTAAAATTCGCGTTAAATTTTTGTTAAATCAGCTCATTTTTTAACC
AATAGGCCGAAATCGGCAAAATCCCTTATAAATCAAAAGAATAGACCGAGATAGGGTTGAGTGTTGTTCCAGTTTGGAACAAGAGTC
CACTATTAAAGAACGTGGACTCCAACGTCAAAGGGCGAAAAACCGTCTATCAGGGCGATGGCCCACTACGTGAACCATCACCCTAAT
CAAGTTTTTTGGGGTCGAGGTGCCGTAAAGCACTAAATCGGAACCCTAAAGGGATGCCCCGATTTAGAGCTTGACGGGGAAAGCCGG
CGAACGTGGCGAGAAAGGAAGGGAAGAAAGCGAAAGGAGCGGGCGCTAGGGCGCTGGCAAGTGTAGCGGTCACGCTGCGCGTAACCA
CCACACCCGCCGCGCTTAATGCGCCGCTACAGGGCGCGTCCCATTCGCCATTCAGGCTGCGCAACTGTTGGGAAGGGCGATCGGTGC
GGGCCTCTTCGCTATTACGCCAGCTGGCGAAAGGGGGATGTGCTGCAAGGCGATTAAGTTGGGTAACGCCAGGGTTTTCCCAGTCAC
GACGTTGTAAAACGACGGCCAGTGAATTAATACGACTCACTATAGTAAAAGAAAAGGAACAACCCTGTTGTTGTTCGACGCTATACT
AAATATATATTATCTTATTAGTGCATTTCTTTTACCACTTCACAGTATGCCGAACGTTTCTTTGACTGCTAAGGGTGGAGGACACTA
CAACGAGGATCAATGGGATACACAAGTTGTGGAAGCCGGAGTATTTGACGATTGGTGGGTCCACGTAGAAGCCTGGAATAAATTTCT
AGACAATTTACGTGGTATCAACTTTAGCGTTGCTTCCTCTCGGTCGCAAGTCGCTGAATGCTTAGCTGCGTTAGATCGTGATCTACC
TGCTGATGTAGACAGACGGTTTGCAGGTGCTAGAGGACAAATTGGTTTACCCAATTATCTTCCTGCGCCAAAATTCTTTCGTCTCGA
TAAGCGAACTATCGCTGAACTGACTAGACTCTCTCGTCTTACGGATCAGCCGCACAACAATCGTGATATAGAGCTTAACCGAGCGAA
AAGAGCCACAACTAACCCATCTCCCCCGGCGCAGGCACCGTCGGAGAATCTTACTCTTCGTGATGTTCAACCGTTAAAGGATAGTGC
GTTGCATTATCAATACGTGTTGATTGACCTACAGAGTGCGAGACTCCCAGTGTATACCAGGAAGACTTTCGAACGTGAACTCGCTTT
GGAATGGATCATTCCAGATGCCGAGGAAGCGTGACCTGCTGTTGAAGCGGTAAAAGGATGTACATATGTATCTTATTTATTTTGTTT
ATCTATTTTCTTTTACTTTTAGTTTTTGCTTTTTACGCGTTAACTAGATGTATTGACTTTAGCCATGGACATGACGAAAACTGTTGA
GGAAAAGAAAACAAATGGAACTGATTCAGTGAAAGGTGTTTTTGAAAACTCGACGATTCCCAAAGTTCCGACTGGACAGGAAATGGG
TGGTGACGATTCTTCTACTTCTAAATTAAAGGAAACTCTAAAAGTTGCCGATCAGACTCCATTGTCCGTTGACAACGGTGCCAAATC
CAAATTGGATTCTTCTGATAGACAAGTTCCTGGTCCTAAGTTGGCAACAACTGTGGAAAAGGAACCTGAGTTGAAACCCAACGTTAA
GAAGTCCAAGAAGAAAAGAATCCAAAAACCTGCTCAACCGAGTAGGCCCAATGACCTTAAAGGCGGGACTAAGGGATCATCTCAAGT
GGGTGAAAATGTGAGTGAGAACTATACTGGGATTTCTAAGGAAGCAGCTAAGCAAAAGCAGAAGACACCCAAGTCTGTGAAAATGCA
AAGCAATCTGGCCGATAAGTTCAAAGCGAATGATACTCGTAGATCGGAATTAATTAACAAGTTTCAGCAATTTGTGCATGAAACCTG
TCTTAAATCTGATTTTGAGTACACTGGTCGACAGTATTTCAGAGCTAGATCAAATTTCTTTGAAATGATTAAGCTCGCATCCTTGTA
TGACAAACATCTAAAGGAATGTATGGCGCGAGCCTGCACCCTAGAACGAGAACGATTGAAGCGTAAGTTACTCCTAGTACGAGCTTT
GAAACCAGCAGTTGACTTCCTTACGGGAATCATCTCTGGAGTTCCTGGCTCAGGAAAATCAACCATTGTGCGTACTTTGCTCAAAGG
TGAATTTCCGGCTGTTTGTGCTTTGGCCAATCCTGCCTTAATGAACGACTATTCTGGTATTGAAGGCGTTTACGGGTTAGATGACCT
GTTGCTTTCTGCAGTTCCGATAACGTCTGATTTATTGATCATAGATGAATATACACTTGCTGAGAGCGCGGAAATCCTGTTGTTACA
ACGAAGACTCAGAGCCTCTATGGTGTTGTTAGTCGGGGATGTAGCTCAAGGAAAAGCCACCACTGCTTCCAGTATTGAGTATTTAAC
TCTGCCGGTGATCTACAGATCAGAGACGACTTATCGTTTGGGACAAGAGACTGCTTCGCTTTGCAGCAAGCAGGGTAACAGAATGGT
TTCAAAGGGTGGAAGGGACACAGTGATCATTACTGATTACGATGGCGAAACAGATGGAACGGAGAAAAATATCGCTTTTACTGTCGA
TACAGTTCGAGATGTGAAAGATTGCGGGTACGATTGTGCCCTGGCAATTGATGTGCAAGGGAAAGAATTCGATTCAGTGACTTTATT

CCTAAGGAACGAAGACCGGAAAGCTTTAGCAGATAAGCATTTGCGTTTAGTCGCTTTGAGCAGACATAAGTCGAAGTTAATCATCAG
GGCCGACGCGGAAATTCGTCAAGCATTCCTGACAGGTGATATTGACTTGAGCTCTAAGGCGAGTAACTCTCATCGTTATTCTGCAAA
ACCGGATGAAGACCACAGTTGGTTCAAGGCCAAATAAGTATTGGCCAATTGTCGCCGGAATCGGTGTCGTTGGATTGTTTGCGTATT
TGATCTTTTCAAATCAAAAACATTCTACGGAATCCGGCGATAATATTCACAAATTCGCCAACGGAGGTAGTTACAGGGACGGGTCAA
AGAGTATAAGTTATAATCGTAATCATCCTTTTGCCTATGGCAATGCCTCATCCCCTGGAATGTTGTTGCCCGCAATGCTTACCATCA
TCGGAATCATTTCCTATTTATGGCGAACAAGAGATTCCGTGCTCGGAGACTCAGGCGGAAACAATTCCTGCGGAGAAGACTGTCAGG
GCGAATGTCTTAACGGACATTCTCGACGATCATTACTATGCGATATTGGCTAGTCTTTTTATCATTGCTCTATGGTTATTGTATATA
TATCTAAGCAGTATACCTACGGAGACTGGTCCCTACTTCTATCAAGATCTGAACTCTGTGAAGATCTATGGAATAGGGGCTACGAAT
CCAGAAGTTATTGCGGCCATCCACCATTGGCAGAAGTACCCTTTTGGGGAATCTCCGATGTGGGGAGGTTTAGTCAGTGTTTTGAGC
GTTCTTCTTAAACCGCTGACGTTAGTTTTTGCGTTAAGCTTTTTTCTCTTACTTTCTTCAAAAAGGTAAAAAAAAAAAAAAAAAAAA
TGTTTGATCAGATCATTCAAATCTGATGGTGCCCATCAACCATATGATGGGAGTGTTTGCAAGTCCACTATAATCGAACTTGAAAAC
GATGCCTGAATTGGAAACCATGAATCTTAACGGATTCTGGAGAGAAAATTTAGGAATTGGTATGTAAGCTACAACTTCCGGTAGCTG
CGTCACACTTTAAGAGTGTGCATACTGAGCCGAAGCTCAGCTTCGGTCCCCCAAGGGAAGACCACTAGTCATGCAAGCTTTCCCTAT
AGTGAGTCGTATTAGAGCTTGGCGTAATCATGGTCATAGCTGTTTCCTGTGTGAAATTGTTATCCGCTCACAATTCCACACAACATA
CGAGCCGGAAGCATAAAGTCTAAAGCCTGGGGTGCCTAATGAGTGAGCTAACTCACATTAATTGCGTTGCGCTCACTGCCCGCTTTC
CAGTCGGGAAACCTGTCGTGCCAGCTGCATTAATGAATCGGCCAACGCGCGGGGAGAGGCGGTTTGCGTATTGGGCGCT

3) BSMV γ genome sequence:

CTTCCGCTTCCTCGCTCACTGACTCGCTGCGCTCGGTCGTTCGGCTGCGGCGAGCGGTATCAGCTCACTCAAAGGCGGTAATACGGT
TATCCACAGAATCAGGGGATAACGCAGGAAAGAACATGTGAGCAAAAGGCCAGCAAAAGGCCAGGAACCGTAAAAAGGCCGCGTTGC
TGGCGTTTTTCCATAGGCTCCGCCCCCCTGACGAGCATCACAAAAATCGACGCTCAAGTCAGAGGTGGCGAAACCCGACAGGACTAT
AAAGATACCAGGCGTTTCCCCCTGGAAGCTCCCTCGTGCGCTCTCCTGTTCCGACCCTGCCGCTTACCGGATACCTGTCCGCCTTTC
TCCCTTCGGGAAGCGTGGCGCTTTCTCATAGCTCACGCTGTAGGTATCTCAGTTCGGTGTAGGTCGTTCGCTCCAAGCTGGGCTGTG
TGCACGAACCCCCCGTTCAGCCCGACCGCTGCGCCTTATCCGGTAACTATCGTCTTGAGTCCAACCCGGTAAGACACGACTTATCGC
CACTGGCAGCAGCCACTGGTAACAGGATTAGCAGAGCGAGGTATGTAGGCGGTGCTACAGAGTTCTTGAAGTGGTGGCCTAACTACG
GCTACACTAGAAGGACAGTATTTGGTATCTGCGCTCTGCTGAAGCCAGTTACCTTCGGAAAAAGAGTTGGTAGCTCTTGATCCGGCA
AACAAACCACCGCTGGTAGCGGTGGTTTTTTTGTTTGCAAGCAGCAGATTACGCGCAGAAAAAAAGGATCTCAAGAAGATCCTTTGA
TCTTTTCTACGGGGTCTGACGCTCAGTGGAACGAAAACTCACGTTAAGGGATTTTGGTCATGAGATTATCAAAAAGGATCTTCACCT
AGATCCTTTTAAATTAAAAATGAAGTTTTAAATCAATCTAAAGTATATATGAGTAAACTTGGTCTGACAGTTACCAATGCTTAATCA
GTGAGGCACCTATCTCAGCGATCTGTCTATTTCGTTCATCCATAGTTGCCTGACTCCCCGTCGTGTAGATAACTACGATACGGGAGG
GCTTACCATCTGGCCCCAGTGCTGCAATGATACCGCGAGACCCACGCTCACCGGCTCCAGATTTATCAGCAATAAACCAGCCAGCCG
GAAGGGCCGAGCGCAGAAGTGGTCCTGCAACTTTATCCGCCTCCATCCAGTCTATTAATTGTTGCCGGGAAGCTAGAGTAAGTAGTT
CGCCAGTTAATAGTTTGCGCAACGTTGTTGCCATTGCTACAGGCATCGTGGTGTCACGCTCGTCGTTTGGTATGGCTTCATTCAGCT
CCGGTTCCCAACGATCAAGGCGAGTTACATGATCCCCCATGTTGTGCAAAAAAGCGGTTAGCTCCTTCGGTCCTCCGATCGTTGTCA
GAAGTAAGTTGGCCGCAGTGTTATCACTCATGGTTATGGCAGCACTGCATAATTCTCTTACTGTCATGCCATCCGTAAGATGCTTTT
CTGTGACTGGTGAGTACTCAACCAAGTCATTCTGAGAATAGTGTATGCGGCGACCGAGTTGCTCTTGCCCGGCGTCAATACGGGATA
ATACCGCGCCACATAGCAGAACTTTAAAAGTGCTCATCATTGGAAAACGTTCTTCGGGGCGAAAACTCTCAAGGATCTTACCGCTGT
TGAGATCCAGTTCGATGTAACCCACTCGTGCACCCAACTGATCTTCAGCATCTTTTACTTTCACCAGCGTTTCTGGGTGAGCAAAAA
CAGGAAGGCAAAATGCCGCAAAAAAGGGAATAAGGGCGACACGGAAATGTTGAATACTCATACTCTTCCTTTTTCAATATTATTGAA
GCATTTATCAGGGTTATTGTCTCATGAGCGGATACATATTTGAATGTATTTAGAAAAATAAACAAATAGGGGTTCCGCGCACATTTC
CCCGAAAAGTGCCACCTGAAATTGTAAACGTTAATATTTTGTTAAAATTCGCGTTAAATTTTTGTTAAATCAGCTCATTTTTTAACC
AATAGGCCGAAATCGGCAAAATCCCTTATAAATCAAAAGAATAGACCGAGATAGGGTTGAGTGTTGTTCCAGTTTGGAACAAGAGTC
CACTATTAAAGAACGTGGACTCCAACGTCAAAGGGCGAAAAACCGTCTATCAGGGCGATGGCCCACTACGTGAACCATCACCCTAAT
CAAGTTTTTTGGGGTCGAGGTGCCGTAAAGCACTAAATCGGAACCCTAAAGGGATGCCCCGATTTAGAGCTTGACGGGGAAAGCCGG
CGAACGTGGCGAGAAAGGAAGGGAAGAAAGCGAAAGGAGCGGGCGCTAGGGCGCTGGCAAGTGTAGCGGTCACGCTGCGCGTAACCA
CCACACCCGCCGCGCTTAATGCGCCGCTACAGGGCGCGTCCCATTCGCCATTCAGGCTGCGCAACTGTTGGGAAGGGCGATCGGTGC
GGGCCTCTTCGCTATTACGCCAGCTGGCGAAAGGGGGATGTGCTGCAAGGCGATTAAGTTGGGTAACGCCAGGGTTTTCCCAGTCAC
GACGTTGTAAAACGACGGCCAGTGAATTAATACGACTCACTATAGTATAGCTTGAGCATTACCGTCGTGTAATTGCAACACTTGGCT
TGCCAAATAACGCTAAAGCGTTCACGAAACAAACAACACTTCGGCATGGATGTTGTGAAGAAATTCGCCGTCATGTCAGTGACTGTA
GTAGCAGGTCCCGTCCTTACGCTTTCATCACCTGTGGTGGTGACGTTTGGAACAGGCTTAATTGCCGTATCTTTGGTGAAACGGTTG
CTACAGGAACAACCCCGTGTAATTGCTCACGATCACGAACATTACCCAGGTGGTTCTGAGAGCAGTTCTAGCTCTTGTGCTACCGCG
CCTATTTTACGTAATCTTTCGCGAGATCAGTGCGATTCAGAGAATATTGGATGCAGTTCTAGCGCCTGTTCTCCGTCTGAAATTGTG
AAAGTTACAAGGCAGGTAGTGGGAGTTGAACGTGGTCTTTACCGGGACATTTTTCAGGACAACGAAATCCCATCAGTCATGGAAGAG
AAACTGCAGAAACTCCTTTACTCTGAGGGTGAGAAGATTCGAAGACGTTGCCAATTTGAAGCATCAACGATGCACTCACGCAAAGTA

AAGGTTCCGGAGGTAGGTACTATCCCAGATATCCAAACTTGGTTCGATGCTACGTTTCCTGGTAACTCCGTTAGGTTTTCTGATTTC
GACGGTTATACTGTTGCTACGGAGGACATTAACATGGATGTTCAGGATTGTAGACTTAAGTTCGGGAAGACTTTTCGACCTTATGAA
TTTAAGGAATCACTGAAACCAGTACTGAGGACAGCAATGCCAGAAAAACGACAGGGTAGTTTGATTGAAAGTGTGCTGGCCTTTCGT
AAAAGAAATTTGGCTGCGCCCAGATTACAAGGAGCTTTGAATGAATGGCACACAATTGAGAATGTGCTAACGAAGGCGTTAAAGGTA
TTCTTCTTTGAAGATTTAATTGATCGAACGGATCACTGCACTTACGAGTCAGCGCTCAGATGGTGGGATAAACAATCAGTGACAGCT
CGAGCGCAGCTCGTGGCGGATCAGCGGAGGTTATGTGATGTTGACTTCACGACTTATAACTTCATGATAAAAAATGATGTAAAGCCG
AAGTTAGATCTAACACCTCAAGTTGAATATGCAGCTTTGCAGACTGTTGTATATCCTGATAAGATAGTCAATGCTTTCTTTGGTCCG
ATCATAAAGGAGATTAATGAACGGATCATCAGAGCGCTTAGACCTCATGTGGTCTTTAATTCTCGTATGACTGCTGATGAACTGAAT
GAAACAGCTGCCTTTTTGACACCTCATAAGTACAGAGCCTTAGAGATTGATTTTTCAAAATTTGATAAATCAAAGACTGGGCTTCAT
ATCAAAGCTGTCATTGGACTCTATAAGCTCTTTGGCCTAGATGGCCTGTTAAAAGTGCTCTGGGAAAAATCGCAATATCAGACTTAC
GTGAAAGATAGAAACTTCGGTCTCGAGGCATATCTATTGTATCAGCAAAAGTCAGGAAATTGTGACACTTACGGTTCGAACACCTGG
TCTGCCGCCTTGGCGTTGTTAGATTGTCTTCCTTTGGAAGATGCACATTTCTGTGTATTTGGTGGTGATGATTCATTGATATTGTTT
GATCAGGGATACATAATTTCCGACCCATGCCGGCAACTTGCCGGTACTTGGAATCTTGAATGTAAAGTGTTCGACTTCAAGTACCCC
GCATTTTGTGGTAAATTTCTGCTGTGCATAGATGGAAAATATCAATTTGTTCCAGATGCGGCAAAATTTATCACAAAATTAGGTAGA
ACTGATGTGAGAGATGTAGAAGTTTTGAGTGAGATTTATATCTCTATCAATGACAATTACAAATCTTACAAAGACTTTAAGGTGCTT
GATGCTTTGGATAAGGCTTTAGTGGATAGATATCGATCCCCTTATAGTGCTATTTCTGCTTTGGTTTCTTTATGTTATCATATCTTT
GACTTTAATAAGTTTAAGTTGCTGTTTAATTGTGAAGGGAAATTTGTGGATAAGAAGCTGAGAAAAGACTTCGAGTGGTGAACTCTA
GGTCCTGATGTTTAAATCTACTGTATTTACCTTCGCATGATGGCTACTTTCTCTTGTGTGTGTTGTGGTACCTTAACTACAAGTACT
TACTGTGGTAAGAGATGTGAGCGAAAGCATGTATATTCTGAAACAAGAAATAAGAGATTGGAACTTTACAAGAAGTATCTATTGGAA
CCGCAAAAATGCGCCCTGAATGGAATCGTTGGACACAGTTGTGGAATGCCATGCTCCATTGCGGAAGAGGCTTGTGATCAACTGCCA
ATCGTGAGTAGGTTCTGTGGCCAAAAGCATGCGGATCTGTATGATTCACTTCTGAAACGTTCTGAACAGGAGTTACTTCTTGAATTT
CTCCAGAAGAAGATGCAGGAGCTGAAACTTTCTCATATCGTAAAAATGGCTAAGCTTGAAAGTGAGGTTAACGCAATACGTAAGTCC
GTAGCTTCTTCTTTTGAAGATTCTGTTGGATGTGATGATTCTTCTTCCGTTTCTAAGTAAAAAAAAAAAAAAAATGTTTGATCAGATC
ATTCAAATCTGATGGTGCCCATCAACCATATGATGGGAGTGTTTGCAAGTCCACTATAATCGAACTTGAAAACGATGCCTGAATTGG
AAACCATGAATCTTAACGGACTCTGGAGAGAAAATTTAGGAATTGGTATGTAAGCTACAACTTCCGGTAGCTGCGTCACACTTTAAG
AGTGTGCATACTGAGCCGAAGCTCAGCTTCGGTCCCCCAAGGGAAGACCACGCGTCATGCAAGCTTTCCCTATAGTGAGTCGTATTA
GAGCTTGGCGTAATCATGGTCATAGCTGTTTCCTGTGTGAAATTGTTATCCGCTCACAATTCCACACAACATACGAGCCGGAAGCAT
AAAGTCTAAAGCCTGGGGTGCCTAATGAGTGAGCTAACTCACATTAATTGCGTTGCGCTCACTGCCCGCTTTCCAGTCGGGAAACCT
GTCGTGCCAGCTGCATTAATGAATCGGCCAACGCGCGGGGAGAGGCGGTTTGCGTATTGGGCGCT

4) pγpds4As sequence:

CTTCCGCTTCCTCGCTCACTGACTCGCTGCGCTCGGTCGTTCGGCTGCGGCGAGCGGTATCAGCTCACTCAAAGGCGGTAATACGGT
TATCCACAGAATCAGGGGATAACGCAGGAAAGAACATGTGAGCAAAAGGCCAGCAAAAGGCCAGGAACCGTAAAAAGGCCGCGTTGC
TGGCGTTTTTCCATAGGCTCCGCCCCCCTGACGAGCATCACAAAAATCGACGCTCAAGTCAGAGGTGGCGAAACCCGACAGGACTAT
AAAGATACCAGGCGTTTCCCCCTGGAAGCTCCCTCGTGCGCTCTCCTGTTCCGACCCTGCCGCTTACCGGATACCTGTCCGCCTTTC
TCCCTTCGGGAAGCGTGGCGCTTTCTCATAGCTCACGCTGTAGGTATCTCAGTTCGGTGTAGGTCGTTCGCTCCAAGCTGGGCTGTG
TGCACGAACCCCCCGTTCAGCCCGACCGCTGCGCCTTATCCGGTAACTATCGTCTTGAGTCCAACCCGGTAAGACACGACTTATCGC
CACTGGCAGCAGCCACTGGTAACAGGATTAGCAGAGCGAGGTATGTAGGCGGTGCTACAGAGTTCTTGAAGTGGTGGCCTAACTACG
GCTACACTAGAAGGACAGTATTTGGTATCTGCGCTCTGCTGAAGCCAGTTACCTTCGGAAAAAGAGTTGGTAGCTCTTGATCCGGCA
AACAAACCACCGCTGGTAGCGGTGGTTTTTTTGTTTGCAAGCAGCAGATTACGCGCAGAAAAAAAGGATCTCAAGAAGATCCTTTGA
TCTTTTCTACGGGGTCTGACGCTCAGTGGAACGAAAACTCACGTTAAGGGATTTTGGTCATGAGATTATCAAAAAGGATCTTCACCT
AGATCCTTTTAAATTAAAAATGAAGTTTTAAATCAATCTAAAGTATATATGAGTAAACTTGGTCTGACAGTTACCAATGCTTAATCA
GTGAGGCACCTATCTCAGCGATCTGTCTATTTCGTTCATCCATAGTTGCCTGACTCCCCGTCGTGTAGATAACTACGATACGGGAGG
GCTTACCATCTGGCCCCAGTGCTGCAATGATACCGCGAGACCCACGCTCACCGGCTCCAGATTTATCAGCAATAAACCAGCCAGCCG
GAAGGGCCGAGCGCAGAAGTGGTCCTGCAACTTTATCCGCCTCCATCCAGTCTATTAATTGTTGCCGGGAAGCTAGAGTAAGTAGTT
CGCCAGTTAATAGTTTGCGCAACGTTGTTGCCATTGCTACAGGCATCGTGGTGTCACGCTCGTCGTTTGGTATGGCTTCATTCAGCT
CCGGTTCCCAACGATCAAGGCGAGTTACATGATCCCCCATGTTGTGCAAAAAAGCGGTTAGCTCCTTCGGTCCTCCGATCGTTGTCA
GAAGTAAGTTGGCCGCAGTGTTATCACTCATGGTTATGGCAGCACTGCATAATTCTCTTACTGTCATGCCATCCGTAAGATGCTTTT
CTGTGACTGGTGAGTACTCAACCAAGTCATTCTGAGAATAGTGTATGCGGCGACCGAGTTGCTCTTGCCCGGCGTCAATACGGGATA
ATACCGCGCCACATAGCAGAACTTTAAAAGTGCTCATCATTGGAAAACGTTCTTCGGGGCGAAAACTCTCAAGGATCTTACCGCTGT
TGAGATCCAGTTCGATGTAACCCACTCGTGCACCCAACTGATCTTCAGCATCTTTTACTTTCACCAGCGTTTCTGGGTGAGCAAAAA
CAGGAAGGCAAAATGCCGCAAAAAAGGGAATAAGGGCGACACGGAAATGTTGAATACTCATACTCTTCCTTTTTCAATATTATTGAA
GCATTTATCAGGGTTATTGTCTCATGAGCGGATACATATTTGAATGTATTTAGAAAAATAAACAAATAGGGGTTCCGCGCACATTTC
CCCGAAAAGTGCCACCTGAAATTGTAAACGTTAATATTTTGTTAAAATTCGCGTTAAATTTTTGTTAAATCAGCTCATTTTTTAACC

AATAGGCCGAAATCGGCAAAATCCCTTATAAATCAAAAGAATAGACCGAGATAGGGTTGAGTGTTGTTCCAGTTTGGAACAAGAGTC
CACTATTAAAGAACGTGGACTCCAACGTCAAAGGGCGAAAAACCGTCTATCAGGGCGATGGCCCACTACGTGAACCATCACCCTAAT
CAAGTTTTTTGGGGTCGAGGTGCCGTAAAGCACTAAATCGGAACCCTAAAGGGATGCCCCGATTTAGAGCTTGACGGGGAAAGCCGG
CGAACGTGGCGAGAAAGGAAGGGAAGAAAGCGAAAGGAGCGGGCGCTAGGGCGCTGGCAAGTGTAGCGGTCACGCTGCGCGTAACCA
CCACACCCGCCGCGCTTAATGCGCCGCTACAGGGCGCGTCCCATTCGCCATTCAGGCTGCGCAACTGTTGGGAAGGGCGATCGGTGC
GGGCCTCTTCGCTATTACGCCAGCTGGCGAAAGGGGGATGTGCTGCAAGGCGATTAAGTTGGGTAACGCCAGGGTTTTCCCAGTCAC
GACGTTGTAAAACGACGGCCAGTGAATTAATACGACTCACTATAGTATAGCTTGAGCATTACCGTCGTGTAATTGCAACACTTGGCT
TGCCAAATAACGCTAAAGCGTTCACGAAACAAACAACACTTCGGCATGGATGTTGTGAAGAAATTCGCCGTCATGTCAGTGACTGTA
GTAGCAGGTCCCGTCCTTACGCTTTCATCACCTGTGGTGGTGACGTTTGGAACAGGCTTAATTGCCGTATCTTTGGTGAAACGGTTG
CTACAGGAACAACCCCGTGTAATTGCTCACGATCACGAACATTACCCAGGTGGTTCTGAGAGCAGTTCTAGCTCTTGTGCTACCGCG
CCTATTTTACGTAATCTTTCGCGAGATCAGTGCGATTCAGAGAATATTGGATGCAGTTCTAGCGCCTGTTCTCCGTCTGAAATTGTG
AAAGTTACAAGGCAGGTAGTGGGAGTTGAACGTGGTCTTTACCGGGACATTTTTCAGGACAACGAAATCCCATCAGTCATGGAAGAG
AAACTGCAGAAACTCCTTTACTCTGAGGGTGAGAAGATTCGAAGACGTTGCCAATTTGAAGCATCAACGATGCACTCACGCAAAGTA
AAGGTTCCGGAGGTAGGTACTATCCCAGATATCCAAACTTGGTTCGATGCTACGTTTCCTGGTAACTCCGTTAGGTTTTCTGATTTC
GACGGTTATACTGTTGCTACGGAGGACATTAACATGGATGTTCAGGATTGTAGACTTAAGTTCGGGAAGACTTTTCGACCTTATGAA
TTTAAGGAATCACTGAAACCAGTACTGAGGACAGCAATGCCAGAAAAACGACAGGGTAGTTTGATTGAAAGTGTGCTGGCCTTTCGT
AAAAGAAATTTGGCTGCGCCCAGATTACAAGGAGCTTTGAATGAATGGCACACAATTGAGAATGTGCTAACGAAGGCGTTAAAGGTA
TTCTTCTTTGAAGATTTAATTGATCGAACGGATCACTGCACTTACGAGTCAGCGCTCAGATGGTGGGATAAACAATCAGTGACAGCT
CGAGCGCAGCTCGTGGCGGATCAGCGGAGGTTATGTGATGTTGACTTCACGACTTATAACTTCATGATAAAAAATGATGTAAAGCCG
AAGTTAGATCTAACACCTCAAGTTGAATATGCAGCTTTGCAGACTGTTGTATATCCTGATAAGATAGTCAATGCTTTCTTTGGTCCG
ATCATAAAGGAGATTAATGAACGGATCATCAGAGCGCTTAGACCTCATGTGGTCTTTAATTCTCGTATGACTGCTGATGAACTGAAT
GAAACAGCTGCCTTTTTGACACCTCATAAGTACAGAGCCTTAGAGATTGATTTTTCAAAATTTGATAAATCAAAGACTGGGCTTCAT
ATCAAAGCTGTCATTGGACTCTATAAGCTCTTTGGCCTAGATGGCCTGTTAAAAGTGCTCTGGGAAAAATCGCAATATCAGACTTAC
GTGAAAGATAGAAACTTCGGTCTCGAGGCATATCTATTGTATCAGCAAAAGTCAGGAAATTGTGACACTTACGGTTCGAACACCTGG
TCTGCCGCCTTGGCGTTGTTAGATTGTCTTCCTTTGGAAGATGCACATTTCTGTGTATTTGGTGGTGATGATTCATTGATATTGTTT
GATCAGGGATACATAATTTCCGACCCATGCCGGCAACTTGCCGGTACTTGGAATCTTGAATGTAAAGTGTTCGACTTCAAGTACCCC
GCATTTTGTGGTAAATTTCTGCTGTGCATAGATGGAAAATATCAATTTGTTCCAGATGCGGCAAAATTTATCACAAAATTAGGTAGA
ACTGATGTGAGAGATGTAGAAGTTTTGAGTGAGATTTATATCTCTATCAATGACAATTACAAATCTTACAAAGACTTTAAGGTGCTT
GATGCTTTGGATAAGGCTTTAGTGGATAGATATCGATCCCCTTATAGTGCTATTTCTGCTTTGGTTTCTTTATGTTATCATATCTTT
GACTTTAATAAGTTTAAGTTGCTGTTTAATTGTGAAGGGAAATTTGTGGATAAGAAGCTGAGAAAAGACTTCGAGTGGTGAACTCTA
GGTCCTGATGTTTAAATCTACTGTATTTACCTTCGCATGATGGCTACTTTCTCTTGTGTGTGTTGTGGTACCTTAACTACAAGTACT
TACTGTGGTAAGAGATGTGAGCGAAAGCATGTATATTCTGAAACAAGAAATAAGAGATTGGAACTTTACAAGAAGTATCTATTGGAA
CCGCAAAAATGCGCCCTGAATGGAATCGTTGGACACAGTTGTGGAATGCCATGCTCCATTGCGGAAGAGGCTTGTGATCAACTGCCA
ATCGTGAGTAGGTTCTGTGGCCAAAAGCATGCGGATCTGTATGATTCACTTCTGAAACGTTCTGAACAGGAGTTACTTCTTGAATTT
CTCCAGAAGAAGATGCAGGAGCTGAAACTTTCTCATATCGTAAAAATGGCTAAGCTTGAAAGTGAGGTTAACGCAATACGTAAGTCC
GTAGCTTCTTCTTTTGAAGATTCTGTTGGATGTGATGATTCTTCTTCCGTTGCTAGCTGAGCGGCCGCCTACTTTCAGGAGGATTAC
CATCCAAGAATGCCATTTTCGAGCCATGCGTCTCCTGGAGAAAACGGTTTAGAGCAATCAGAATGCACTGCATGGATAACTCGTCAG
GGTTTATGAAATTGAGGGCCTTGGACATTGCAATGAAAACCTCGTCGTTGACTCGATCAGGAACACCCTGCTTTTCCATCCAGTTAA
TTAATCAGCTAGCTAAAAAAAAAAAAAAAAATGTTTGATCAGATCATTCAAATCTGATGGTGCCCATCAACCATATGATGGGAGTGTTT
GCAAGTCCACTATAATCGAACTTGAAAACGATGCCTGAATTGGAAACCATGAATCTTAACGGACTCTGGAGAGAAAATTTAGGAATT
GGTATGTAAGCTACAACTTCCGGTAGCTGCGTCACACTTTAAGAGTGTGCATACTGAGCCGAAGCTCAGCTTCGGTCCCCCAAGGGA
AGACCAATTTAAATGCGCGCGTCATGCAAGCTTTCCCTATAGTGAGTCGTATTAGAGCTTGGCGTAATCATGGTCATAGCTGTTTCC
TGTGTGAAATTGTTATCCGCTCACAATTCCACACAACATACGAGCCGGAAGCATAAAGTCTAAAGCCTGGGGTGCCTAATGAGTGAG
CTAACTCACATTAATTGCGTTGCGCTCACTGCCCGCTTTCCAGTCGGGAAACCTGTCGTGCCAGCTGCATTAATGAATCGGCCAACG
CGCGGGGAGAGGCGGTTTGCGTATTGGGCGCT

APPENDIX B

CT-VALUES OF QRT-PCR EXPERIMENTS

MAP kinase

Well	Well Name	Ct (dR)
A1	18s c-6	11.88
A2	18s c-6	11.7
A3	18s c-6	11.73
A4	18s c-12	12.88
A5	18s c-12	13.1
A6	18s c-12	13.07
A7	18s c-24	14.1
A8	18s c-24	13.6
A9	18s c-24	13.8
A10	18s c-48	12.1
A11	18s c-48	12.7
A12	18s c-48	12.3
B1	18s b95-6	13.08
B2	18s b95-6	12.58
B3	18s b95-6	12.65
B4	18s b95-12	10.94
B5	18s b95-12	10.91
B6	18s b95-12	10.2
B7	18s b95-24	23.51
B8	18s b95-24	23.53
B9	18s b95-24	21.04
B10	18s b95-48	15.72
B11	18s b95-48	15.8
B12	18s b95-48	15.73
C1	18s b103-6	11.55
C2	18s b103-6	11.94
C3	18s b103-6	12.39
C4	18s b103-12	15.04
C5	18s b103-12	14.84
C6	18s b103-12	14.84
C7	18s b103-24	21.25
C8	18s b103-24	21.91
C9	18s b103-24	24.14
C10	18s b103-48	17.71
C11	18s b103-48	19.39
C12	18s b103-48	19.81
D1	MAPk c-6	19.84
D2	MAPk c-6	19.42
D3	MAPk c-6	19.56
D4	MAPk c-12	23.8
D5	MAPk c-12	23.64
D6	MAPk c-12	24.19
D7	MAPk c-24	34.14
D8	MAPk c-24	34.93
D9	MAPk c-24	34.36
E1	MAPk b95-6	23.25
E2	MAPk b95-6	23.12
E3	MAPk b95-6	23.14
E4	MAPk b95-12	20.29
E5	MAPk b95-12	20.16
E10	MAPk b95-48	27.35
E11	MAPk b95-48	29.64
E12	MAPk b95-48	30.13
F1	MAPk b103-6	23.68
F2	MAPk b103-6	23.49
F3	MAPk b103-6	23.71
F4	MAPk b103-12	23.7
F5	MAPk b103-12	23.62
F6	MAPk b103-12	24.12
F11	MAPk b103-48	24.8
F12	MAPk b103-48	24.61

GAMyb

Well	Well Name	Ct (dR)
A1	18s control 6	13.1
A2	18s control 6	13.02
A3	18s control 6	12.82
A4	18s control 12	12.62
A5	18s control 12	12.52
A6	18s control 12	12.66
A7	18s control 24	13.01
A8	18s control 24	13.18
A9	18s control 24	12.74
A10	18s control 48	12.38
A11	18s control 48	12.32
A12	18s control 48	12.17
B1	18 s b95 6	12
B2	18 s b95 6	11.99
B3	18 s b95 6	11.73
B4	18 s b95 12	12.27
B5	18 s b95 12	12.63
B6	18 s b95 12	12.21
B7	18 s b95 24	12.54
B8	18 s b95 24	12.67
B9	18 s b95 24	12.55
B10	18 s b95 48	12.24
B11	18 s b95 48	12.21
B12	18 s b95 48	12.27
C1	18 s b103 6	13.61
C2	18 s b103 6	13.25
C3	18 s b103 6	13.36
C4	18 s b103 12	12.92

GAMyb		
C8	18 s b103 24	11.45
C9	18 s b103 24	11.59
C10	18 s b103 48	12.11
C11	18 s b103 48	12.01
C12	18 s b103 48	12.26
E1	myb control 6	29.32
E2	myb control 6	28.97
E3	myb control 6	29.21
E4	myb control 12	29.19
E5	myb control 12	28.99
E6	myb control 12	29.01
E7	myb control 24	29.61
E8	myb control 24	29.73
E9	myb control 24	29.02
E10	myb control 48	28.51
E11	myb control 48	28.47
E12	myb control 48	28.49
F1	myb b95 6	39.15
F2	myb b95 6	28.48
F3	myb b95 6	28.1
F4	myb b95 12	27.44
F5	myb b95 12	27.2
F6	myb b95 12	27.09
F7	myb b95 24	28.51
F8	myb b95 24	29.09
F9	myb b95 24	28.36
F10	myb b95 48	28.04
F11	myb b95 48	28.11
F12	myb b95 48	28.31
G1	myb b103 6	34.96
G3	myb b103 6	29.49
G4	myb b103 12	27.72
G6	myb b103 12	27.3
G7	myb b103 24	26.77
G8	myb b103 24	27.03
G9	myb b103 24	26.87
G10	myb b103 48	28.45
G11	myb b103 48	28.55
G12	myb b103 48	28.32

	DNA J	
Well	Well Name	Ct (dR)
A1	18s control 6	12.91
A2	18s control 6	13.04
A3	18s control 6	13.09
A4	18s control 12	12.55
A5	18s control 12	12.74
A6	18s control 12	12.73
A7	18s control 24	12.98
A8	18s control 24	13.06
A9	18s control 24	13.31
A10	18s control 48	12.29
A11	18s control 48	12.17
A12	18s control 48	12.31
B1	18s b95 6	11.26
B2	18s b95 6	11.09
B3	18s b95 6	11.09
B4	18s b95 12	11.71
B5	18s b95 12	11.56
B6	18s b95 12	11.88
B7	18s b95 24	12.26
B8	18s b95 24	12.3
B9	18s b95 24	12.18
B10	18s b95 48	11.82
B11	18s b95 48	11.91
B12	18s b95 48	12.23
C1	18s b103 6	13.36
C2	18s b103 6	13.36
C3	18s b103 6	13.17
C4	18s b103 12	13.14
C5	18s b103 12	13.05
C6	18s b103 12	13.22
C7	18s b103 24	11.34
C8	18s b103 24	11.79
C9	18s b103 24	11.75
C10	18s b103 48	12.11
C11	18s b103 48	12.26
C12	18s b103 48	12.68
D1	dnaj control 6	24.57
D2	dnaj control 6	24.51
D3	dnaj control 6	24.7
D4	dnaj control 12	24.24
D5	dnaj control 12	23.85
D6	dnaj control 12	24.09
D7	dnaj control 24	24.26
D8	dnaj control 24	24.24
D9	dnaj control 24	24.28
D10	dnaj control 48	24.37
D11	dnaj control 48	23.73
D12	dnaj control 48	24.2
E1	dnaj b95 6	29.59
E2	dnaj b95 6	23.8
E3	dnaj b95 6	23.17
E4	dnaj b95 12	23.03
E5	dnaj b95 12	22.67
E6	dnaj b95 12	22.53
E7	dnaj b95 24	23.42
E8	dnaj b95 24	23.37
E9	dnaj b95 24	23.27
E10	dnaj b95 48	23.8
E11	dnaj b95 48	24.03
E12	dnaj b95 48	23.53
F1	dnaj b103 6	24.9
F2	dnaj b103 6	24.76
F3	dnaj b103 6	24.59
F4	dnaj b103 12	22.23
F5	dnaj b103 12	22.3
F6	dnaj b103 12	22.42
F7	dnaj b103 24	22.69
F8	dnaj b103 24	22.28
F9	dnaj b103 24	22.14

Cellulose synthase		
Well	Well Name	Ct
A1	18s control 6	13.46
A2	18s control 6	13.26
A3	18s control 6	13.37
A4	18s control 12	13.16
A5	18s control 12	12.93
A6	18s control 12	13.29
A7	18s control 24	13.36
A8	18s control 24	13.48
A9	18s control 24	13.19
A10	18s control 48	12.63
A11	18s control 48	12.72
A12	18s control 48	12.63
B1	18s b95 6	11.97
B2	18s b95 6	11.8
B3	18s b95 6	14.43
B4	18s b95 12	12.31
B5	18s b95 12	12.29
B6	18s b95 12	12.41
B7	18s b95 24	12.82
B8	18s b95 24	13.1
B9	18s b95 24	12.44
B10	18s b95 48	12.6
B11	18s b95 48	12.63
B12	18s b95 48	12.18
C1	18s b103 6	14.03
C2	18s b103 6	13.33
C3	18s b103 6	13.26
C4	18s b103 12	13.07
C5	18s b103 12	13.25
C6	18s b103 12	13.25
C7	18s b103 24	11.75
C8	18s b103 24	11.98
C9	18s b103 24	11.92
C10	18s b103 48	12.39
C11	18s b103 48	12.28
C12	18s b103 48	12.24
D1	cell synthase	26.09
D2	cell synthase	25.68
D3	cell synthase	25.56
D4	cell synthase	26.21
D5	cell synthase	26.23
D6	cell synthase	26.03
D7	cell synthase	26.08
D8	cell synthase	26.16
D9	cell synthase	26.1
D10	cell synthase	25.17
D11	cell synthase	25.15
D12	cell synthase	25.24
E1	cell synthase b95	25.22
E2	cell synthase b95	24.61
E3	cell synthase b95	24.66
E4	cell synthase b95	24.54
E5	cell synthase b95	24.45
E6	cell synthase b95	24.31
E7	cell synthase b95	25.31
E8	cell synthase b95	25.36
E9	cell synthase b95	26
E10	cell synthase b95	25.21
E11	cell synthase b95	24.78
E12	cell synthase b95	25.19
F1	cell synthase	26.76
F2	cell synthase	26.35
F3	cell synthase	26.14
F4	cell synthase	24.32
F5	cell synthase	24.63
F6	cell synthase	24.89
F7	cell synthase	24.19
F8	cell synthase	24.08
F9	cell synthase	24.17
F10	cell synthase	26.02
F11	cell synthase	25.61
F12	cell synthase	25.57

Hsp90		
Well	Well Name	Ct (dR)
A1	18s c 6	15.17
A2	18s c 12	14.65
A3	18s c 24	14.51
A4	18s c 48	13.75
A5	18s b95 6	12.32
A6	18s b95 12	13.16
A7	18s b95 24	13.67
A8	18s b95 48	14.04
A9	18s b103 6	14.74
A10	18s b103 12	14.05
A11	18s b103 24	13.32
A12	18s b103 48	15.09
B1	hsp90 control 6	26.86
B2	hsp90 control 6	27.11
B3	hsp90 control 6	27.03
B4	hsp90 control 12	27.56
B5	hsp90 control 12	27.53
B6	hsp90 control 12	27.04
B7	hsp90 control 24	27.41
B8	hsp90 control 24	29.24
B9	hsp90 control 24	28.26
B10	hsp90 control 48	27.62
B11	hsp90 control 48	31.73
B12	hsp90 control 48	27.46
C1	hsp90 b95 6	26.45
C2	hsp90 b95 6	26.06
C3	hsp90 b95 6	26.28
C4	hsp90 b95 12	26.85
C5	hsp90 b95 12	26.09
C6	hsp90 b95 12	27.05
C7	hsp90 b95 24	27.05
C8	hsp90 b95 24	27.17
C9	hsp90 b95 24	26.97
C10	hsp90 b95 48	26.89
C11	hsp90 b95 48	26.67

APPENDIX C

miRNA MICROARRAY ANALYSIS RESULTS

Chip: 01_METU_071010

Sample A: 232b – Cy3
Sample B: mock-a – Cy5

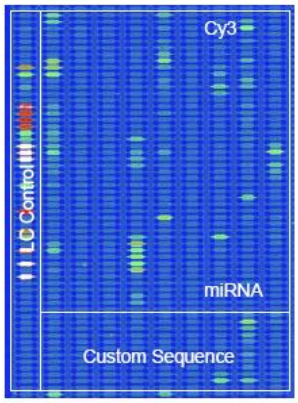

Sample A

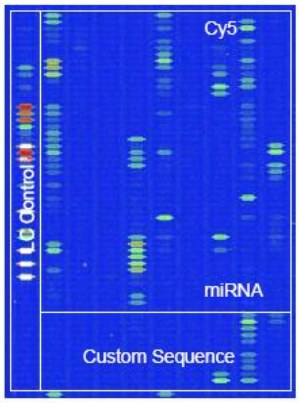

Sample B

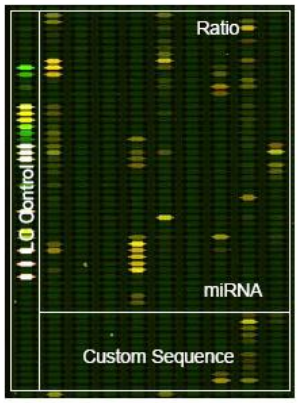

Cy3/Cy5

Table 1 Call list (differentially expressed transcripts with p-value < 0.01)

No.	Probe_ID	Sample A Signal	Sample B Signal	log2 (Sample B / Sample A)
1	ath-miR319a	1,396.78	2,200.81	0.63
2	ath-miR319c	3,915.89	5,192.48	0.38
3	gma-miR319a	2,346.34	3,258.66	0.52
4	osa-miR168a	11,798.37	8,782.30	-0.46
5	osa-miR396d	12,227.89	8,974.55	-0.45
6	ppt-miR319a	3,958.52	5,518.33	0.47
7	ppt-miR319c	1,855.11	2,907.20	0.68
8	ptc-miR159f	1,250.98	2,297.16	0.88
9	sof-miR159e	2,448.12	4,072.46	0.78
10	sof-miR168b	10,250.75	8,353.98	-0.34
11	C-ath-miR319a-19a	4,916.66	6,358.39	0.37
12	C-ptc-miR159f-1g	1,269.93	2,281.58	0.85

Chip: 02_METU_071011

Sample A: 169b – Cy3
Sample B: mock-b – Cy5

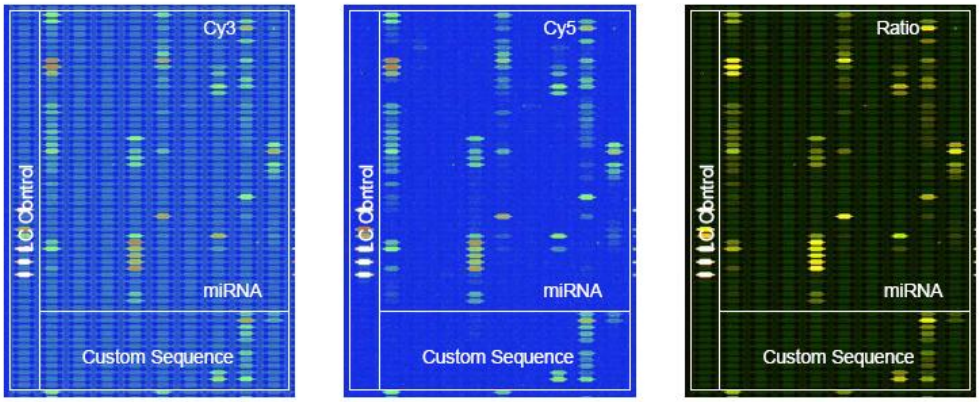

Sample A Sample B Cy3/Cy5

Table 2 Call list (differentially expressed transcripts with p-value < 0.01)

No.	Probe_ID	Sample A Signal	Sample B Signal	log2 (Sample B / Sample A)
1	ath-miR168a	9,205.47	5,972.34	-0.53
2	ppt-miR894	13,060.51	9,160.52	-0.51
3	bna-miR156a	7,402.61	5,331.29	-0.47
4	osa-miR168a	16,740.53	13,869.41	-0.33
5	ath-miR159b	22,230.46	25,682.16	0.19

Chip: 03_METU_071012

Sample A: R41 – Cy3
Sample B: R67 – Cy5

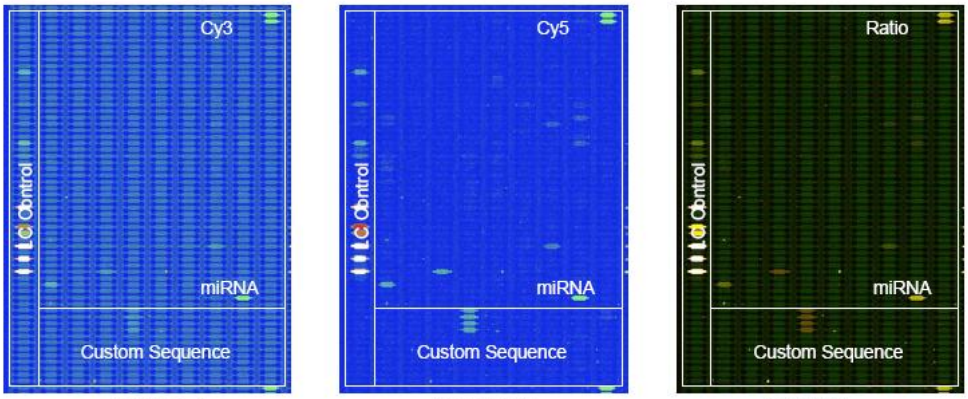

Sample A Sample B Cy3/Cy5

Table 3 Call list (differentially expressed transcripts with p-value < 0.01)

No.	Probe_ID	Sample A Signal	Sample B Signal	log2 (Sample B / Sample A)
1	ath-miR854a	1,106.00	2,490.30	1.17
2	ptc-miR474a	10,930.07	7,394.63	-0.64
3	ptc-miR474b	10,788.46	6,435.40	-0.74
4	ptc-miR474c	10,895.23	6,830.56	-0.67
5	C-ath-miR854a	1,153.12	2,452.53	1.04
6	C-ath-miR854b	1,228.00	2,564.68	1.09
7	C-ath-miR854c	1,193.21	2,664.11	0.97
8	C-ath-miR854d	1,301.77	2,599.15	0.96

Group A: 232b

Group B: 169b

			Group A	Group B	Log2 (B/A)
No.	Reporter Name	p-value	Mean	Mean	
24	ath-miR169b	2.14E-07	1,011	704	-0.52
23	ath-miR169a	4.80E-07	888	599	-0.57
305	ppt-miR894	9.93E-07	7,189	10,161	0.50
387	sof-miR159e	3.97E-06	3,159	4,690	0.57
392	zma-miR169e	1.92E-05	185	11	-4.07
27	ath-miR169h	3.31E-05	1,004	696	-0.53
21	ath-miR167d	4.10E-05	2,758	2,270	-0.28
330	ptc-miR169o	5.27E-05	952	645	-0.56
180	osa-miR164d	6.28E-05	2,040	1,711	-0.25
320	ptc-miR159f	1.36E-04	1,684	3,341	0.99
19	ath-miR167a	2.91E-04	2,687	2,301	-0.22
175	osa-miR159f	3.88E-04	18,750	17,070	-0.14
171	osa-miR159a	5.14E-04	20,777	18,769	-0.15
390	zma-miR162	5.18E-04	25	0	-13.22
343	ptc-miR172i	5.84E-04	45	13	-1.78
202	osa-miR393b	6.05E-04	1,947	1,635	-0.25
307	ppt-miR896	6.89E-04	441	655	0.57
382	sbi-miR164c	7.20E-04	2,575	2,156	-0.26
179	osa-miR164c	8.68E-04	2,344	2,042	-0.20
212	osa-miR396d	8.77E-04	15,672	13,981	-0.16
20	ath-miR167c	1.15E-03	1,612	1,347	-0.26
346	ptc-miR395a	1.35E-03	18	3	-2.77
349	ptc-miR397b	1.56E-03	20	0	-6.22
388	sof-miR168b	2.22E-03	13,392	11,805	-0.18
326	ptc-miR167f	2.23E-03	2,964	2,469	-0.26
25	ath-miR169d	2.35E-03	976	752	-0.38
283	ppt-miR319c	3.65E-03	2,290	3,135	0.45
204	osa-miR395b	4.33E-03	114	63	-0.86
187	osa-miR167d	5.06E-03	3,086	2,665	-0.21
385	sbi-miR172a	5.70E-03	51	22	-1.21
38	ath-miR390a	6.74E-03	45	25	-0.86
91	ath-miR823	7.10E-03	32	61	0.91
181	osa-miR164e	7.86E-03	3,173	2,856	-0.15
3	ath-miR156h	7.93E-03	281	561	1.00
380	ptc-miR482	1.00E-02	32	12	-1.43
270	ppt-miR1219a	1.06E-02	35	15	-1.23

Group A:232b

Group B:169b

240	osa-miR528	1.08E-02	73	124	0.76
162	mtr-miR395a	1.11E-02	115	66	-0.81
96	ath-miR828	1.13E-02	7	24	1.84
191	osa-miR169e	1.20E-02	942	754	-0.32
383	sbi-miR166a	1.24E-02	915	705	-0.38
94	ath-miR826	1.25E-02	23	44	0.92
51	ath-miR399b	1.32E-02	75	120	0.69
389	sof-miR408e	1.52E-02	25	4	-2.59
107	ath-miR835-3p	1.53E-02	26	51	0.96
384	sbi-miR171f	1.70E-02	74	28	-1.39
282	ppt-miR319a	1.73E-02	5,203	6,249	0.26
386	sbi-miR172b	1.73E-02	48	19	-1.32
106	ath-miR834	1.73E-02	21	40	0.94
159	gma-miR319a	1.75E-02	3,251	3,724	0.20
325	ptc-miR166p	1.79E-02	225	327	0.54
41	ath-miR394a	1.82E-02	63	41	-0.61
144	ath-miR864-3p	1.84E-02	32	55	0.79
185	osa-miR166k	1.87E-02	987	843	-0.23
150	ath-miR867	1.88E-02	26	53	1.01
5	ath-miR157d	1.91E-02	195	341	0.80
188	osa-miR168a	1.98E-02	14,876	13,104	-0.18
317	ptc-miR156k	1.99E-02	2,579	3,129	0.28
345	ptc-miR319i	2.05E-02	39	17	-1.18
42	ath-miR395a	2.09E-02	66	40	-0.73
11	ath-miR160a	2.11E-02	102	154	0.59
332	ptc-miR169s	2.28E-02	846	701	-0.27
93	ath-miR825	2.32E-02	15	35	1.24
95	ath-miR827	2.39E-02	42	196	2.22
205	osa-miR395c	2.51E-02	70	36	-0.96
157	bna-miR393	2.65E-02	2,092	1,901	-0.14
329	ptc-miR169ab	2.84E-02	49	96	0.99
130	ath-miR853	3.02E-02	12	31	1.40
146	ath-miR865-3p	3.02E-02	28	49	0.78
173	osa-miR159d	3.11E-02	12,474	11,763	-0.08
4	ath-miR157a	3.16E-02	279	410	0.56
234	osa-miR441a	3.32E-02	5	28	2.41
362	ptc-miR474c	3.48E-02	54	33	-0.71
229	osa-miR435	3.80E-02	28	45	0.68
158	gma-miR156b	3.97E-02	2,882	3,368	0.23
55	ath-miR400	4.03E-02	20	46	1.20
190	osa-miR169d	4.04E-02	41	92	1.19

Group A:232b

Group B:169b

99	ath-miR830	4.12E-02	27	55	1.01
207	osa-miR395o	4.21E-02	71	32	-1.12
43	ath-miR395b	4.54E-02	69	45	-0.62
108	ath-miR835-5p	4.80E-02	7	22	1.72
145	ath-miR864-5p	4.89E-02	10	29	1.56
246	osa-miR807a	4.96E-02	20	6	-1.83

Group 1 b95 inf. 6 hpi
Group 2 b103 inf. 6 hpi

			Group 1	Group 2	Log2 (G2/G1)
No.	Reporter Name	p-value	Mean	Mean	
255	C-osa-miR168a-9g	1.16E-03	631	424	-0.57
291	osa-miR1436	1.28E-03	2,183	1,271	-0.78
250	C-gma-miR319a-17g	2.24E-03	612	846	0.47
260	C-ptc-miR159f-1g	2.41E-03	1,300	1,705	0.39
268	gma-miR319a	3.01E-03	857	1,280	0.58
788	vvi-miR319b	7.80E-03	846	1,189	0.49
578	pta-miR319	8.89E-03	589	769	0.39
263	C-sof-miR159e-18c	1.19E-02	714	1,081	0.60
737	sof-miR168b	1.64E-02	559	409	-0.45
575	pta-miR159c	1.80E-02	764	948	0.31
574	pta-miR159b	2.37E-02	622	745	0.26
604	ptc-miR159f	2.56E-02	1,289	1,708	0.41
2	ath-miR156g	2.66E-02	462	342	-0.43
1	ath-miR156a	2.67E-02	454	341	-0.41
573	pta-miR159a	4.35E-02	1,240	1,441	0.22
545	ppt-miR894	4.75E-02	1,166	1,331	0.19
36	ath-miR319a	5.16E-02	744	889	0.26
600	ptc-miR1450	5.28E-02	61,631	46,632	-0.40
313	osa-miR168a	5.74E-02	604	448	-0.43
Following transcripts are statistically significant but have low signals (signal < 500)					
651	ptc-miR474a	2.14E-04	52	181	1.79
652	ptc-miR474b	3.14E-04	53	191	1.85
653	ptc-miR474c	3.28E-04	56	180	1.68
789	vvi-miR319e	3.32E-04	48	209	2.14
157	bna-miR156a	4.67E-04	436	274	-0.67
307	osa-miR164d	4.90E-04	237	137	-0.79
16	ath-miR164c	1.85E-03	242	145	-0.74
168	C-ath-miR168a-15a	2.38E-03	159	123	-0.38
365	osa-miR528	2.66E-03	75	49	-0.62
254	C-osa-miR156l-21c	2.77E-03	439	271	-0.70
167	C-ath-miR156g-10u	3.06E-03	323	228	-0.50
207	C-ath-miR854b	3.42E-03	32	50	0.65
208	C-ath-miR854c	3.45E-03	34	50	0.56
635	ptc-miR396f	3.93E-03	15	35	1.23
676	sbi-miR164c	5.53E-03	314	197	-0.67
298	osa-miR156l	8.39E-03	358	236	-0.60
306	osa-miR164c	8.48E-03	276	184	-0.59
131	ath-miR854a	9.23E-03	28	48	0.76
324	osa-miR319a	1.14E-02	28	58	1.05
206	C-ath-miR854a	1.16E-02	33	49	0.57
15	ath-miR164a	1.44E-02	224	132	-0.76
209	C-ath-miR854d	1.53E-02	33	48	0.56

40	ath-miR393a	1.78E-02	97	114	0.24
264	C-sof-miR168b-16c	1.83E-02	88	73	-0.28
608	ptc-miR164f	1.99E-02	356	235	-0.60
269	gma-miR319c	2.25E-02	40	80	1.00
308	osa-miR164e	2.79E-02	360	261	-0.46
359	osa-miR444b.1	2.93E-02	184	161	-0.19
754	tae-miR1132	3.70E-02	18	32	0.84
27	ath-miR169h	4.10E-02	23	31	0.41
20	ath-miR167c	4.21E-02	127	152	0.26
22	ath-miR168a	4.85E-02	317	247	-0.36
765	vvi-miR159a	5.16E-02	326	246	-0.40
767	vvi-miR166b	5.47E-02	46	37	-0.30
675	sbi-miR156e	5.88E-02	443	329	-0.43
265	ghr-miR156c	8.33E-02	368	272	-0.44
17	ath-miR165a	8.74E-02	29	39	0.42
3	ath-miR156h	8.83E-02	86	110	0.34

Group 1 b95 inf. 12 hpi
Group 2 b103 inf. 12 hpi

			Group 1	Group 2	Log2 (G2/G1)
No.	Reporter Name	p-value	Mean	Mean	
545	ppt-miR894	2.42E-08	4,559	314	-3.86
255	C-osa-miR168a-9g	3.61E-08	1,441	220	-2.71
169	C-ath-miR319a-19a	1.27E-07	1,160	2,356	1.02
308	osa-miR164e	1.64E-07	1,281	421	-1.60
307	osa-miR164d	2.19E-07	1,022	313	-1.71
313	osa-miR168a	3.64E-07	1,631	268	-2.60
16	ath-miR164c	1.19E-06	1,082	314	-1.79
306	osa-miR164c	1.48E-06	1,092	344	-1.67
260	C-ptc-miR159f-1g	2.46E-06	546	1,136	1.06
676	sbi-miR164c	5.07E-06	1,111	326	-1.77
208	C-ath-miR854c	6.13E-06	51	602	3.57
737	sof-miR168b	6.18E-06	1,355	205	-2.73
15	ath-miR164a	9.45E-06	1,050	304	-1.79
209	C-ath-miR854d	1.71E-05	55	611	3.47
632	ptc-miR319e	2.19E-05	954	1,907	1.00
207	C-ath-miR854b	2.28E-05	52	601	3.53
302	osa-miR159e	2.48E-05	1,698	2,815	0.73
573	pta-miR159a	2.97E-05	902	1,711	0.92
788	vvi-miR319b	3.08E-05	660	1,204	0.87
37	ath-miR319c	3.18E-05	930	1,952	1.07
600	ptc-miR1450	3.68E-05	73,699	16,519	-2.16
206	C-ath-miR854a	4.89E-05	47	602	3.68
300	osa-miR159c	5.04E-05	1,602	2,770	0.79
21	ath-miR167d	5.73E-05	603	270	-1.16
291	osa-miR1436	7.47E-05	1,480	746	-0.99
574	pta-miR159b	8.13E-05	219	493	1.17
602	ptc-miR159d	8.42E-05	1,661	2,694	0.70
575	pta-miR159c	9.73E-05	531	967	0.87
736	sof-miR159e	1.48E-04	1,254	2,408	0.94
513	ppt-miR319a	1.59E-04	1,132	2,273	1.01
365	osa-miR528	1.61E-04	684	275	-1.31
301	osa-miR159d	1.65E-04	1,943	2,967	0.61
608	ptc-miR164f	1.89E-04	1,207	372	-1.70
268	gma-miR319a	1.94E-04	700	1,251	0.84
36	ath-miR319a	2.02E-04	510	1,031	1.02
19	ath-miR167a	2.94E-04	500	240	-1.06
604	ptc-miR159f	4.66E-04	553	1,173	1.09
131	ath-miR854a	5.77E-04	53	612	3.53
22	ath-miR168a	1.10E-03	578	59	-3.30
10	ath-miR159c	1.89E-03	1,880	2,826	0.59
1	ath-miR156a	5.31E-03	303	525	0.79
611	ptc-miR167e	6.64E-03	556	273	-1.03
2	ath-miR156g	6.73E-03	312	518	0.73

157	bna-miR156a	7.48E-03	264	469	0.83
612	ptc-miR167f	7.51E-03	489	240	-1.03
299	osa-miR159a	9.44E-02	4,714	4,370	-0.11
Following transcripts are statistically significant but have low signals (signal < 500)					
264	C-sof-miR168b-16c	1.12E-06	75	11	-2.75
167	C-ath-miR156g-10u	3.07E-06	29	194	2.75
263	C-sof-miR159e-18c	3.31E-05	111	383	1.78
257	C-ppt-miR319a-2a	6.85E-05	35	152	2.13
259	C-ptc-miR156k-3g	1.02E-04	40	118	1.57
250	C-gma-miR319a-17g	2.02E-04	51	285	2.47
168	C-ath-miR168a-15a	2.49E-04	298	22	-3.75
609	ptc-miR166n	3.09E-04	92	43	-1.09
677	sbi-miR166a	3.81E-04	248	95	-1.38
254	C-osa-miR156l-21c	5.55E-04	194	399	1.04
314	osa-miR168b	5.78E-04	176	22	-3.00
578	pta-miR319	5.97E-04	211	449	1.09
653	ptc-miR474c	6.33E-04	54	13	-2.03
675	sbi-miR156e	6.56E-04	253	434	0.78
312	osa-miR166m	7.14E-04	276	100	-1.46
18	ath-miR166a	1.09E-03	278	107	-1.38
166	C-ath-miR156a-11c	1.19E-03	17	168	3.27
613	ptc-miR167h	1.30E-03	243	130	-0.91
335	osa-miR396d	1.32E-03	268	411	0.62
765	vvi-miR159a	1.48E-03	29	146	2.35
651	ptc-miR474a	1.67E-03	44	13	-1.80
298	osa-miR156l	2.11E-03	151	349	1.20
769	vvi-miR166d	2.12E-03	189	76	-1.31
262	C-sbi-miR156e-12g	2.48E-03	20	155	2.98
767	vvi-miR166b	3.29E-03	181	74	-1.29
747	tae-miR1125	4.59E-03	25	101	1.99
267	gma-miR156b	5.00E-03	49	191	1.96
265	ghr-miR156c	1.15E-02	108	269	1.32
601	ptc-miR156k	1.48E-02	72	198	1.46
547	ppt-miR896	1.74E-02	39	10	-1.95
652	ptc-miR474b	2.68E-02	39	16	-1.34
763	vvi-miR156e	2.83E-02	43	165	1.94
159	bna-miR167a	3.19E-02	78	53	-0.56
605	ptc-miR160e	3.21E-02	20	33	0.75
510	ppt-miR167	3.51E-02	253	135	-0.90
164	bna-miR393	3.67E-02	79	48	-0.73
792	vvi-miR396a	3.78E-02	10	32	1.68
249	C-gma-miR156b-20a	4.71E-02	14	59	2.03
770	vvi-miR167c	4.96E-02	95	64	-0.56
793	vvi-miR396b	8.59E-02	9	33	1.78

Group 1 b95 inf. 24 hpi

Group 2 b103 inf. 24 hpi

			Group 1	Group 2	Log2 (G2/G1)
No.	Reporter Name	p-value	Mean	Mean	
254	C-osa-miR156l-21c	5.02E-06	300	530	0.82
255	C-osa-miR168a-9g	7.31E-06	903	476	-0.93
545	ppt-miR894	1.22E-05	2,508	862	-1.54
157	bna-miR156a	1.54E-05	340	582	0.78
298	osa-miR156l	4.04E-05	246	472	0.94
169	C-ath-miR319a-19a	8.65E-05	1,635	1,937	0.24
291	osa-miR1436	2.43E-04	1,061	632	-0.75
1	ath-miR156a	5.58E-04	366	620	0.76
313	osa-miR168a	7.44E-04	941	540	-0.80
675	sbi-miR156e	1.03E-03	355	568	0.68
600	ptc-miR1450	1.41E-03	46,787	33,329	-0.49
335	osa-miR396d	1.73E-03	568	263	-1.11
737	sof-miR168b	4.27E-03	828	445	-0.90
301	osa-miR159d	4.52E-03	2,896	3,195	0.14
2	ath-miR156g	5.44E-03	374	619	0.73
578	pta-miR319	8.38E-03	385	469	0.29
300	osa-miR159c	8.38E-03	2,639	2,919	0.15
302	osa-miR159e	1.12E-02	2,713	3,031	0.16
788	vvi-miR319b	1.28E-02	744	824	0.15
10	ath-miR159c	1.33E-02	2,746	3,097	0.17
9	ath-miR159b	2.48E-02	3,575	3,921	0.13
299	osa-miR159a	2.75E-02	3,803	4,080	0.10
8	ath-miR159a	2.92E-02	3,585	3,888	0.12
303	osa-miR159f	3.16E-02	3,611	3,875	0.10
308	osa-miR164e	3.57E-02	548	475	-0.21
608	ptc-miR164f	4.41E-02	519	425	-0.29
602	ptc-miR159d	5.32E-02	2,704	2,923	0.11
573	pta-miR159a	5.57E-02	1,005	1,112	0.15
736	sof-miR159e	6.64E-02	1,376	1,720	0.32
260	C-ptc-miR159f-1g	7.01E-02	1,045	1,124	0.10
632	ptc-miR319e	8.87E-02	1,233	1,353	0.13
268	gma-miR319a	9.98E-02	790	831	0.07
Following transcripts are statistically significant but have low signals (signal < 500)					
747	tae-miR1125	1.29E-06	15	353	4.59
168	C-ath-miR168a-15a	7.84E-05	77	20	-1.94
365	osa-miR528	1.27E-04	86	249	1.53
167	C-ath-miR156g-10u	2.06E-04	178	248	0.48
265	ghr-miR156c	2.85E-04	243	441	0.86
264	C-sof-miR168b-16c	5.39E-04	48	11	-2.11
756	tae-miR1134	6.14E-04	120	40	-1.59
596	ptc-miR1446a	7.16E-04	38	315	3.07
164	bna-miR393	1.20E-03	263	125	-1.08

547	ppt-miR896	1.71E-03	132	24	-2.44
166	C-ath-miR156a-11c	1.76E-03	173	124	-0.48
19	ath-miR167a	3.54E-03	283	349	0.30
574	pta-miR159b	3.57E-03	293	430	0.55
651	ptc-miR474a	5.53E-03	95	41	-1.22
652	ptc-miR474b	6.21E-03	96	30	-1.66
59	ath-miR404	6.25E-03	10	37	1.85
40	ath-miR393a	8.87E-03	65	27	-1.28
609	ptc-miR166n	1.05E-02	53	28	-0.93
325	osa-miR393b	1.46E-02	228	118	-0.95
22	ath-miR168a	1.46E-02	304	161	-0.92
653	ptc-miR474c	1.50E-02	104	39	-1.41
763	vvi-miR156e	1.65E-02	143	221	0.62
769	vvi-miR166d	1.91E-02	54	37	-0.55
18	ath-miR166a	2.00E-02	113	47	-1.28
312	osa-miR166m	2.49E-02	91	46	-0.98
677	sbi-miR166a	3.19E-02	91	43	-1.06
17	ath-miR165a	3.30E-02	66	25	-1.40
767	vvi-miR166b	4.16E-02	71	38	-0.90
259	C-ptc-miR156k-3g	4.24E-02	116	85	-0.46
16	ath-miR164c	4.95E-02	302	332	0.14
309	osa-miR166e	6.46E-02	36	19	-0.90
314	osa-miR168b	7.84E-02	52	27	-0.98
21	ath-miR167d	8.35E-02	330	381	0.21
267	gma-miR156b	8.72E-02	147	199	0.43

Group 1 b95 inf. 48 hpi

Group 2 b103 inf. 48 hpi

			Group 1	Group 2	Log2 (G2/G1)
No.	Reporter Name	p-value	Mean	Mean	
545	ppt-miR894	2.94E-05	1,725	1,237	-0.48
737	sof-miR168b	1.63E-03	542	353	-0.62
313	osa-miR168a	2.67E-03	569	396	-0.52
600	ptc-miR1450	3.30E-03	49,112	35,001	-0.49
255	C-osa-miR168a-9g	3.78E-03	558	400	-0.48
250	C-gma-miR319a-17g	4.63E-03	779	648	-0.27
574	pta-miR159b	7.00E-03	860	724	-0.25
575	pta-miR159c	1.32E-02	1,014	957	-0.08
788	vvi-miR319b	1.47E-02	1,089	1,164	0.10
169	C-ath-miR319a-19a	1.75E-02	1,980	1,947	-0.02
268	gma-miR319a	4.30E-02	1,129	1,242	0.14
8	ath-miR159a	4.50E-02	3,064	3,322	0.12
302	osa-miR159e	7.36E-02	2,397	2,502	0.06
263	C-sof-miR159e-18c	8.22E-02	925	834	-0.15
303	osa-miR159f	8.88E-02	3,118	3,286	0.08
9	ath-miR159b	9.51E-02	3,115	3,369	0.11
Following transcripts are statistically significant but have low signals (signal < 500)					
206	C-ath-miR854a	1.53E-06	52	109	1.07
252	C-hsa-miR-675	1.64E-06	55	11	-2.38
208	C-ath-miR854c	2.25E-06	57	114	1.01
27	ath-miR169h	2.85E-06	15	54	1.86
207	C-ath-miR854b	4.92E-06	58	115	1.00
314	osa-miR168b	1.18E-05	87	27	-1.68
264	C-sof-miR168b-16c	1.27E-05	73	27	-1.42
131	ath-miR854a	2.83E-05	56	111	0.99
25	ath-miR169d	3.61E-05	14	52	1.86
618	ptc-miR169s	4.86E-05	13	48	1.87
24	ath-miR169b	1.05E-04	15	44	1.56
168	C-ath-miR168a-15a	1.43E-04	135	39	-1.80
166	C-ath-miR156a-11c	1.58E-04	144	206	0.52
312	osa-miR166m	1.87E-04	85	61	-0.48
357	osa-miR444a.1	2.31E-04	38	17	-1.18
775	vvi-miR169o	2.42E-04	12	29	1.28
617	ptc-miR169q	3.14E-04	11	34	1.59
335	osa-miR396d	5.12E-04	235	316	0.43
209	C-ath-miR854d	5.40E-04	56	107	0.95
508	ppt-miR166j	5.94E-04	38	20	-0.91
269	gma-miR319c	7.58E-04	43	20	-1.14
325	osa-miR393b	1.01E-03	125	79	-0.66
677	sbi-miR166a	1.23E-03	87	69	-0.34
159	bna-miR167a	1.34E-03	146	107	-0.45
254	C-osa-miR156l-21c	1.43E-03	301	377	0.33

22	ath-miR168a	1.59E-03	251	156	-0.68
359	osa-miR444b.1	2.15E-03	137	107	-0.36
316	osa-miR169e	2.64E-03	16	50	1.62
616	ptc-miR169o	2.99E-03	13	52	2.00
157	bna-miR156a	3.75E-03	318	405	0.35
756	tae-miR1134	4.51E-03	34	16	-1.06
596	ptc-miR1446a	5.32E-03	149	34	-2.16
2	ath-miR156g	6.54E-03	341	467	0.46
23	ath-miR169a	8.01E-03	10	40	1.95
547	ppt-miR896	8.61E-03	44	21	-1.08
811	zma-miR171c	9.11E-03	31	21	-0.55
773	vvi-miR169l	9.76E-03	12	27	1.17
652	ptc-miR474b	1.02E-02	47	168	1.83
765	vvi-miR159a	1.05E-02	408	201	-1.02
40	ath-miR393a	1.12E-02	56	27	-1.03
257	C-ppt-miR319a-2a	1.15E-02	156	118	-0.40
767	vvi-miR166b	1.16E-02	77	57	-0.42
298	osa-miR156l	1.19E-02	252	333	0.40
259	C-ptc-miR156k-3g	1.29E-02	156	117	-0.42
651	ptc-miR474a	1.32E-02	47	160	1.78
160	bna-miR169c	1.40E-02	13	38	1.54
653	ptc-miR474c	1.54E-02	52	169	1.70
609	ptc-miR166n	1.66E-02	55	41	-0.42
1	ath-miR156a	1.66E-02	347	468	0.43
675	sbi-miR156e	1.66E-02	338	423	0.32
789	vvi-miR319e	2.30E-02	64	43	-0.56
727	smo-miR156c	2.55E-02	60	33	-0.85
621	ptc-miR169v	2.56E-02	12	32	1.47
613	ptc-miR167h	2.56E-02	290	238	-0.28
265	ghr-miR156c	2.63E-02	253	324	0.35
249	C-gma-miR156b-20a	2.68E-02	98	61	-0.67
770	vvi-miR167c	2.71E-02	153	121	-0.34
164	bna-miR393	3.40E-02	127	92	-0.47
533	ppt-miR533a*	3.67E-02	27	5	-2.44
16	ath-miR164c	4.15E-02	205	178	-0.20
21	ath-miR167d	5.04E-02	284	250	-0.19
311	osa-miR166k	5.04E-02	63	49	-0.37
19	ath-miR167a	5.26E-02	265	230	-0.20
20	ath-miR167c	5.32E-02	154	122	-0.34
610	ptc-miR166p	6.92E-02	31	21	-0.54
764	vvi-miR156h	7.51E-02	85	58	-0.56
763	vvi-miR156e	7.75E-02	191	227	0.25

Sample A: b95 inf. 6 hpi – Cy3
Sample B: b95-control 6 hpi – Cy5

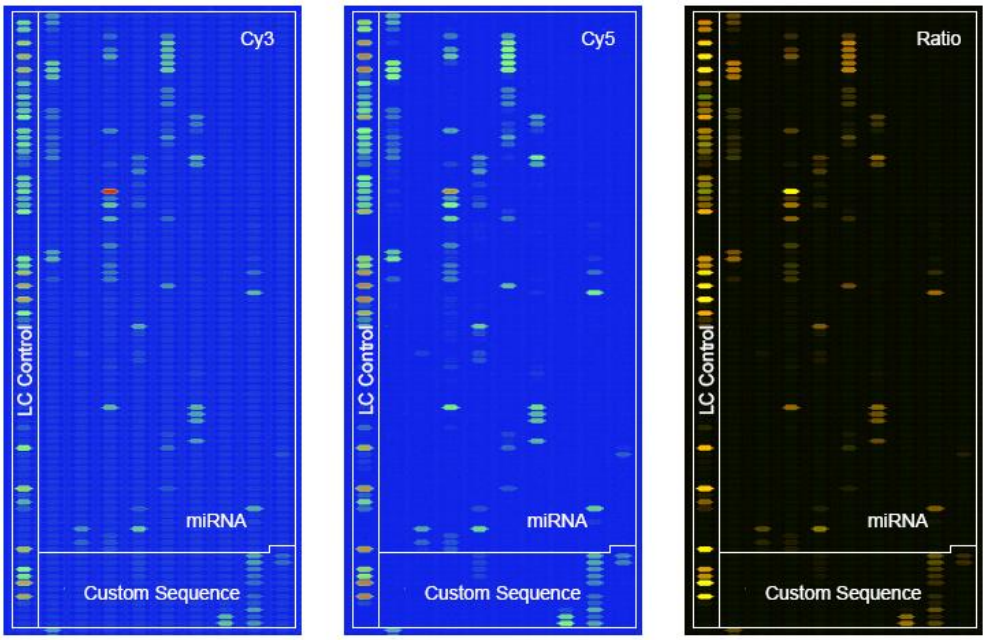

Sample A Sample B Cy3/Cy5

Sample A: b95 inf. 12 hpi – Cy3
Sample B: b95-control 12 hpi – Cy5

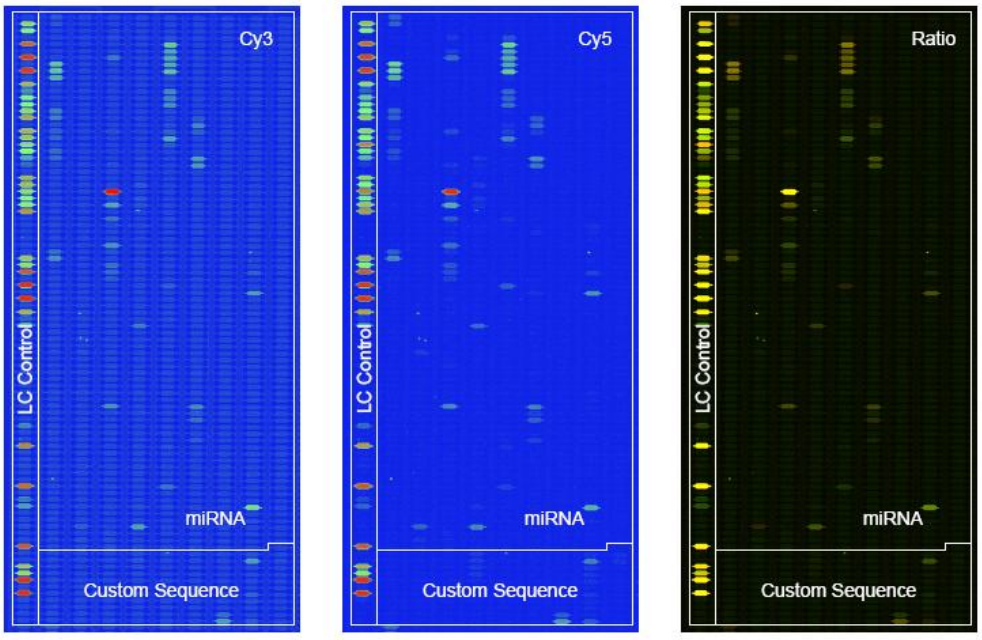

Sample A Sample B Cy3/Cy5

Table 2 Call list (differentially expressed transcripts with p-value < 0.01)

No.	Probe_ID	Sample A Signal	Sample B Signal	log2 (Sample B / Sample A)
1	ath-miR156a	182.53	529.47	1.50
2	ath-miR156g	195.03	529.07	1.44
3	ath-miR159a	4,035.35	4,933.70	0.29
4	ath-miR159b	4,122.37	4,741.43	0.24
5	ath-miR159c	2,201.38	2,859.48	0.38
6	ath-miR164a	789.11	501.88	-0.67
7	ath-miR164c	797.52	513.89	-0.63
8	ath-miR166a	197.77	108.79	-0.87
9	ath-miR168a	360.71	170.30	-1.11
10	bna-miR156a	160.50	422.48	1.45
11	ghr-miR156c	66.86	226.15	1.71
12	gma-miR156b	22.22	102.27	2.21
13	osa-miR1436	1,584.20	1,166.76	-0.44
14	osa-miR156l	79.54	275.04	1.78
15	osa-miR159a	4,350.78	5,075.10	0.22
16	osa-miR159c	1,813.49	2,463.96	0.38
17	osa-miR159d	2,244.58	2,846.47	0.36
18	osa-miR159e	1,952.97	2,478.00	0.31
19	osa-miR164c	869.74	512.37	-0.72
20	osa-miR164d	738.20	462.59	-0.67
21	osa-miR164e	1,068.97	676.67	-0.69
22	osa-miR168a	1,614.14	1,020.87	-0.70
23	osa-miR168b	132.93	53.57	-1.31
24	osa-miR396d	170.70	425.40	1.35
25	osa-miR528	368.96	112.75	-1.76
26	ppt-miR319a	1,185.98	1,613.49	0.44
27	ppt-miR894	4,810.64	2,500.66	-0.99
28	ptc-miR1450	70,214.47	37,257.11	-0.95
29	ptc-miR159d	1,929.94	2,584.93	0.39
30	ptc-miR164f	1,048.48	658.69	-0.67
31	ptc-miR319e	999.05	1,283.09	0.36
32	sbi-miR156e	147.09	404.18	1.47
33	sbi-miR164c	864.16	526.70	-0.73
34	sof-miR168b	1,294.73	851.36	-0.56
35	vvi-miR156e	19.77	88.87	2.17
36	C-ath-miR156a-11c	9.10	87.70	3.18
37	C-ath-miR156g-10u	17.88	105.10	2.87
38	C-ath-miR168a-15a	187.95	64.56	-1.43
39	C-ath-miR319a-19a	1,316.53	1,718.93	0.41
40	C-ath-miR854a	31.24	108.96	1.86
41	C-ath-miR854b	38.91	109.02	1.40
42	C-ath-miR854c	38.03	100.86	1.42
43	C-osa-miR156l-21c	115.31	393.45	1.81
44	C-osa-miR168a-9g	1,399.72	971.35	-0.55

Table 1 Call list (differentially expressed transcripts with p-value < 0.01)

No.	Probe_ID	Sample A Signal	Sample B Signal	log2 (Sample B / Sample A)
1	ath-miR156h	218.53	367.38	0.75
2	ath-miR164a	853.71	646.29	-0.41
3	ath-miR164c	859.15	648.09	-0.37
4	ath-miR168a	1,165.54	790.94	-0.57
5	ath-miR319c	3,962.92	4,649.23	0.23
6	osa-miR1432	321.32	207.27	-0.67
7	osa-miR1436	5,594.28	4,155.41	-0.39
8	osa-miR159a	6,316.46	7,628.63	0.27
9	osa-miR159c	4,682.26	5,587.82	0.26
10	osa-miR159d	4,897.43	5,825.96	0.25
11	osa-miR159e	4,721.93	5,670.59	0.26
12	osa-miR159f	6,032.59	7,373.97	0.29
13	osa-miR164c	1,045.97	757.62	-0.47
14	osa-miR164d	811.41	590.28	-0.46
15	osa-miR164e	1,293.38	898.06	-0.42
16	osa-miR168a	2,029.90	1,522.00	-0.39
17	osa-miR396d	1,850.48	2,715.39	0.54
18	osa-miR444b.1	636.23	424.20	-0.59
19	ppt-miR319a	4,381.22	5,132.53	0.23
20	ppt-miR894	3,012.81	3,560.52	0.24
21	pta-miR159a	3,631.24	4,329.98	0.27
22	pta-miR159c	2,614.90	3,062.20	0.23
23	ptc-miR1450	71,180.86	17,368.92	-2.01
24	ptc-miR156k	951.14	1,281.57	0.43
25	ptc-miR164f	1,202.32	889.60	-0.50
26	ptc-miR167e	891.34	621.54	-0.52
27	ptc-miR167f	816.62	610.37	-0.42
28	ptc-miR319e	3,809.60	4,584.12	0.27
29	sbi-miR164c	1,087.21	825.68	-0.37
30	sof-miR159e	4,432.81	5,257.85	0.26
31	tae-miR1134	7.86	53.82	2.73
32	vvi-miR156e	990.47	1,266.28	0.35
33	vvi-miR156h	284.64	433.58	0.62
34	vvi-miR319b	2,782.64	3,357.85	0.27
35	C-ath-miR156a-11c	965.12	1,282.23	0.42
36	C-ath-miR319a-19a	4,811.32	5,728.72	0.29
37	C-gma-miR156b-20a	388.45	602.92	0.71
38	C-ppt-miR319a-2a	624.46	1,023.37	0.62
39	C-ptc-miR156k-3g	591.52	911.22	0.55
40	C-sbi-miR156e-12g	682.67	1,012.58	0.57

Sample A: b95 inf. 24 hpi – Cy3
Sample B: b95-control 24 hpi – Cy5

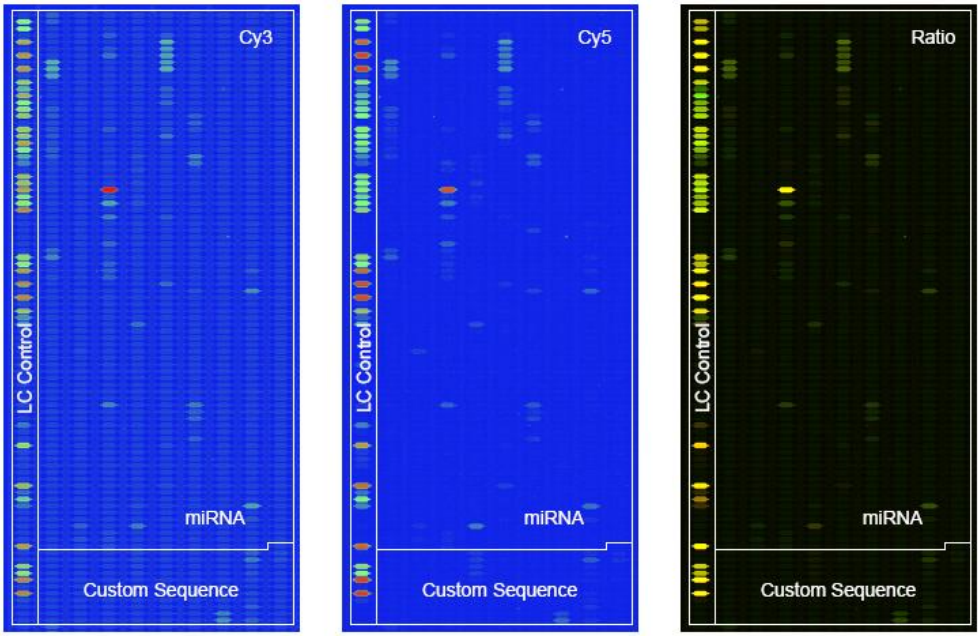

Sample A Sample B Cy3/Cy5

Table 3 Call list (differentially expressed transcripts with p-value < 0.01)

No.	Probe_ID	Sample A Signal	Sample B Signal	log2 (Sample B / Sample A)
1	ath-miR156a	158.40	66.63	-1.31
2	ath-miR156g	165.88	65.19	-1.30
3	ath-miR164a	132.05	284.59	1.08
4	ath-miR164c	135.81	290.16	1.12
5	ath-miR167a	134.48	54.50	-1.30
6	ath-miR167c	64.65	24.46	-1.40
7	ath-miR167d	150.13	54.47	-1.46
8	ath-miR854a	35.29	120.20	1.77
9	bna-miR156a	147.59	54.04	-1.45
10	bna-miR393	126.48	37.20	-1.65
11	ghr-miR156c	116.29	39.24	-1.40
12	osa-miR1432	55.94	12.74	-2.15
13	osa-miR1436	459.40	1,195.88	1.39
14	osa-miR156l	115.55	46.93	-1.30
15	osa-miR164c	174.34	405.34	1.26
16	osa-miR164d	139.55	323.04	1.19
17	osa-miR164e	238.88	515.53	1.11
18	osa-miR393b	106.46	30.17	-1.78
19	osa-miR396d	248.58	66.04	-1.91
20	osa-miR528	44.85	133.57	1.53
21	ppt-miR167	119.89	48.20	-1.37
22	ptc-miR1446a	20.07	98.30	2.06
23	ptc-miR1450	46,817.11	42,250.92	-0.15
24	ptc-miR159f	460.86	269.07	-0.78
25	ptc-miR164f	228.23	538.55	1.25
26	ptc-miR167e	152.28	66.97	-1.16
27	ptc-miR167f	146.40	57.58	-1.28
28	ptc-miR167h	142.60	60.28	-1.26
29	sbi-miR156e	154.84	74.57	-1.11
30	sbi-miR164c	193.13	403.87	1.06
31	tae-miR1125	10.24	153.83	3.91
32	tae-miR1134	65.34	155.65	1.25
33	C-ath-miR854a	38.35	121.17	1.65
34	C-ath-miR854b	35.63	107.20	1.81
35	C-ath-miR854c	35.50	119.66	1.71
36	C-ath-miR854d	37.84	108.03	1.60
37	C-osa-miR156l-21c	136.00	52.51	-1.31
38	C-ptc-miR159f-1g	452.15	251.16	-0.85
39	C-sof-miR159e-18c	204.98	81.56	-1.33

Sample A: b95 inf. 48 hpi – Cy3
Sample B: b95-control 48 hpi – Cy5

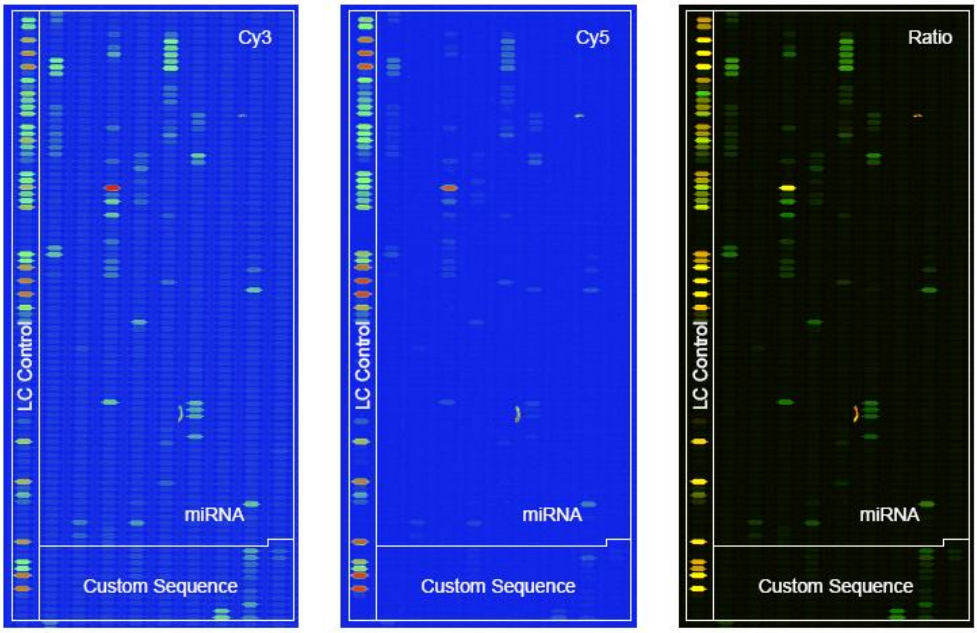

Sample A Sample B Cy3/Cy5

Table 4 Call list (differentially expressed transcripts with p-value < 0.01)

No.	Probe_ID	Sample A Signal	Sample B Signal	log2 (Sample B / Sample A)
1	ath-miR156h	35.89	4.83	-2.76
2	ath-miR319a	664.33	200.42	-1.71
3	ath-miR319c	1,025.43	592.65	-0.80
4	gma-miR319a	768.03	298.82	-1.40
5	gma-miR319c	31.08	2.97	-3.34
6	osa-miR166k	44.23	149.42	1.74
7	osa-miR166m	60.99	222.19	1.87
8	osa-miR168a	359.09	1,022.81	1.47
9	osa-miR168b	65.72	18.04	-1.91
10	osa-miR396d	178.42	439.87	1.29
11	ppt-miR319a	1,170.59	861.01	-0.43
12	ppt-miR894	1,062.54	2,885.34	1.46
13	pta-miR159a	954.15	467.81	-1.01
14	pta-miR159b	633.40	109.19	-2.55
15	pta-miR159c	708.56	171.73	-2.06
16	pta-miR319	597.45	112.03	-2.43
17	ptc-miR159f	1,118.93	285.28	-1.99
18	ptc-miR319e	1,036.88	620.63	-0.74
19	ptc-miR474a	42.45	8.28	-2.43
20	ptc-miR474b	45.52	5.85	-2.96
21	ptc-miR474c	49.78	12.39	-2.04
22	sbi-miR164c	199.66	317.45	0.67
23	sbi-miR166a	62.23	202.13	1.69
24	smo-miR156c	44.68	8.16	-2.54
25	sof-miR159e	1,259.19	544.85	-1.21
26	sof-miR168b	354.29	1,088.13	1.61
27	tae-miR1134	21.58	249.94	3.54
28	vvi-miR156h	68.62	20.16	-1.77
29	vvi-miR159a	297.48	44.32	-2.75
30	vvi-miR166b	56.27	179.03	1.65
31	vvi-miR166d	48.26	146.69	1.60
32	vvi-miR319b	731.42	299.00	-1.31
33	vvi-miR319e	48.41	10.80	-1.92
34	C-ath-miR156a-11c	110.54	48.31	-1.21
35	C-gma-miR156b-20a	69.44	15.47	-2.23
36	C-gma-miR319a-17g	602.74	88.79	-2.77
37	C-osa-miR168a-9g	363.41	1,063.03	1.56
38	C-ptc-miR159f-1g	1,096.93	308.53	-1.85
39	C-sbi-miR156e-12g	88.89	30.02	-1.55
40	C-sof-miR159e-18c	727.04	93.47	-3.01

Sample A: b103 inf. 6 hpi – Cy3
Sample B: b103 control 6 hpi – Cy5

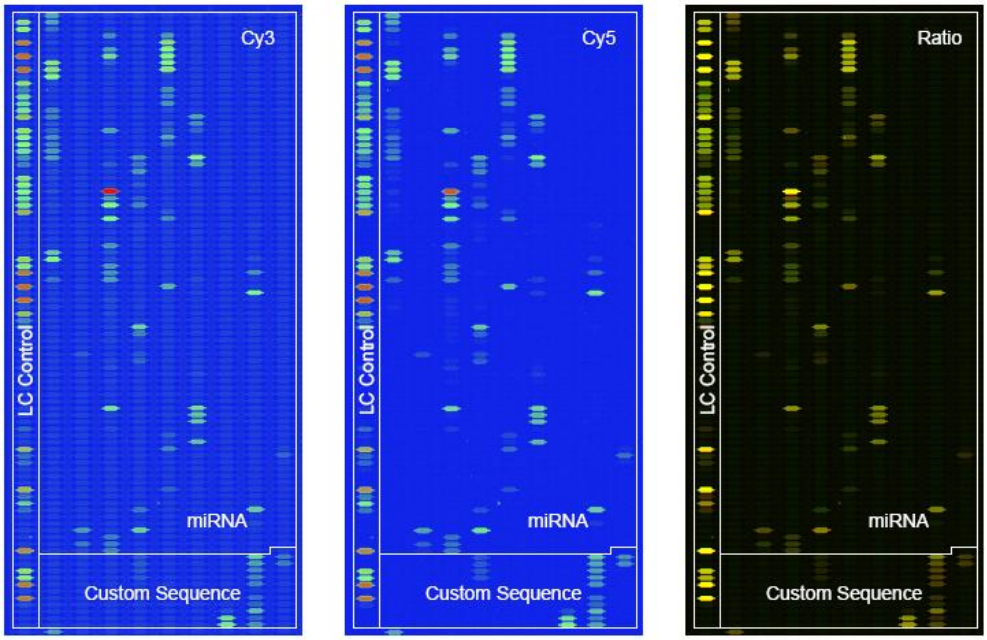

Sample A Sample B Cy3/Cy5

Table 5 Call list (differentially expressed transcripts with p-value < 0.01)

No.	Probe_ID	Sample A Signal	Sample B Signal	log2 (Sample B / Sample A)
1	ath-miR156a	1,746.95	2,289.73	0.41
2	ath-miR156g	1,778.15	2,274.01	0.39
3	ath-miR156h	384.77	666.12	0.79
4	ath-miR159c	7,612.73	6,667.38	-0.19
5	ath-miR164c	881.43	690.72	-0.35
6	ath-miR165a	171.52	83.36	-1.04
7	ath-miR166a	292.48	133.50	-1.11
8	ath-miR167a	1,201.40	760.26	-0.76
9	ath-miR167c	880.26	586.89	-0.62
10	ath-miR167d	1,275.92	754.46	-0.75
11	ath-miR319a	4,094.35	3,601.35	-0.18
12	ath-miR396a	30.53	79.50	1.41
13	ath-miR854a	222.43	383.30	0.79
14	bna-miR156a	1,550.93	1,989.29	0.53
15	bna-miR167a	699.54	421.98	-0.69
16	ghr-miR156c	1,576.41	2,080.41	0.41
17	gma-miR156b	1,520.83	2,113.71	0.48
18	gma-miR319a	5,131.33	4,481.53	-0.19
19	osa-miR1432	565.88	229.99	-1.30
20	osa-miR1436	4,447.74	5,874.36	0.40
21	osa-miR156l	1,370.38	1,920.15	0.50
22	osa-miR166k	241.25	144.33	-0.74
23	osa-miR168b	397.54	625.16	0.67
24	osa-miR396d	2,666.88	3,569.85	0.45
25	osa-miR444b.1	913.37	654.97	-0.48
26	ppt-miR167	1,049.10	668.79	-0.65
27	pta-miR159b	3,600.74	3,145.40	-0.23
28	ptc-miR1450	54,217.10	34,839.28	-0.71
29	ptc-miR156k	1,582.12	2,140.90	0.41
30	ptc-miR159f	6,863.70	5,876.70	-0.26
31	ptc-miR167e	1,309.21	841.45	-0.65
32	ptc-miR167f	1,236.42	804.24	-0.65
33	ptc-miR167h	1,577.49	1,012.08	-0.61
34	ptc-miR319e	6,182.83	5,432.08	-0.19
35	sbi-miR156e	1,534.47	2,175.31	0.51
36	sbi-miR166a	237.82	116.57	-1.03
37	smo-miR156c	409.37	761.06	0.87
38	tae-miR1134	30.75	125.32	2.12
39	vvi-miR156e	1,446.21	2,006.65	0.47
40	vvi-miR156h	570.36	940.53	0.75
41	vvi-miR159a	1,300.82	929.77	-0.49
42	vvi-miR167c	793.57	510.95	-0.72
43	vvi-miR396a	183.55	358.03	0.98
44	vvi-miR396b	253.97	466.81	0.80
45	C-ath-miR156a-11c	1,236.15	2,001.20	0.66
46	C-ath-miR156g-10u	1,368.50	2,167.07	0.62

47	C-ath-miR854a	242.96	406.58	0.67
48	C-ath-miR854b	258.46	384.52	0.61
49	C-ath-miR854c	262.41	384.07	0.59
50	C-ath-miR854d	244.08	391.22	0.68
51	C-gma-miR156b-20a	566.26	1,104.17	0.94
52	C-osa-miR156l-21c	1,551.57	2,165.64	0.50
53	C-osa-miR396d-13u	207.16	385.91	0.83
54	C-ppt-miR319a-2a	1,059.49	1,782.39	0.67
55	C-ptc-miR156k-3g	1,060.19	1,700.92	0.63
56	C-ptc-miR159f-1g	7,042.89	6,335.20	-0.15
57	C-sbi-miR156e-12g	1,107.07	1,804.72	0.68
58	C-sof-miR159e-18c	5,964.84	5,144.52	-0.25
59	C-sof-miR168b-16c	308.65	496.51	0.66

Sample A: b103 inf. 12 hpi – Cy3
Sample B: b103 control 12 hpi – Cy5

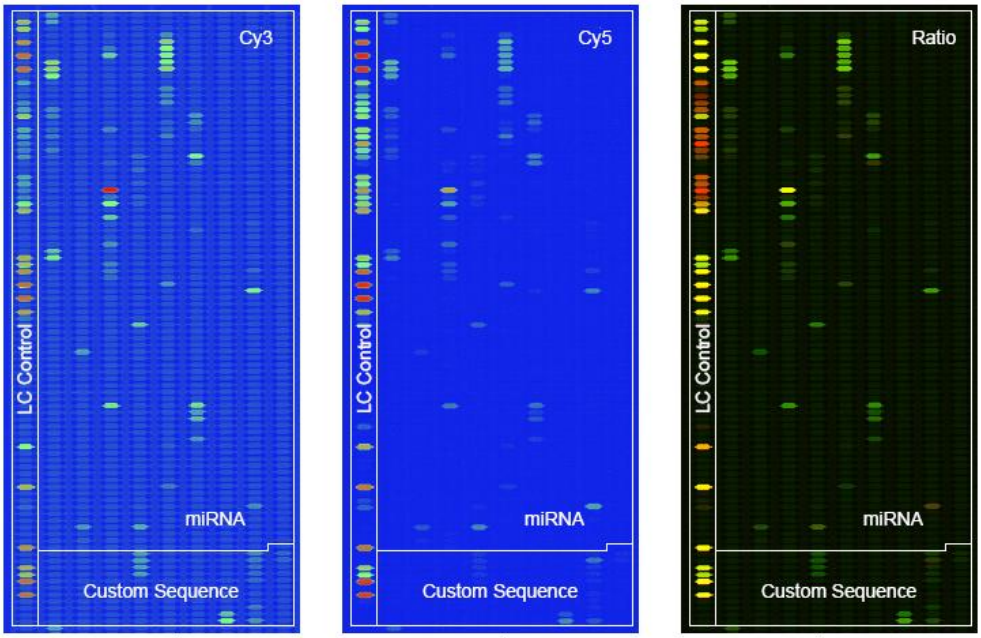

Sample A Sample B Cy3/Cy5

Table 6 Call list (differentially expressed transcripts with p-value < 0.01)

No.	Probe_ID	Sample A Signal	Sample B Signal	log2 (Sample B / Sample A)
1	ath-miR159a	5,584.07	6,692.51	0.27
2	ath-miR159b	5,658.75	6,775.49	0.23
3	ath-miR159c	3,808.85	3,383.62	-0.17
4	ath-miR164a	333.17	821.16	1.30
5	ath-miR164c	354.39	830.75	1.25
6	ath-miR168a	51.53	278.83	2.28
7	ath-miR319a	1,447.64	744.29	-0.99
8	ath-miR319c	2,707.75	1,719.68	-0.70
9	ath-miR854a	641.84	145.23	-2.16
10	gma-miR319a	1,774.77	943.14	-0.93
11	osa-miR1436	1,030.35	2,324.70	1.19
12	osa-miR159a	5,960.72	7,354.20	0.30
13	osa-miR159f	5,413.32	6,256.61	0.20
14	osa-miR164c	410.02	914.90	1.22
15	osa-miR164d	353.29	836.33	1.24
16	osa-miR164e	520.72	1,218.91	1.18
17	osa-miR166m	93.40	194.45	1.07
18	osa-miR168a	349.17	1,795.70	2.37
19	osa-miR168b	14.80	73.61	2.34
20	osa-miR393b	36.32	91.76	1.40
21	osa-miR528	268.41	162.53	-0.72
22	ppt-miR319a	3,053.74	1,966.43	-0.63
23	ppt-miR894	442.87	3,934.38	3.16
24	pta-miR159a	2,398.49	1,359.19	-0.79
25	pta-miR159b	622.32	194.31	-1.68
26	pta-miR159c	1,359.86	654.90	-1.04
27	pta-miR319	557.82	200.65	-1.47
28	ptc-miR1450	25,188.67	36,920.12	0.60
29	ptc-miR159f	1,602.55	599.12	-1.42
30	ptc-miR164f	450.38	1,070.94	1.29
31	ptc-miR319e	2,636.75	1,557.33	-0.72
32	sbi-miR164c	385.99	943.47	1.27
33	sof-miR159e	3,376.29	1,840.07	-0.88
34	sof-miR168b	250.68	1,487.40	2.59
35	tae-miR1125	110.83	24.32	-2.12
36	tae-miR1134	16.08	119.81	2.91
37	vvi-miR159a	126.58	34.70	-1.78
38	vvi-miR319b	1,698.39	871.02	-0.88
39	C-ath-miR168a-15a	24.13	103.11	2.13
40	C-ath-miR319a-19a	3,185.18	2,227.04	-0.50
41	C-ath-miR854a	626.23	151.13	-2.05
42	C-ath-miR854b	629.38	149.28	-2.06
43	C-ath-miR854c	628.78	142.48	-2.17
44	C-ath-miR854d	644.58	155.01	-2.06
45	C-gma-miR319a-17g	321.71	73.63	-2.12
46	C-osa-miR168a-9g	274.39	1,510.73	2.48

Sample A: b103 inf. 24 hpi – Cy3
Sample B: b103 control 24 hpi – Cy5

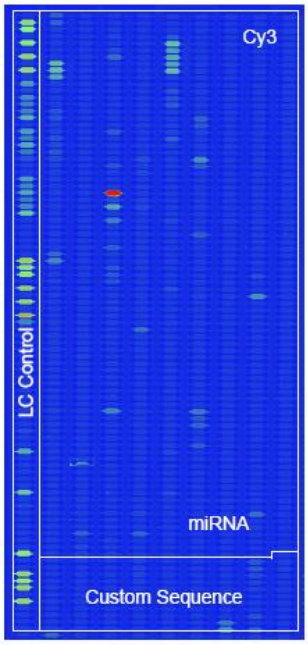

Sample A

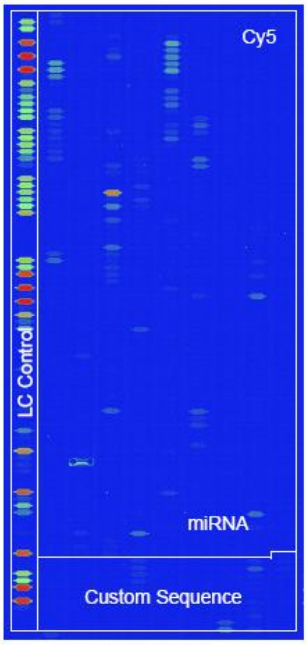

Sample B

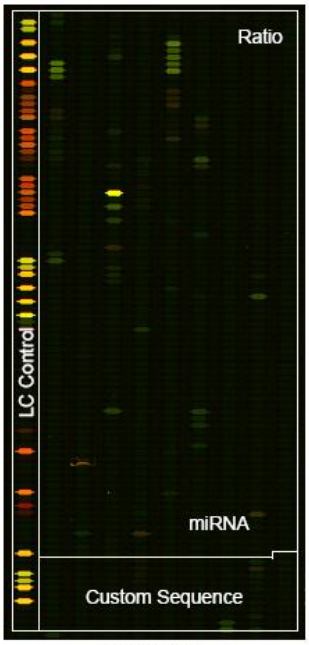

Cy3/Cy5

Table 7 Call list (differentially expressed transcripts with p-value < 0.01)

No.	Probe_ID	Sample A Signal	Sample B Signal	log2 (Sample B / Sample A)
1	ath-miR156a	233.86	76.75	-1.69
2	ath-miR156g	238.56	72.37	-1.73
3	ath-miR159c	1,458.39	1,155.56	-0.33
4	ath-miR164a	105.96	324.84	1.62
5	ath-miR164c	113.84	326.70	1.54
6	ath-miR166a	15.58	77.66	2.44
7	ath-miR167a	124.18	62.83	-0.98
8	ath-miR167d	139.76	69.16	-1.02
9	ath-miR319a	239.80	143.49	-0.76
10	bna-miR156a	215.26	69.17	-1.57
11	ghr-miR156c	150.08	43.88	-1.67
12	osa-miR1436	260.16	997.02	1.94
13	osa-miR156l	164.55	54.49	-1.51
14	osa-miR159a	2,345.28	2,897.33	0.30
15	osa-miR164c	134.21	445.62	1.70
16	osa-miR164d	117.99	377.48	1.65
17	osa-miR164e	179.91	589.34	1.71
18	osa-miR166e	9.44	46.62	2.47
19	osa-miR166k	11.19	61.50	2.57
20	osa-miR166m	20.52	118.31	2.54
21	osa-miR168a	214.12	464.11	1.08
22	osa-miR528	83.66	160.09	0.94
23	ppt-miR166j	5.71	36.42	2.67
24	ppt-miR894	366.48	836.47	1.18
25	pta-miR159b	158.45	56.81	-1.41
26	pta-miR319	175.61	77.80	-1.16
27	ptc-miR1447	6.90	47.46	2.83
28	ptc-miR159d	1,315.94	1,092.09	-0.27
29	ptc-miR159f	487.86	253.22	-1.01
30	ptc-miR164f	158.09	567.37	1.85
31	ptc-miR166n	11.13	73.98	2.52
32	ptc-miR167f	117.05	66.24	-0.82
33	sbi-miR156e	223.44	70.90	-1.53
34	sbi-miR164c	139.13	436.61	1.62
35	sbi-miR166a	19.47	90.31	2.27
36	sof-miR159e	842.38	540.20	-0.65
37	sof-miR168b	185.01	424.47	1.22
38	tae-miR1125	154.02	13.80	-3.27
39	vvi-miR156e	79.86	25.94	-1.63
40	vvi-miR166b	18.36	98.49	2.52
41	vvi-miR166d	16.48	93.99	2.54
42	C-ath-miR156g-10u	81.01	27.44	-1.56
43	C-ath-miR319a-19a	877.05	657.73	-0.42
44	C-ath-miR854a	26.05	91.34	1.91
45	C-ath-miR854b	27.68	84.66	1.61
46	C-ath-miR854c	29.07	89.29	1.46

Sample A: b103 inf. 48 hpi – Cy3
Sample B: b103 control 48 hpi – Cy5

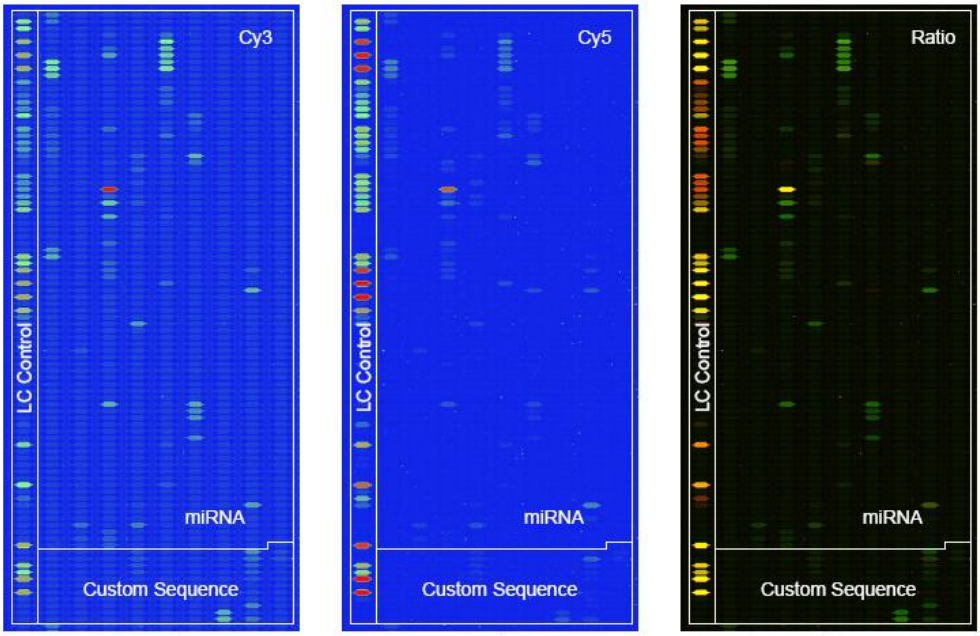

Sample A Sample B Cy3/Cy5

Table 8 Call list (differentially expressed transcripts with p-value < 0.01)

No.	Probe_ID	Sample A Signal	Sample B Signal	log2 (Sample B / Sample A)
1	ath-miR166a	38.64	127.34	1.72
2	ath-miR168a	88.28	273.88	1.55
3	ath-miR319a	521.56	156.33	-1.74
4	ath-miR319c	919.32	525.03	-0.83
5	gma-miR319a	689.22	240.83	-1.48
6	osa-miR166m	34.23	125.83	1.88
7	osa-miR168a	210.61	977.67	2.23
8	osa-miR396d	175.08	401.87	1.19
9	osa-miR528	84.10	26.47	-1.69
10	ppt-miR319a	1,049.19	656.05	-0.74
11	ppt-miR894	656.07	2,554.22	1.97
12	pta-miR159a	782.68	315.90	-1.35
13	pta-miR159b	413.81	54.94	-2.96
14	pta-miR159c	527.97	112.18	-2.24
15	pta-miR319	439.16	63.44	-2.82
16	ptc-miR1447	5.47	68.11	3.62
17	ptc-miR1450	49,359.72	37,763.35	-0.23
18	ptc-miR159f	952.83	214.54	-2.13
19	ptc-miR319e	895.41	489.63	-0.88
20	ptc-miR474a	84.54	22.56	-1.84
21	ptc-miR474b	91.45	17.45	-2.44
22	ptc-miR474c	94.82	24.73	-1.99
23	sof-miR159e	1,127.61	396.10	-1.53
24	sof-miR168b	186.36	859.03	2.31
25	tae-miR1134	9.55	287.39	5.14
26	vvi-miR159a	119.47	10.10	-3.77
27	vvi-miR166b	32.54	130.14	2.00
28	vvi-miR166d	35.49	125.19	1.82
29	vvi-miR319b	635.85	239.98	-1.42
30	C-ath-miR319a-19a	1,100.71	628.78	-0.79
31	C-gma-miR319a-17g	376.01	38.87	-3.26
32	C-osa-miR168a-9g	210.63	992.32	2.23
33	C-ptc-miR159f-1g	928.20	171.46	-2.45
34	C-sof-miR159e-18c	476.28	34.31	-3.78

Sample A: b95 inf. 6 hpi R2 – Cy3
Sample B: b95-control 6 hpi R2 – Cy5

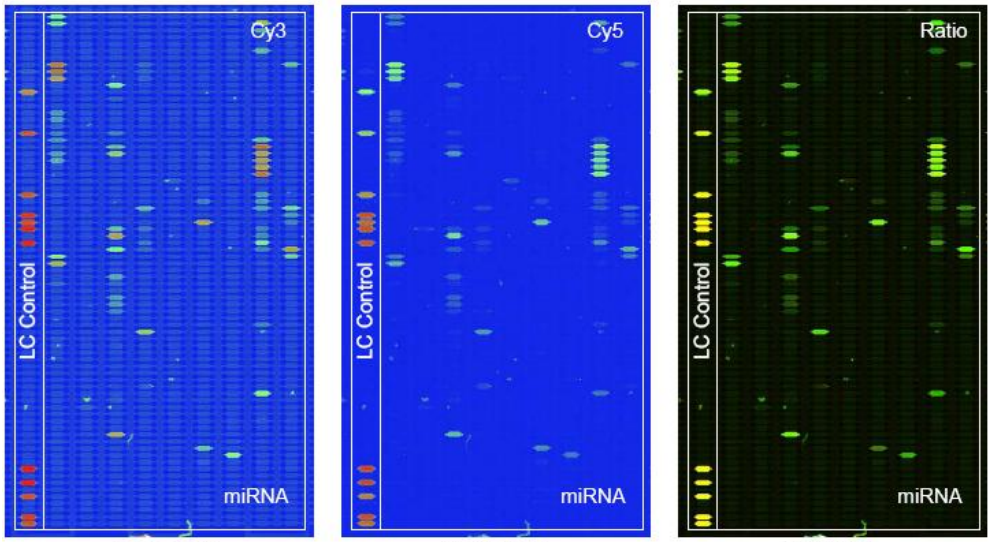

Sample A Sample B Cy3/Cy5

Table 1 Call list (differentially expressed transcripts with p-value < 0.01)

No.	Probe_ID	Sample A Signal	Sample B Signal	log2 (Sample B / Sample A)
1	ptc-miR474b	112.27	22.84	-2.39
2	ptc-miR474a	124.16	23.61	-2.38
3	pta-miR159b	1,096.66	247.40	-1.90
4	ptc-miR159f	3,071.30	988.67	-1.64
5	pta-miR319	1,231.81	411.44	-1.57
6	ptc-miR156k	1,439.95	510.38	-1.50
7	vvi-miR156e	1,349.70	484.99	-1.48
8	osa-miR168b	369.36	143.38	-1.40
9	gma-miR156b	1,289.66	512.18	-1.33
10	ppt-miR894	1,315.68	2,797.00	1.14
11	smo-miR159	3,114.72	1,694.96	-0.87
12	ath-miR167a	493.32	816.81	0.76
13	osa-miR396d	3,029.74	1,758.01	-0.76
14	ath-miR168a	767.63	459.32	-0.74
15	ptc-miR167e	689.87	1,113.54	0.73
16	ath-miR167d	608.52	943.44	0.66
17	ptc-miR167f	546.39	833.14	0.64
18	ath-miR319a	3,804.35	2,524.33	-0.59
19	vvi-miR319b	5,550.29	3,750.79	-0.54
20	osa-miR159a	14,928.10	21,677.59	0.52
21	ath-miR159b	13,986.33	19,764.65	0.48
22	ath-miR159a	14,056.39	18,757.06	0.48
23	osa-miR159f	13,851.33	19,139.90	0.46
24	sof-miR159e	9,430.11	6,846.72	-0.46
25	pta-miR159a	6,929.84	5,288.87	-0.40
26	gma-miR319a	5,864.91	4,392.12	-0.40
27	ptc-miR319e	8,051.08	6,496.61	-0.31
28	osa-miR168a	2,517.12	3,058.79	0.30
29	ath-miR159c	10,327.96	12,213.18	0.27
30	ath-miR319c	7,462.68	6,162.96	-0.26
31	osa-miR159d	10,520.09	12,242.87	0.25
32	osa-miR159e	10,110.36	11,427.28	0.21
33	osa-miR159c	9,757.96	11,332.58	0.21

Sample A: b95 inf. 12 hpi R2 – Cy3
Sample B: b95-control 12 hpi R2 – Cy5

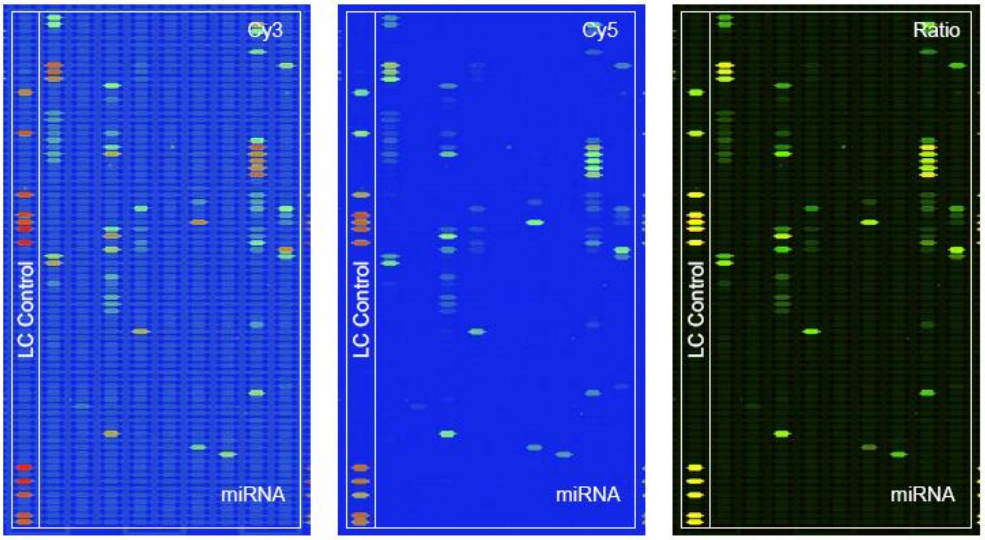

Sample A Sample B Cy3/Cy5

Table 2 Call list (differentially expressed transcripts with p-value < 0.01)

No.	Probe_ID	Sample A Signal	Sample B Signal	log2 (Sample B / Sample A)
1	ath-miR398a	63.62	12.27	-2.37
2	ath-miR398b	61.77	11.72	-2.36
3	gma-miR156b	1,781.54	541.56	-1.62
4	vvi-miR156e	1,799.06	649.92	-1.39
5	ptc-miR156k	1,979.08	727.83	-1.35
6	ath-miR393a	223.16	93.75	-1.28
7	pta-miR159b	2,573.01	1,205.58	-1.21
8	ptc-miR159f	5,163.47	2,261.32	-1.13
9	osa-miR528	4,547.42	2,183.09	-1.11
10	pta-miR319	2,398.28	1,159.99	-1.09
11	ppt-miR894	1,630.76	3,389.11	1.04
12	osa-miR396d	4,639.56	2,459.13	-0.88
13	osa-miR156l	1,959.70	1,232.75	-0.66
14	sbi-miR156e	2,950.79	1,852.93	-0.64
15	ath-miR167d	603.15	941.61	0.64
16	ptc-miR167e	830.92	1,254.64	0.59
17	ath-miR159a	16,962.26	25,359.98	0.56
18	osa-miR159a	18,177.24	26,304.23	0.55
19	ath-miR159b	17,022.54	25,352.46	0.55
20	osa-miR159f	17,012.54	24,573.96	0.52
21	osa-miR168a	2,397.81	3,206.43	0.47
22	ath-miR156a	3,618.45	2,549.86	-0.45
23	smo-miR159	5,032.11	3,493.95	-0.43
24	ath-miR156g	3,574.58	2,573.15	-0.42
25	ptc-miR159d	12,578.94	15,846.59	0.39
26	ath-miR319a	4,872.69	3,561.36	-0.37
27	ath-miR159c	12,372.41	16,096.28	0.32
28	osa-miR159d	12,984.24	16,616.60	0.32
29	osa-miR159c	12,452.48	15,444.66	0.31
30	osa-miR159e	12,373.40	15,501.77	0.29
31	ppt-miR319a	12,341.75	14,968.96	0.28
32	pta-miR159a	8,951.13	7,673.47	-0.22

Sample A: b95 inf. 24 hpi R2 – Cy3
Sample B: b95-control 24 hpi R2 – Cy5

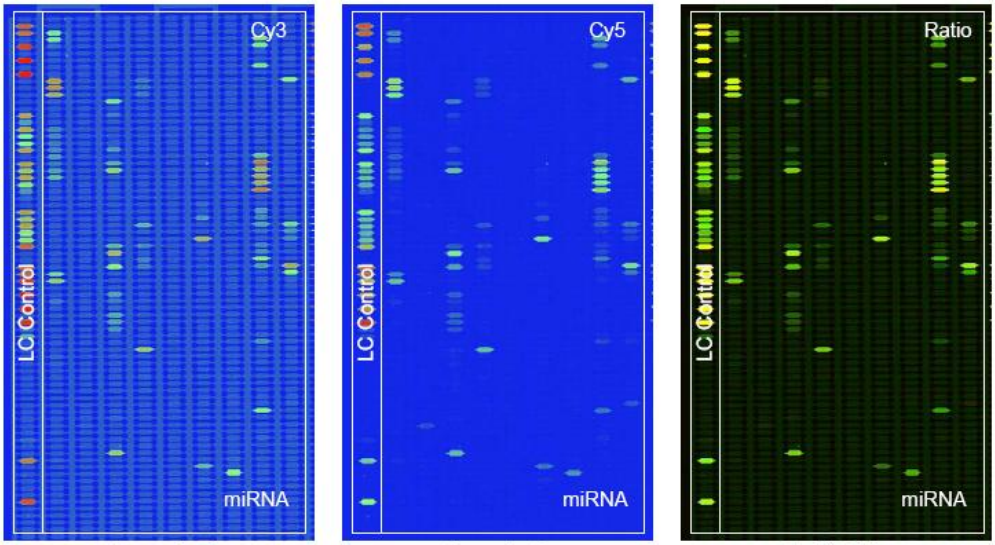

Sample A Sample B Cy3/Cy5

Table 3 Call list (differentially expressed transcripts with p-value < 0.01)

No.	Probe_ID	Sample A Signal	Sample B Signal	log2 (Sample B / Sample A)
1	tae-miR1134	26.12	686.44	5.06
2	ath-miR854a	54.90	562.92	3.40
3	ath-miR398b	70.35	10.32	-2.84
4	ath-miR398a	69.69	10.75	-2.73
5	osa-miR168b	626.16	105.79	-2.69
6	ath-miR168a	1,401.53	466.56	-1.63
7	sof-miR168b	3,626.63	1,798.67	-1.07
8	osa-miR168a	4,302.09	2,132.67	-0.99
9	osa-miR396d	3,122.13	1,535.07	-0.99
10	vvi-miR156e	1,005.56	547.03	-0.87
11	gma-miR156b	962.73	559.23	-0.78
12	bna-miR393	558.41	317.48	-0.78
13	osa-miR393b	434.65	260.73	-0.75
14	ptc-miR156k	1,047.86	707.30	-0.73
15	ath-miR159a	13,777.85	20,211.35	0.57
16	ath-miR159b	13,892.59	20,451.75	0.55
17	osa-miR159a	15,154.99	21,456.90	0.50
18	pta-miR319	2,062.70	1,462.90	-0.49
19	osa-miR156l	1,423.38	1,022.46	-0.48
20	sbi-miR156e	2,175.18	1,571.34	-0.47
21	osa-miR159f	13,809.63	18,923.22	0.45
22	pta-miR159b	2,593.38	1,893.34	-0.45
23	ptc-miR167e	776.74	1,056.74	0.44
24	bna-miR156a	2,088.36	1,553.95	-0.43
25	ptc-miR159f	4,330.72	3,236.09	-0.42
26	ath-miR159c	8,904.60	11,598.50	0.38
27	ptc-miR159d	9,010.15	10,871.21	0.38
28	osa-miR159d	9,519.89	12,190.17	0.36
29	ath-miR156a	2,363.41	1,844.18	-0.36
30	osa-miR159e	9,059.47	11,157.95	0.30
31	osa-miR159c	8,814.40	10,843.32	0.30
32	ppt-miR319a	8,895.09	10,132.93	0.19

Sample A: b95 inf. 48 hpi R2 – Cy3
Sample B: b95-control 48 hpi R2 – Cy5

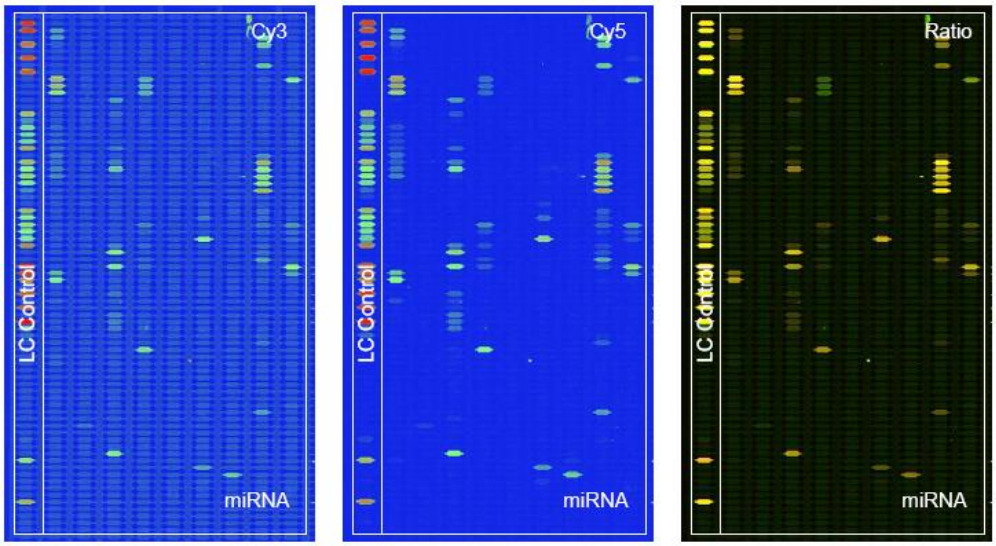

Sample A | Sample B | Cy3/Cy5

Table 4 Call list (differentially expressed transcripts with p-value < 0.01)

No.	Probe_ID	Sample A Signal	Sample B Signal	log2 (Sample B / Sample A)
1	ath-miR398b	105.42	6.90	-3.93
2	ath-miR398a	111.15	9.92	-3.04
3	ptc-miR474c	1,955.52	469.09	-2.12
4	ptc-miR474b	1,882.92	460.66	-2.10
5	ptc-miR474a	2,059.99	501.18	-2.02
6	tae-miR1134	180.29	44.16	-1.95
7	ath-miR854a	386.30	140.03	-1.49
8	osa-miR168b	129.25	410.85	1.46
9	osa-miR528	6,181.10	2,859.38	-1.10
10	gma-miR156b	445.15	899.50	0.94
11	vvi-miR156e	704.63	1,183.24	0.66
12	ath-miR156g	1,421.06	1,852.98	0.46
13	ath-miR156a	1,353.72	1,833.59	0.46
14	sbi-miR156e	1,338.54	1,730.11	0.39
15	osa-miR168a	2,179.33	2,750.56	0.35
16	sof-miR168b	1,936.20	2,483.10	0.35
17	vvi-miR319b	5,474.07	6,553.14	0.29
18	ppt-miR319a	9,125.61	10,357.49	0.18

Sample A: b95-control 6 hpi R3 – Cy3
Sample B: b95 inf. 6 hpi R3 – Cy5

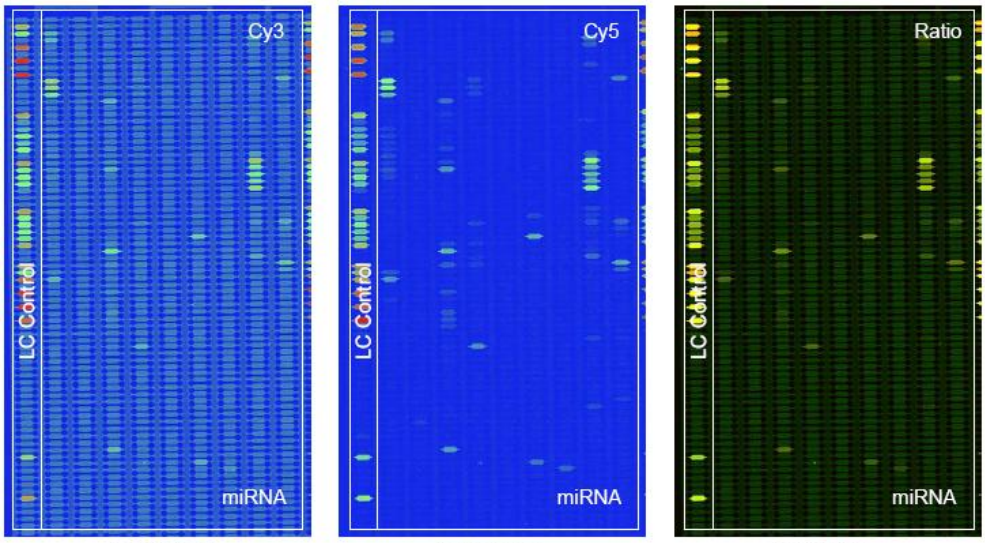

Sample A Sample B Cy3/Cy5

Table 5 Call list (differentially expressed transcripts with p-value < 0.01)

No.	Probe_ID	Sample A Signal	Sample B Signal	log2 (Sample B / Sample A)
1	osa-miR393b	79.45	237.08	1.58
2	bna-miR156a	1,127.60	629.96	-0.79
3	sbi-miR156e	1,100.44	606.22	-0.67
4	ath-miR156a	1,269.62	797.74	-0.67
5	ath-miR156g	1,307.60	799.64	-0.67
6	ath-miR319c	1,479.36	2,183.23	0.49
7	ppt-miR319a	2,621.44	3,437.75	0.41
8	sof-miR159e	2,162.85	2,934.77	0.40

Sample A: b95-control 12 hpi R3 – Cy3
Sample B: b95 inf. 12 hpi R3 – Cy5

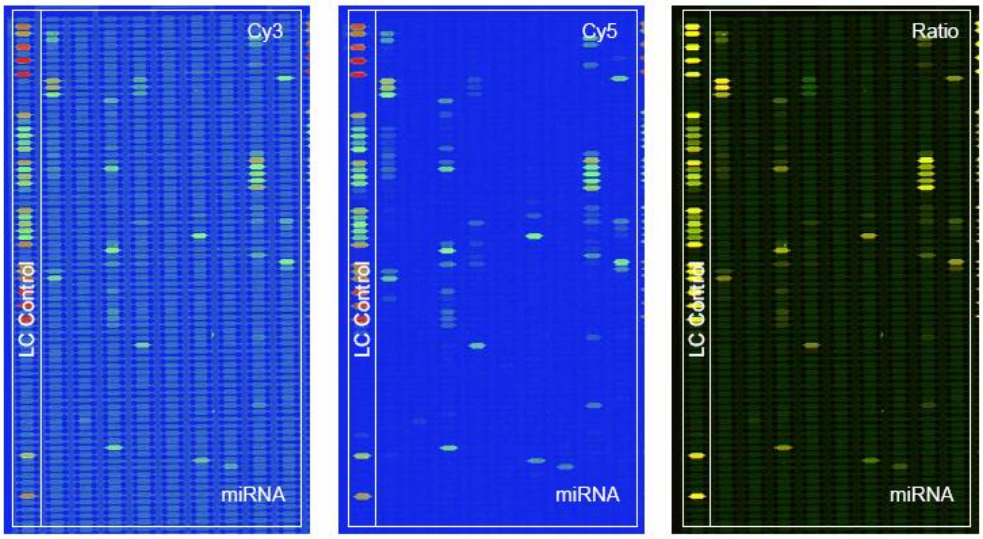

Sample A Sample B Cy3/Cy5

Table 6 Call list (differentially expressed transcripts with p-value < 0.01)

No.	Probe_ID	Sample A Signal	Sample B Signal	log2 (Sample B / Sample A)
1	ptc-miR474b	1,000.97	120.99	-3.03
2	ptc-miR474c	1,085.10	146.47	-2.95
3	ptc-miR474a	1,329.05	171.84	-2.92
4	ath-miR854a	363.66	102.13	-1.87
5	osa-miR396d	489.11	1,177.94	1.26
6	ppt-miR894	2,935.91	2,059.73	-0.62
7	pta-miR159b	832.07	1,160.47	0.52
8	osa-miR528	5,161.08	3,936.21	-0.39
9	ath-miR159a	14,965.95	13,065.25	-0.18
10	osa-miR159a	18,129.38	16,131.73	-0.15

Sample A: b95-control 24 hpi R3 – Cy3
Sample B: b95 inf. 24 hpi R3 – Cy5

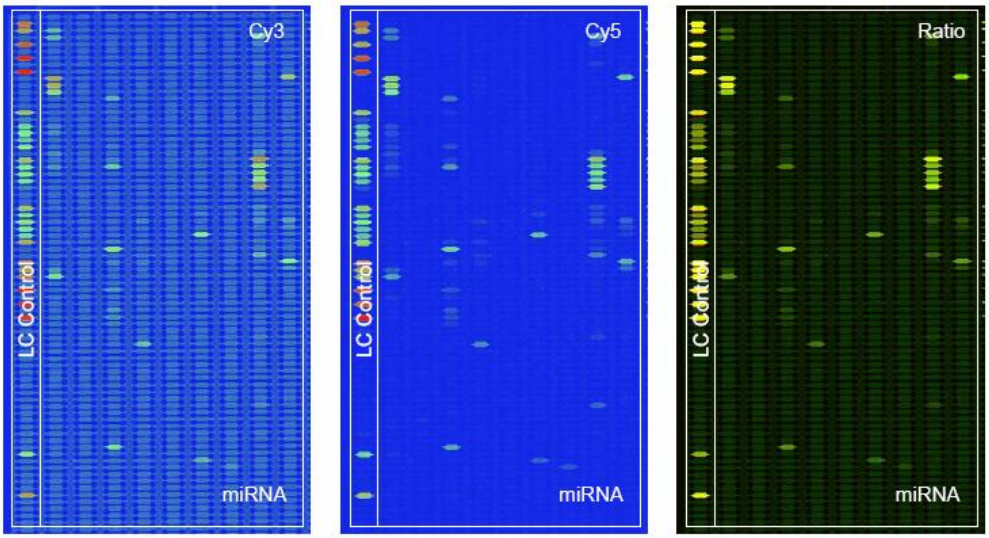

Sample A Sample B Cy3/Cy5

Table 7 Call list (differentially expressed transcripts with p-value < 0.01)

No.	Probe_ID	Sample A Signal	Sample B Signal	log2 (Sample B / Sample A)
1	osa-miR396d	305.61	769.38	1.34
2	ppt-miR894	1,460.38	692.04	-0.91
3	osa-miR528	7,331.08	4,741.53	-0.54
4	osa-miR159f	12,115.32	13,768.78	0.19

Sample A: b95-control 48 hpi R3 – Cy3
Sample B: b95 inf. 48 hpi R3 – Cy5

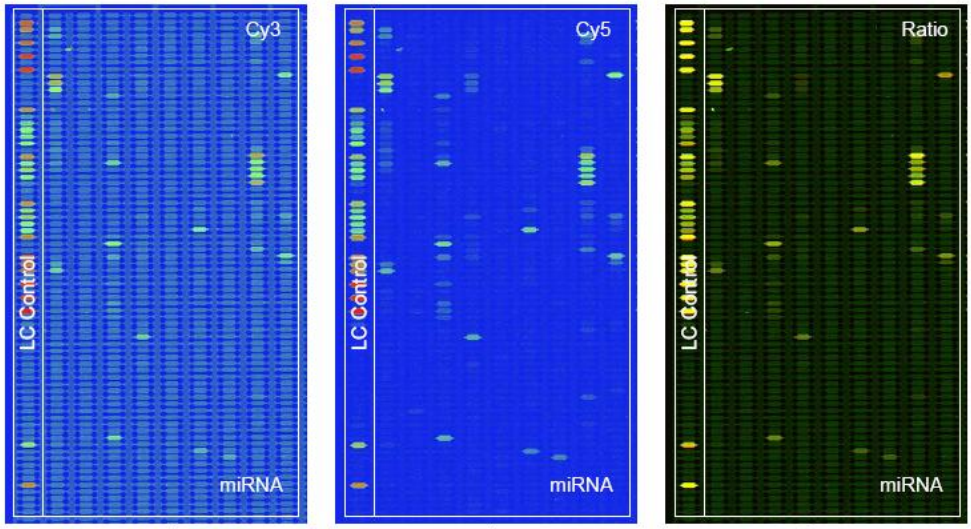

Sample A Sample B Cy3/Cy5

Table 8 Call list (differentially expressed transcripts with p-value < 0.01)

No.	Probe_ID	Sample A Signal	Sample B Signal	log2 (Sample B / Sample A)
1	ptc-miR474c	146.64	405.40	1.82
2	ptc-miR474b	144.38	441.51	1.80
3	ptc-miR474a	137.16	462.36	1.69
4	osa-miR396d	223.98	491.84	1.04
5	osa-miR528	3,929.78	7,075.26	0.91
6	osa-miR168a	1,921.09	1,130.56	-0.84
7	sof-miR168b	1,283.90	861.68	-0.63

Sample A: b103 inf. 6 hpi R2 – Cy3
Sample B: b103 control 6 hpi R2 – Cy5

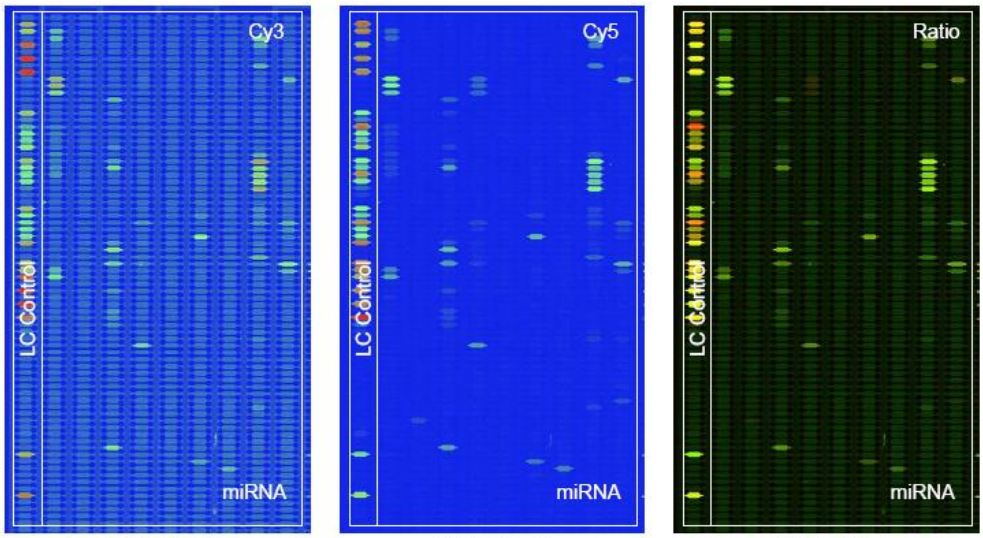

Sample A Sample B Cy3/Cy5

Table 9 Call list (differentially expressed transcripts with p-value < 0.01)

No.	Probe_ID	Sample A Signal	Sample B Signal	log2 (Sample B / Sample A)
1	ptc-miR474c	49.64	1,012.35	4.34
2	ptc-miR474a	67.59	1,118.54	4.02
3	ptc-miR474b	63.58	1,007.17	3.98
4	tae-miR1134	64.10	513.38	3.29
5	ath-miR854a	77.01	456.03	2.36
6	osa-miR156l	979.18	417.07	-1.23
7	sbi-miR156e	1,442.92	588.73	-1.22
8	ath-miR156g	1,443.68	641.04	-1.17
9	ath-miR156a	1,489.00	646.48	-1.16
10	osa-miR168a	1,552.81	670.99	-1.15
11	sof-miR168b	1,423.66	652.99	-1.15

12	osa-miR528	1,686.41	3,425.03	1.02
13	bna-miR156a	1,315.82	598.74	-0.96
14	vvi-miR156e	537.70	283.35	-0.92
15	ppt-miR894	900.16	1,486.35	0.70
16	sof-miR159e	3,899.85	5,098.38	0.39
17	smo-miR159	1,649.28	2,056.25	0.34
18	vvi-miR319b	2,593.81	3,124.24	0.30
19	ppt-miR319a	4,117.60	4,836.55	0.28
20	ptc-miR319e	3,562.54	4,187.59	0.28

Sample A: b103 inf. 12 hpi R2 – Cy3
Sample B: b103 control 12 hpi R2 – Cy5

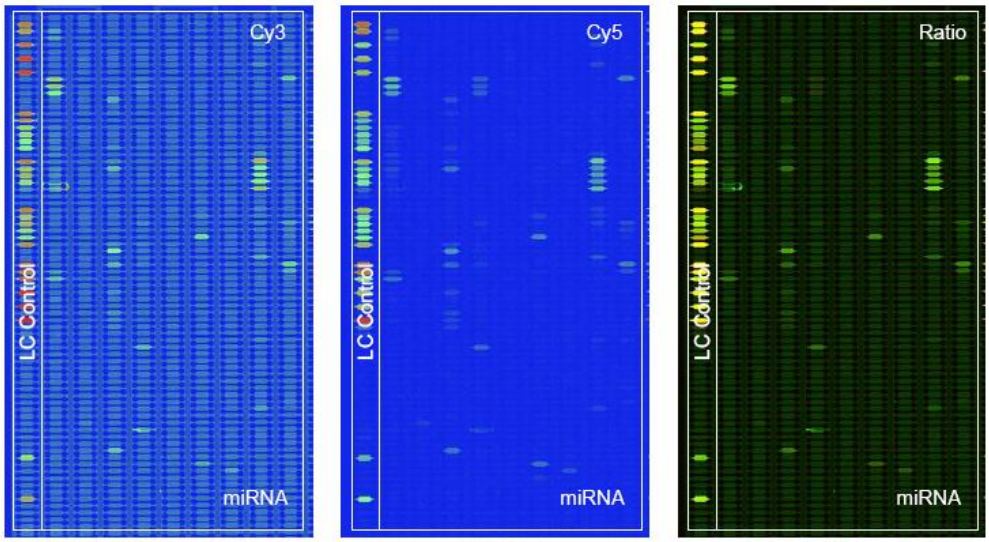

Sample A Sample B Cy3/Cy5

Table 10 Call list (differentially expressed transcripts with p-value < 0.01)

No.	Probe_ID	Sample A Signal	Sample B Signal	log2 (Sample B / Sample A)
1	ptc-miR474c	118.91	641.99	2.43
2	ptc-miR474a	140.87	743.56	2.41
3	ptc-miR474b	123.02	590.08	2.25
4	ppt-miR894	685.33	1,404.57	1.07
5	osa-miR396d	400.03	199.53	-1.00
6	osa-miR168a	955.41	601.59	-0.78

Chip: 11_P10.1_090152

Sample A: b103 inf. 24 hpi R2 – Cy3
Sample B: b103 control 24 hpi R2 – Cy5

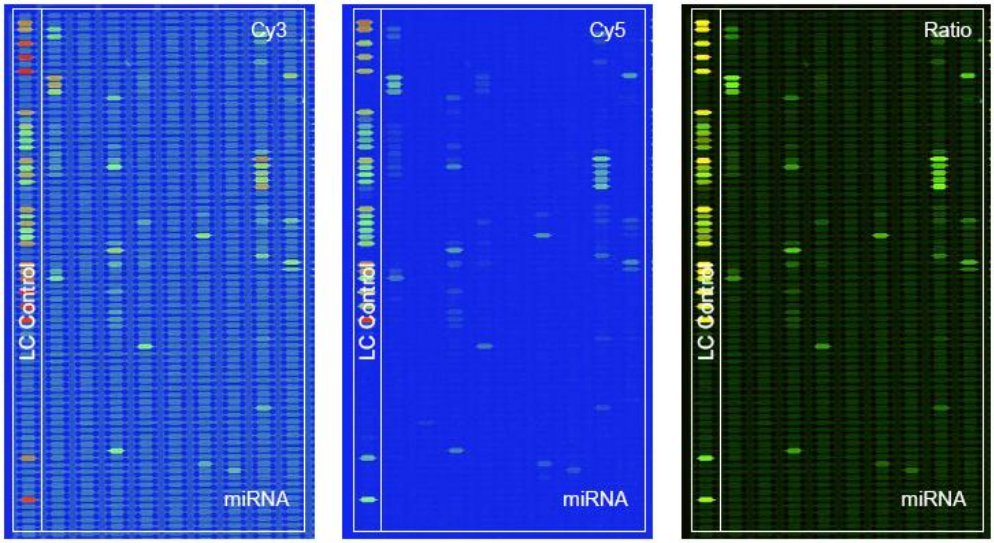

Sample A | Sample B | Cy3/Cy5

Table 11 Call list (differentially expressed transcripts with p-value < 0.01)

No.	Probe_ID	Sample A Signal	Sample B Signal	log2 (Sample B / Sample A)
1	vvi-miR156e	424.36	210.53	-1.01
2	osa-miR156l	693.47	343.85	-0.95
3	osa-miR396d	779.84	411.74	-0.92
4	bna-miR156a	1,097.58	635.84	-0.89
5	sbi-miR156e	1,124.45	607.31	-0.89
6	ath-miR156a	1,310.78	772.51	-0.80
7	ath-miR156g	1,347.60	790.11	-0.77
8	osa-miR159a	8,763.11	11,945.31	0.41
9	osa-miR159f	7,384.14	9,833.93	0.41
10	ath-miR159b	7,445.22	9,988.46	0.38
11	ath-miR159a	7,606.65	9,945.12	0.38

Chip: 12_P10.1_090153

Sample A: b103 inf. 48 hpi R2 – Cy3
Sample B: b103 control 48 hpi R2 – Cy5

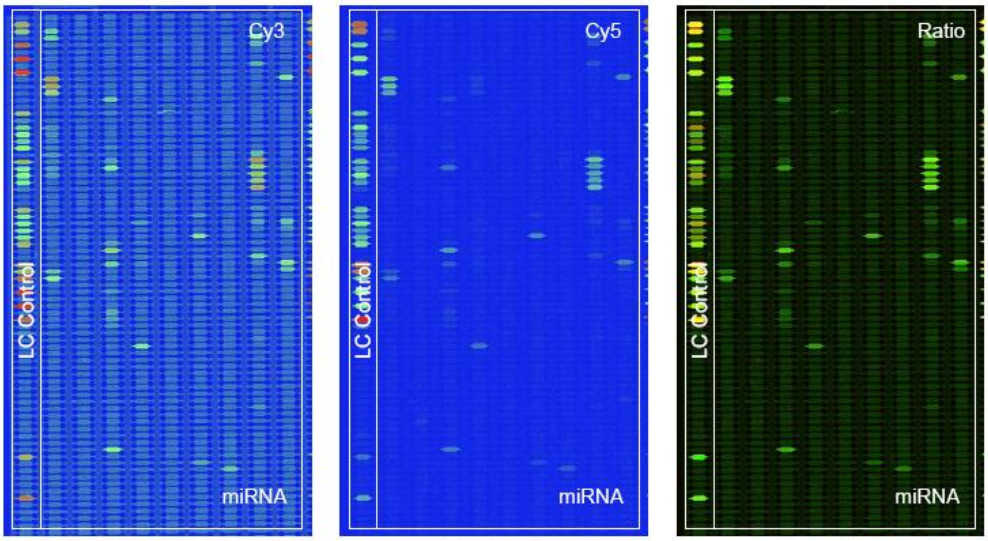

Sample A | Sample B | Cy3/Cy5

Table 12 Call list (differentially expressed transcripts with p-value < 0.01)

No.	Probe_ID	Sample A Signal	Sample B Signal	log2 (Sample B / Sample A)
1	ptc-miR474a	45.62	277.83	2.72
2	vvi-miR156e	342.24	104.55	-1.72
3	gma-miR156b	331.02	108.24	-1.64
4	bna-miR156a	857.13	343.78	-1.49
5	osa-miR156l	702.82	255.12	-1.46
6	sbi-miR156e	860.18	320.05	-1.42
7	ath-miR156a	1,067.72	383.21	-1.38
8	osa-miR168a	1,219.15	499.50	-1.38
9	ath-miR156g	1,038.21	403.50	-1.36
10	sof-miR168b	1,030.65	421.95	-1.29
11	osa-miR528	1,708.46	2,862.48	0.70
12	osa-miR159a	7,592.60	10,204.58	0.42

13	osa-miR159f	6,538.16	8,838.46	0.40
14	osa-miR159c	3,753.89	4,733.66	0.38
15	ath-miR159b	6,731.90	8,886.30	0.35
16	osa-miR159e	3,904.34	5,124.05	0.34
17	ath-miR159a	6,597.22	8,747.12	0.34
18	ptc-miR159d	3,854.54	4,863.07	0.33
19	osa-miR159d	4,367.27	5,673.90	0.33
20	ath-miR159c	4,064.41	5,099.57	0.28

Sample A: b103 control 6 hpi R3 – Cy3
Sample B: b103 inf. 6 hpi R3 – Cy5

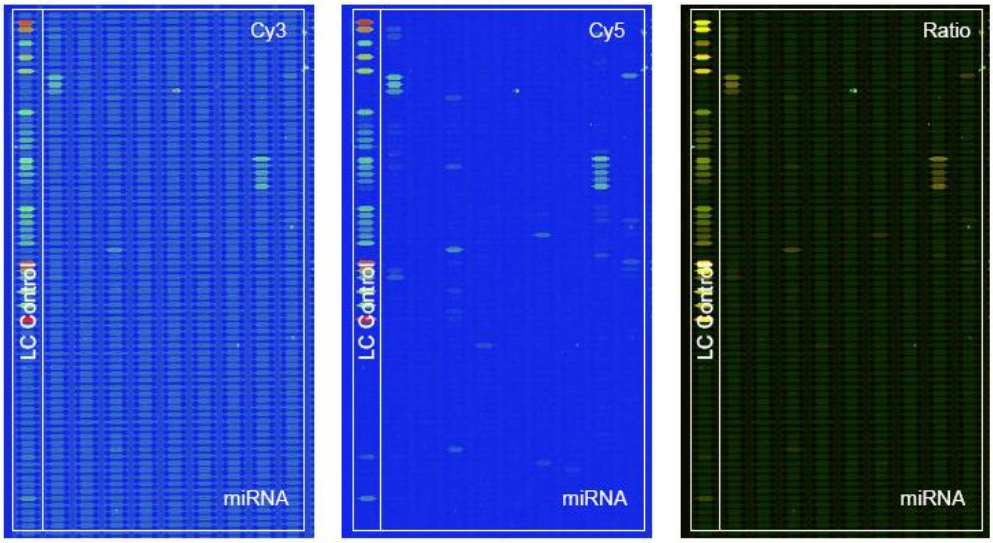

Sample A Sample B Cy3/Cy5

Table 13 Call list (differentially expressed transcripts with p-value < 0.01)

No.	Probe_ID	Sample A Signal	Sample B Signal	log2 (Sample B / Sample A)
1	osa-miR528	348.73	894.22	1.35
2	sof-miR159e	129.64	266.27	1.04
3	osa-miR159a	3,917.43	2,511.52	-0.64
4	ath-miR159a	3,187.06	2,257.32	-0.53
5	osa-miR159f	2,852.12	1,996.66	-0.51
6	ath-miR159b	2,865.36	2,185.20	-0.50

Sample A: b103 control 12 hpi R3 – Cy3
Sample B: b103 inf. 12 hpi R3 – Cy5

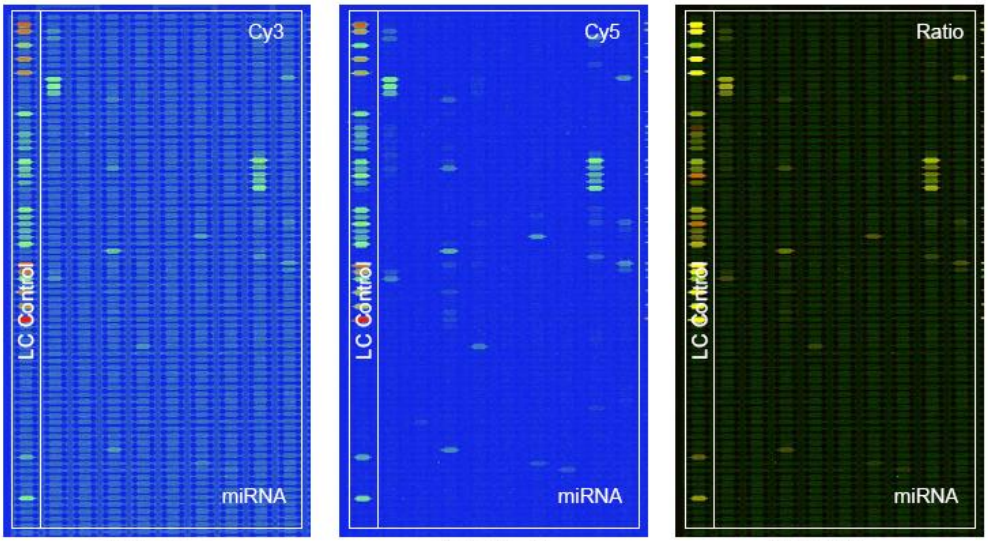

Sample A | Sample B | Cy3/Cy5

Table 14 Call list (differentially expressed transcripts with p-value < 0.01)

No.	Probe_ID	Sample A Signal	Sample B Signal	log2 (Sample B / Sample A)
1	ath-miR398b	98.05	12.66	-2.99
2	ath-miR398a	97.28	16.40	-2.60

Sample A: b103 control 24 hpi R3 – Cy3
Sample B: b103 inf. 24 hpi R3 – Cy5

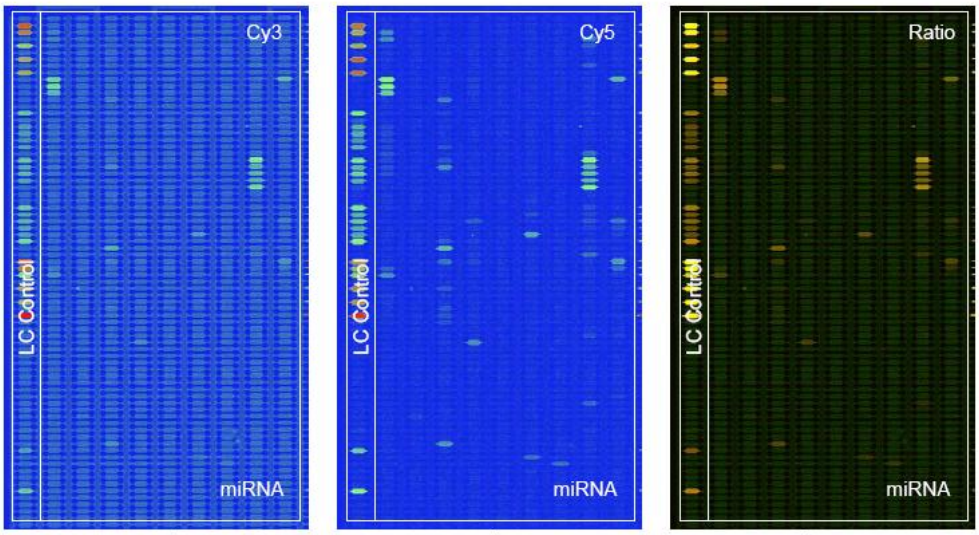

Sample A Sample B Cy3/Cy5

Table 15 Call list (differentially expressed transcripts with p-value < 0.01)

No.	Probe_ID	Sample A Signal	Sample B Signal	log2 (Sample B / Sample A)
1	osa-miR396d	88.21	391.94	2.14
2	osa-miR156l	230.37	535.79	1.18
3	osa-miR528	3,396.06	2,007.91	-0.82
4	osa-miR159a	8,747.80	5,251.33	-0.74
5	osa-miR159f	7,064.83	4,643.54	-0.66
6	ath-miR159b	7,129.59	4,626.64	-0.60
7	ath-miR159a	7,184.51	4,649.92	-0.58
8	ptc-miR159d	3,060.49	2,086.35	-0.55
9	osa-miR159d	3,713.18	2,648.14	-0.47
10	osa-miR159e	3,192.42	2,447.11	-0.44
11	osa-miR159c	3,056.01	2,266.47	-0.43

Sample A: b103 control 48 hpi R3 – Cy3
Sample B: b103 inf. 48 hpi R3 – Cy5

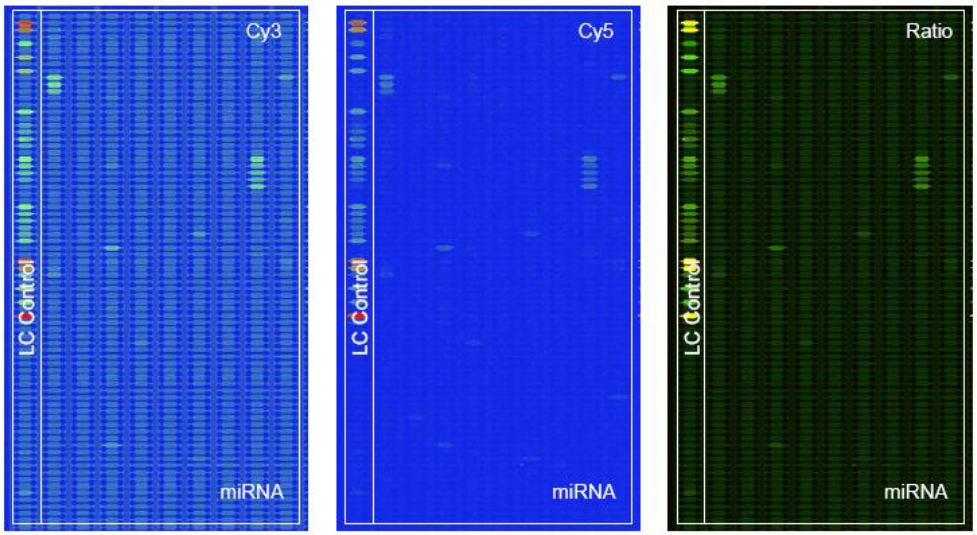

Sample A | Sample B | Cy3/Cy5